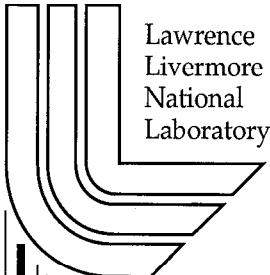


Microstructural Analyses of Topopah Spring Tuff from the Large Block Test at Fran Ridge, Nevada

E.D. Carlberg and J.J. Roberts

January 10, 2000

U.S. Department of Energy



DISCLAIMER

This document was prepared as an account of work sponsored by an agency of the United States Government. Neither the United States Government nor the University of California nor any of their employees, makes any warranty, express or implied, or assumes any legal liability or responsibility for the accuracy, completeness, or usefulness of any information, apparatus, product, or process disclosed, or represents that its use would not infringe privately owned rights. Reference herein to any specific commercial product, process, or service by trade name, trademark, manufacturer, or otherwise, does not necessarily constitute or imply its endorsement, recommendation, or favoring by the United States Government or the University of California. The views and opinions of authors expressed herein do not necessarily state or reflect those of the United States Government or the University of California, and shall not be used for advertising or product endorsement purposes.

Work performed under the auspices of the U. S. Department of Energy by the University of California Lawrence Livermore National Laboratory under Contract W-7405-Eng-48.

This report has been reproduced
directly from the best available copy.

Available to DOE and DOE contractors from the
Office of Scientific and Technical Information
P.O. Box 62, Oak Ridge, TN 37831
Prices available from (423) 576-8401
<http://apollo.osti.gov/bridge/>

Available to the public from the
National Technical Information Service
U.S. Department of Commerce
5285 Port Royal Rd.,
Springfield, VA 22161
<http://www.ntis.gov/>

OR

Lawrence Livermore National Laboratory
Technical Information Department's Digital Library
<http://www.llnl.gov/tid/Library.html>

Microstructural Analyses of Topopah Spring Tuff from the Large Block Test at Fran Ridge, Nevada

Eric D. Carlberg and Jeffery J. Roberts

Lawrence Livermore National Laboratory

Introduction

Microstructural information (e.g., porosity, pore size distribution, and surface area) of porous media is critical to understanding water transport mechanisms and physical properties and their bearing on geophysical measurements. We report microstructural data obtained by mercury injection porosimetry (MIP) on 33 samples of densely welded Topopah Spring tuff from Fran Ridge, Yucca Mountain, Nevada Test Site (NTS), Nevada. The characterization of these samples is also important for the interpretation and analysis of the Large Block Test (LBT) performed in support of the Yucca Mountain Project (YMP). This report includes previously published data on samples from the same location (Roberts and Lin, 1996). We also present information from the Yucca Mountain Site Characterization Project/Lawrence Livermore National Laboratory (YMSCP/LLNL) Large Block Test Engineering Plan (Wilder, 1995) to allow correlation of our data directly to various planes within the Large Block.

The Large Block Test

Thorough descriptions of the LBT are available in numerous reports and articles (e.g., Lin et al., 1994; Blair and Wood, 1997; Lin et al., 1997; Ramirez and Daily, 1997; Wilder et al., 1997). Since the purpose of this paper is to report detailed microstructural results, only a brief description of the test is presented here.

Location of the Large Block Test, borehole nomenclature, and sampling

The LBT is a coupled thermo-hydrological-mechanical-chemical field test of a 3 meter square by 5 meter tall block of densely welded Topopah Spring Tuff. The block is located on an eastern facing slope at Fran Ridge, Nevada, at the Nevada Test Site. Prior to excavation of the Large Block, detailed fracture mapping of the surface was performed in an effort to find the best location for the test. Vertical boreholes were drilled with nearly continuous coring after an area with suitable fracture density was located and roughly graded with a bulldozer (Fig. 1).

An approximately 3 meter square (10 foot by 10 foot) horizontal aluminum template was positioned over the site as a borehole guide. All borehole depths are reported as depth below this template. The template was not parallel to the uneven rock surface, thus, the cores for each borehole start at a different depth. The elevation of the template as well as the borehole elevations at the final cut block were surveyed (Table 1).

Borehole designations correlate to a borehole diameter (N=3 inch or 7.6 cm; E=1.5 inch or 3.8 cm) and a sequential number. Boreholes were renamed after final excavation of the Large Block to reflect location and use (e.g., N1 became TN1 for Top Neutron 1; see Table 1 for remaining names).

Video logging of boreholes was performed, the videos examined and described in detail (Wagoner, 1999). Recovered core was logged and packaged at the YMP Sample Management Facility (SMF) at the NTS. Representative sections from each hole were sent to LLNL (nearly 12 meters of the approximately 45 meters total recovered core). Samples for laboratory core plug tests and microstructural analyses were selected and prepared. Samples with large cavities and inhomogeneous inclusions were excluded from these tests. Subcores were sent to an outside facility for MIP testing while gravimetric analyses as described by Roberts and Lin (1996) were conducted on other samples from approximately the same location as the subcores. Gravimetric test data including dry density, wet density and porosity from Roberts and Lin (1996) are presented in Table 2.

Results and Discussion

Since our data are from boreholes that predate the final excavation of the Large Block, Table 3 is provided to allow cross referencing of our data to significant horizons within the block. Table 4 contains summary data for each sample where MIP testing was conducted.

The appendix contains the plots of incremental pore surface and incremental pore volume. Some plots were not available due to the lack of electronic data. Each data table lists the incremental values for pressure, pore diameter, intrusion volume of mercury, pore surface area, as well as the mean and standard deviation for pore diameter. In Table 4 we report total pore area, median pore diameter by volume, median pore diameter by area, average pore diameter by $4V/A$ where V is volume and A is area, bulk density, skeletal density, and porosity as determined by mercury injection porosimetry.

Mercury Injection Porosimetry

Mercury injection porosimetry is a commonly used tool for the analysis of microstructural properties of porous media, including rocks and soils. Since mercury is a non-wetting fluid (for most materials), it is forced into the pore space by applying pressure rather than by capillary action. By accurately measuring pressure and volume of mercury incrementally intruded into a sample, information is obtained regarding the porosity and pore size distribution in the sample. The simplest equation to model the rate of capillary penetration into a porous medium is attributed to Washburn (1921; cited in Dullien, 1992). Simply stated, the equation describes how far the meniscus of a fluid penetrates into a capillary for a given pressure differential.

Bulk volume of a sample is determined by immersion of the sample in mercury (Dullien, 1992). After evacuating the sample vessel, hydrostatic pressure is incrementally increased. At each pressure, the size and total volume of pores invaded by mercury is calculated. The maximum pressure is 60,000 psia (414 MPa). At this pressure, only a very small amount of the pore space remains unfilled by the mercury. Penetration is never quite complete because it would take infinite pressure to perfectly fill all the edges and corners of the pores (Dullien, 1992).

Total pore area is the surface area within the pores based on the assumption of cylindrical pore geometry and summing over the pressure range of mercury injection into the pores. Median pore diameters are taken as the 50% values from the pressure vs. area and volume curves (assuming cylindrical pores). By comparing the cumulative pore surface area vs. pore diameter and the cumulative pore volume vs. pore diameter plots, it can be seen that area distribution tends to shift towards the smaller pore sizes when

compared to the volume distribution. This is caused by the relatively larger contribution to surface area made by small pores.

Average pore diameter by $4V/A$ is calculated by dividing the formulas for volume and area then solving for diameter. Equation 1 gives the formula for the volume (V) of a cylindrical pore having diameter (d) and length (h); Equation 2 gives the cross-sectional area (A) of such a pore. Therefore, the pore diameter can be estimated using equation 3.

$$V = \pi d^2 h / 4 \quad (1)$$

$$A = \pi d h \quad (2)$$

$$d = 4V/A \quad (3)$$

Bulk density (ρ_{bulk}) is calculated using the sample weight together with the sample volume obtained during initial filling of the mercury porosimeter chamber. Skeletal density (ρ_{skeletal}) is determined by adjusting the bulk density for the volume of the injected mercury (Hg inj);

$$\rho_{\text{skeletal}} = \rho_{\text{bulk}} - (M_{\text{Hg inj}} / V_{\text{sample}}), \quad (4)$$

where M is mass.

Statistical Analyses

For 33 samples tested, mean total pore area is $7.3715 \pm 1.5795 \text{ m}^2/\text{g}$. Skeletal density mean value is $2.5591 \pm 0.0456 \text{ g/cm}^3$. With few exceptions, MIP data closely match gravimetric data in Table 2. Bulk density by MIP results provide a mean value of $2.2633 \pm 0.0596 \text{ g/cm}^3$. Compare this to gravimetric results from Table 2 which has a mean dry density of $2.25 \pm 0.03 \text{ g/cm}^3$. Mean porosity from Table 2 is 0.104 ± 0.013 as compared to MIP results which is 0.1154 ± 0.0228 . Sample N1-13.4 was resubmitted due to suspect data; secondary testing results are reported as sample N1-13.4b (Table 4). Mean and standard deviation data exclude sample N1-13.4a. Refer to Tables 2 and 4 as well as appendix data for further analysis.

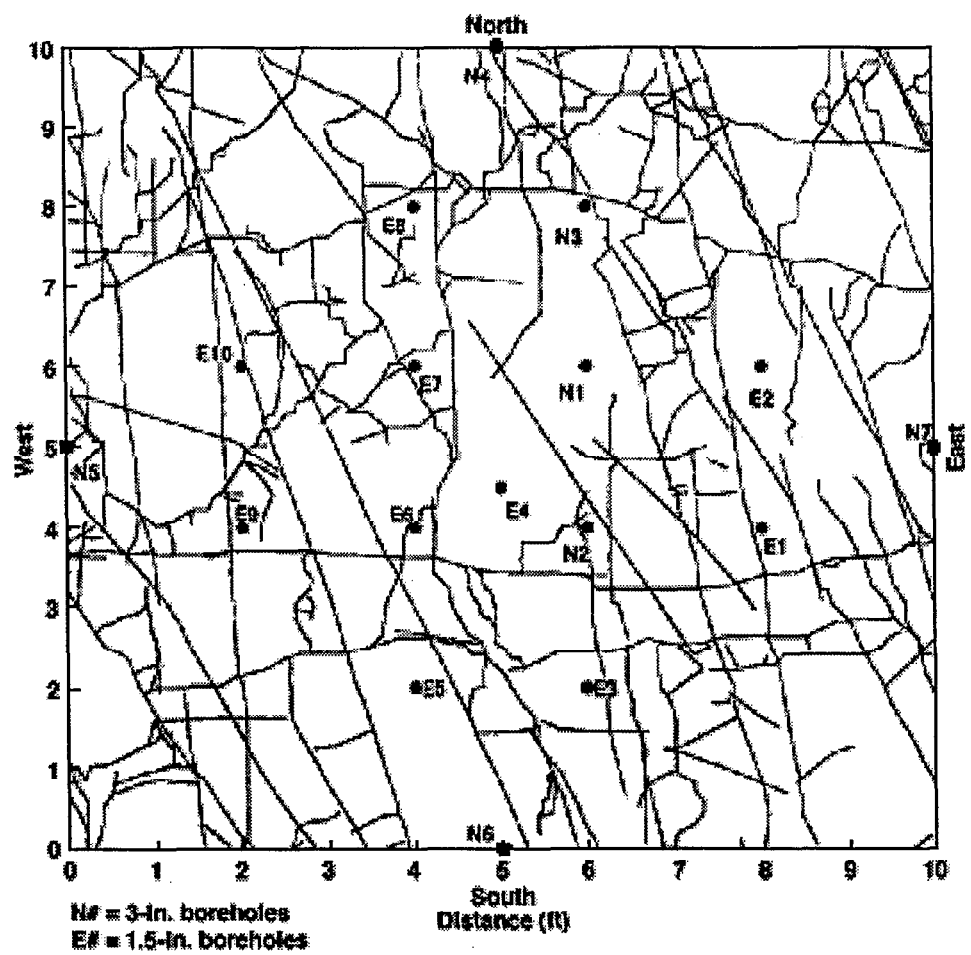


Figure 1 Fracture map of the top surface of large block with top borehole locations (Wilder et al., 1997).

Table 1. Borehole Names and Elevations

| Borehole ¹ | LBT borehole reference | Distance, template to rock surface ² | | Surface elevation ³ | | Surveyed final elevation ⁴ | |
|-----------------------|------------------------|---|----------|--------------------------------|----------|---------------------------------------|----------|
| | | (feet) | (meters) | (feet) | (meters) | (feet) | (meters) |
| N1 | TH1 | 0.30 | 0.09 | 3417.40 | 1041.62 | 3416.34 | 1041.30 |
| N2 | TM1 | 0.56 | 0.17 | 3417.14 | 1041.54 | 3416.32 | 1041.29 |
| N3 | TM2 | 0.53 | 0.16 | 3417.17 | 1041.55 | 3416.35 | 1041.30 |
| N4 | TERT1 (N rockbolt) | 0.37 | 0.11 | 3417.33 | 1041.60 | 3416.37 | 1041.31 |
| N5 | TERT16 (W rockbolt) | 0.42 | 0.13 | 3417.28 | 1041.59 | 3416.37 | 1041.31 |
| N6 | TERT11 (S rockbolt) | 0.28 | 0.09 | 3417.42 | 1041.63 | 3416.36 | 1041.31 |
| N7 | TERT25 (E rockbolt) | 1.00 | 0.30 | 3416.70 | 1041.41 | 3416.38 | 1041.31 |
| E2 | TN4 | 0.56 | 0.17 | 3417.14 | 1041.54 | 3416.34 | 1041.30 |

¹ Prefix N is for a 3 inch borehole; E is for 1.5 inch hole.

² Surveyed template elevation was 3417.7 ft (1041.71 m) at all boreholes.

³ Surveyed elevation of rough surface prior to cutting of the Large Block.

⁴ Surveyed final elevation is in reference to the cut surface of the Large Block.

Table 2. LBT Samples Prepared for Moisture Retention Experiments (Roberts and Lin, 1996)

| Sample [†] | Sample ID | Depth, m | Dry wt, g | Wet wt, g | Dry density, g/cm ³ | Wet density, g/cm ³ | Porosity |
|---------------------|------------|----------|-----------|-----------|-----------------------------------|-----------------------------------|-------------|
| N1-6.3 | 0032079.3 | 1.92 | 1.5352 | 1.6111 | 2.23 | 2.35 | 0.110 |
| N1-6.3A | 0032079.3A | 1.92 | 1.7890 | 1.8680 | 2.26 | 2.36 | 0.0997 |
| N1-6.3B | 0032079.3B | 1.92 | 1.6358 | 1.7098 | 2.28 | 2.39 | 0.103 |
| N1-11.0 | 0032081.3 | 3.35 | 1.6352 | 1.7181 | 2.25 | 2.37 | 0.114 |
| N1-11.0A | 0032081.3A | 3.35 | 1.5920 | 1.6734 | 2.26 | 2.38 | 0.116 |
| N1-11.0B | 0032081.3B | 3.35 | 1.6762 | 1.7525 | 2.30 | 2.41 | 0.105 |
| N1-13.45 | 0032082.3 | 4.10 | 1.4982 | 1.5752 | 2.27 | 2.39 | 0.117 |
| N1-13.45A | 0032082.3A | 4.10 | 1.7118 | 1.7951 | 2.27 | 2.38 | 0.110 |
| N1-13.45B | 0032082.3B | 4.10 | 1.6954 | 1.7781 | 2.26 | 2.37 | 0.110 |
| N1-16.9 | 0032083.3 | 5.15 | 1.6499 | 1.7522 | 2.20 | 2.33 | 0.136 |
| N1-16.9A | 0032083.3A | 5.15 | 1.6094 | 1.6987 | 2.23 | 2.35 | 0.124 |
| N1-16.9B | 0032083.3B | 5.15 | 1.6885 | 1.7670 | 2.27 | 2.38 | 0.106 |
| N1-20.3 | 0032084.3 | 6.19 | 1.5438 | 1.6133 | 2.22 | 2.32 | 0.0998 |
| N1-20.3A | 0032084.3A | 6.19 | 1.5567 | 1.6244 | 2.26 | 2.36 | 0.0982 |
| N1-20.3B | 0032084.3B | 6.19 | 1.5109 | 1.5849 | 2.21 | 2.32 | 0.108 |
| N4-11.6 | 0032104.3 | 3.54 | 1.5429 | 1.6036 | 2.26 | 2.34 | 0.0887 |
| N4-11.6A | 0032104.3A | 3.54 | 1.6222 | 1.6864 | 2.24 | 2.33 | 0.0886 |
| N4-11.6B | 0032104.3B | 3.54 | 1.6375 | 1.6969 | 2.27 | 2.35 | 0.0823 |
| N5-4.9 | 0032107.3 | 1.49 | 1.6998 | 1.7687 | 2.25 | 2.34 | 0.0911 |
| N5-4.9A | 0032107.3A | 1.49 | 1.6501 | 1.7104 | 2.28 | 2.37 | 0.0834 |
| N5-4.9B | 0032107.3B | 1.49 | 1.8818 | 1.9569 | 2.31 | 2.40 | 0.0922 |
| N5-20.4 | 0032111.3 | 6.22 | 1.5230 | 1.5909 | 2.22 | 2.32 | 0.0992 |
| N5-20.4A | 0032111.3A | 6.22 | 1.4883 | 1.5593 | 2.21 | 2.32 | 0.106 |
| N5-20.4B | 0032111.3B | 6.22 | 1.4765 | 1.5463 | 2.22 | 2.32 | 0.105 |
| N6-4.75 | 0032112.3 | 1.43 | 1.7549 | 1.8228 | 2.25 | 2.33 | 0.0869 |
| N6-4.75A | 0032112.3A | 1.43 | 1.6761 | 1.7374 | 2.29 | 2.37 | 0.0837 |
| N6-4.75B | 0032112.3B | 1.43 | 1.7136 | 1.7755 | 2.27 | 2.35 | 0.0819 |
| N6-14.2 | 0032116.3 | 4.33 | 1.6590 | 1.7398 | 2.26 | 2.37 | 0.110 |
| N6-14.2A | 0032116.3A | 4.33 | 1.6869 | 1.7706 | 2.24 | 2.35 | 0.111 |
| N6-14.2B | 0032116.3B | 4.33 | 1.6285 | 1.7137 | 2.23 | 2.35 | 0.117 |
| N7-5.7 | 0032120.3 | 1.74 | 1.6161 | 1.7003 | 2.24 | 2.36 | 0.117 |
| N7-5.7A | 0032120.3A | 1.74 | 1.6320 | 1.7051 | 2.29 | 2.39 | 0.102 |
| N7-5.7B | 0032120.3B | 1.74 | 1.7091 | 1.7834 | 2.28 | 2.38 | 0.0991 |
| N7-11.0 | 0032123.3 | 3.35 | 1.5850 | 1.6705 | 2.25 | 2.37 | 0.121 |
| N7-11.0A | 0032123.3A | 3.35 | 1.6353 | 1.7171 | 2.26 | 2.38 | 0.113 |
| N7-11.0B | 0032123.3B | 3.35 | 1.6318 | 1.7112 | 2.27 | 2.38 | 0.110 |
| mean * | 36 samples | | | | 2.25±0.03 | 2.36±0.02 | 0.104±0.013 |

[†] Sample name consists of borehole designation followed by depth in feet below the template used to locate vertical boreholes.

* Statistical mean for 36 samples. Errors represent one standard deviation for all samples collectively.

Table 3. Cross References for Borehole Data to Large Block Horizons

| Horizon | Surveyed elevation (feet) | Surveyed elevation (meters) | Borehole depth below template (feet) | Borehole depth below template (meters) | Large Block reference depth (feet) | Large Block reference depth (meters) |
|--------------|------------------------------|--------------------------------|---|---|---------------------------------------|---|
| Template | 3417.7 | 1141.7 | 0 | 0 | N/A | N/A |
| Top of LB | 3416.3 | 1141.29 | 1.4 | 0.43 m | 0 | 0 |
| Heated plane | N/A | | 10.4 | 3.17 | -9 | -2.74 |
| Bottom of LB | N/A | | 15.4 | 4.69 | -14 | -4.27 |

Table 4. Mercury Injection Porosimetry Summary Data

| Sample [†] | Total pore area (m ² /g) | Median pore diameter by volume (μm) | Median pore diameter by area (μm) | Average pore diameter by 4V/A (μm) | Bulk density (g/cm ³) | Skeletal density (g/cm ³) | Porosity |
|---------------------|-------------------------------------|-------------------------------------|-----------------------------------|------------------------------------|-----------------------------------|---------------------------------------|----------|
| N1-5.7 to 6.3 | 4.6429 | 0.0932 | 0.0080 | 0.0350 | 2.3372 | 2.5825 | 0.0950 |
| N1-10.9 to 11.5 | 6.9868 | 0.0611 | 0.0171 | 0.0345 | 2.2427 | 2.5930 | 0.1351 |
| N1-11.0 | 8.8620 | 0.0303 | 0.0148 | 0.0224 | 2.3089 | 2.6081 | 0.1148 |
| N1-13.4a | 8.3196 | 37.8102 | 0.0180 | 0.0931 | 1.7272 | 2.5948 | 0.3344 |
| N1-13.4b | 9.6257 | 0.0272 | 0.152 | 0.0207 | 2.3102 | 2.6113 | 0.1153 |
| N1-16.9 | 4.0976 | 0.2434 | 0.0116 | 0.0589 | 2.2421 | 2.5927 | 0.1352 |
| N1-20.3 | 11.1302 | 0.0513 | 0.0063 | 0.0212 | 2.2239 | 2.5595 | 0.1311 |
| N2-4.0 | 5.5900 | 0.1616 | 0.0071 | 0.0367 | 2.2850 | 2.5883 | 0.1172 |
| N2-4.3 | 8.7110 | 0.0383 | 0.0070 | 0.0169 | 2.2967 | 2.5088 | 0.0845 |
| N2-11.1 | 8.2266 | 0.0570 | 0.0075 | 0.0231 | 2.2461 | 2.5150 | 0.1069 |
| N2-11.25 | 5.8431 | 0.1435 | 0.0073 | 0.0362 | 2.2900 | 2.6057 | 0.1211 |
| N2-13.9 | 6.3615 | 0.2336 | 0.0071 | 0.0469 | 2.1707 | 2.5894 | 0.1617 |
| N2-19.2 | 8.4895 | 0.0480 | 0.0085 | 0.0224 | 2.2567 | 2.5277 | 0.1072 |
| N3-4.5 | 5.4111 | 0.2110 | 0.0068 | 0.0389 | 2.2894 | 2.6029 | 0.1204 |
| N3-4.75 | 6.9874 | 0.0665 | 0.0081 | 0.0263 | 2.2555 | 2.5167 | 0.1038 |
| N3-11.0 | 9.0228 | 0.0728 | 0.0073 | 0.0227 | 2.3177 | 2.6305 | 0.1189 |
| N3-15.2 | 7.2965 | 0.1026 | 0.0074 | 0.0325 | 2.2679 | 2.6196 | 0.1343 |
| N3-20.4 | 9.4214 | 0.0339 | 0.0087 | 0.0187 | 2.2528 | 2.5019 | 0.0996 |
| N4-5.3 | 8.9013 | 0.0544 | 0.0059 | 0.0200 | 2.2611 | 2.5135 | 0.1004 |
| N4-11.6 | 6.9084 | 0.0505 | 0.0084 | 0.0235 | 2.2616 | 2.4903 | 0.0918 |
| N4-14.5 | 6.0849 | 0.1298 | 0.0075 | 0.0316 | 2.3096 | 2.5983 | 0.1111 |
| N4-19.0 | 7.4861 | 0.0456 | 0.0125 | 0.0266 | 2.2459 | 2.5281 | 0.1116 |

Table 4 (cont'd). Mercury Injection Porosimetry Summary Data

| Sample [†] | Total pore area (m ² /g) | Median pore diameter by volume (μm) | Median pore diameter by area (μm) | Average pore diameter by 4V/A (μm) | Bulk density (g/cm ³) | Skeletal density (g/cm ³) | Porosity |
|---------------------|-------------------------------------|-------------------------------------|-----------------------------------|------------------------------------|-----------------------------------|---------------------------------------|-------------------|
| N5-4.9 | 6.5621 | 0.0476 | 0.0085 | 0.0232 | 2.3276 | 2.5534 | 0.0884 |
| N5-11.15 | 5.7744 | 0.0889 | 0.0082 | 0.0360 | 2.2889 | 2.5981 | 0.1190 |
| N5-14.8 | 5.9586 | 0.0911 | 0.0087 | 0.0378 | 2.2465 | 2.5717 | 0.1265 |
| N5-20.1 | 9.2912 | 0.0457 | 0.0076 | 0.0196 | 2.2422 | 2.4963 | 0.1018 |
| N6-4.8 | 7.6122 | 0.0371 | 0.0078 | 0.0188 | 2.3001 | 2.5065 | 0.0823 |
| N6-11.0 | 6.6135 | 0.0515 | 0.0106 | 0.0275 | 2.2825 | 2.5464 | 0.1036 |
| N6-14.5 | 6.4598 | 0.1186 | 0.0065 | 0.0338 | 2.2666 | 2.5861 | 0.1235 |
| N6-20.2 | 8.7303 | 1.0908 | 0.0062 | 0.0464 | 1.9941 | 2.4982 | 0.2018 |
| N7-5.0 | 8.1133 | 0.0536 | 0.0071 | 0.0212 | 2.2718 | 2.5177 | 0.0977 |
| N7-10.9 | 6.4128 | 0.0682 | 0.0105 | 0.0310 | 2.3060 | 2.6045 | 0.1146 |
| N7-14.3 | 7.2915 | 0.0543 | 0.0146 | 0.0301 | 2.2768 | 2.6013 | 0.1248 |
| E2-19.5 | 8.3521 | 0.0552 | 0.0086 | 0.0235 | 2.2147 | 2.4850 | 0.1087 |
| mean* | 7.3715 ±1.5795 | | | | 2.2633 ±0.0596 | 2.5591 ±0.0456 | 0.1154 ±0.0228 |

[†] Sample name consists of borehole designation followed by depth in feet below the template used to locate vertical boreholes.

* Statistical mean for 33 samples. Errors represent one standard deviation for all samples collectively. Sample N1-13.4a has been excluded from statistical analyses.

Acknowledgments

Dave Ruddle provided technical support. This work was supported by the Yucca Mountain Site Characterization Project. Work performed under the auspices of the US. Department of Energy by Lawrence Livermore National Laboratory under contract W-7405-ENG-48.

References

- Blair, S. C., and S. A. Wood, Geomechanical observations during the Large Block test, UCRL-JC-128797-EXT-ABS, Lawrence Livermore Natl. Lab., Livermore, CA, 1997.
- Dullien, F. A. L., *Porous Media, Fluid transport and pore structure*, 2nd ed., Academic Press, Inc., San Diego, 574 pp., 1992.
- Lin, W., D. G. Wilder, J. Blink, P. Berge, S. Blair, S. Boyd, V. Brugman, P. Burklund, T. Buscheck, Y. Chang, D. Chesnut, W. Daily, R. S. Glass, W. Glassley, L. Hall, C. Landram, K. Lee, J. Nitao, J. Noring, M. Owens, R. Pletcher, A. Ramirez, N. Rector, T. Reitter, J. Roberts, D. Ruddle, S. Sommer, D. Trummer, J. Ueng, J. Wagoner, R. J. Glass, G. Danko, A progress report for the Large Block Test of the coupled thermal-mechanical-hydrological-chemical processes, UCRL-ID-119101, Lawrence Livermore Natl. Lab., Livermore, CA, 1994.
- Lin, W., D. Wilder, S. Blair, T. Buscheck, W. Daily, G. Gdowski, W. Glassley, K. Lee, A. Meike, A. Ramirez, J. Roberts, D. Ruddle, J. Wagoner, D. Watwood, T. Williams, R. Carlson, D. Neubauer, Overview of progress on the Large Block test, UCRL-JC-128796-EXT-ABS, Lawrence Livermore Natl. Lab., Livermore, CA, 1997.
- Ramirez, A. L., and W. Daily, Electrical resistance tomography of the large block test near Yucca Mountain, UCRL-JC-128798-EXT-ABS, Lawrence Livermore Natl. Lab., Livermore, CA, 1997.
- Roberts, J. J., and W. Lin, Report on laboratory tests of drying and re-wetting of intact rocks, Rep. UCRL-ID-121513, Lawrence Livermore Natl. Lab., Livermore, CA, 1996.
- Wagoner, J. L., Fracture Characterization of the Large Block Test, Fran Ridge, Yucca Mountain, Nevada, UCRL-ID-133846, Lawrence Livermore Natl. Lab., Livermore, CA, 1999.

Wilder, D. G., Yucca mountain site characterization project, Lawrence Livermore National Laboratory, Large Block test engineering plan, LLNL-EP-1, Rev 0, Draft B, Lawrence Livermore Natl. Lab., Livermore, CA, 1995.

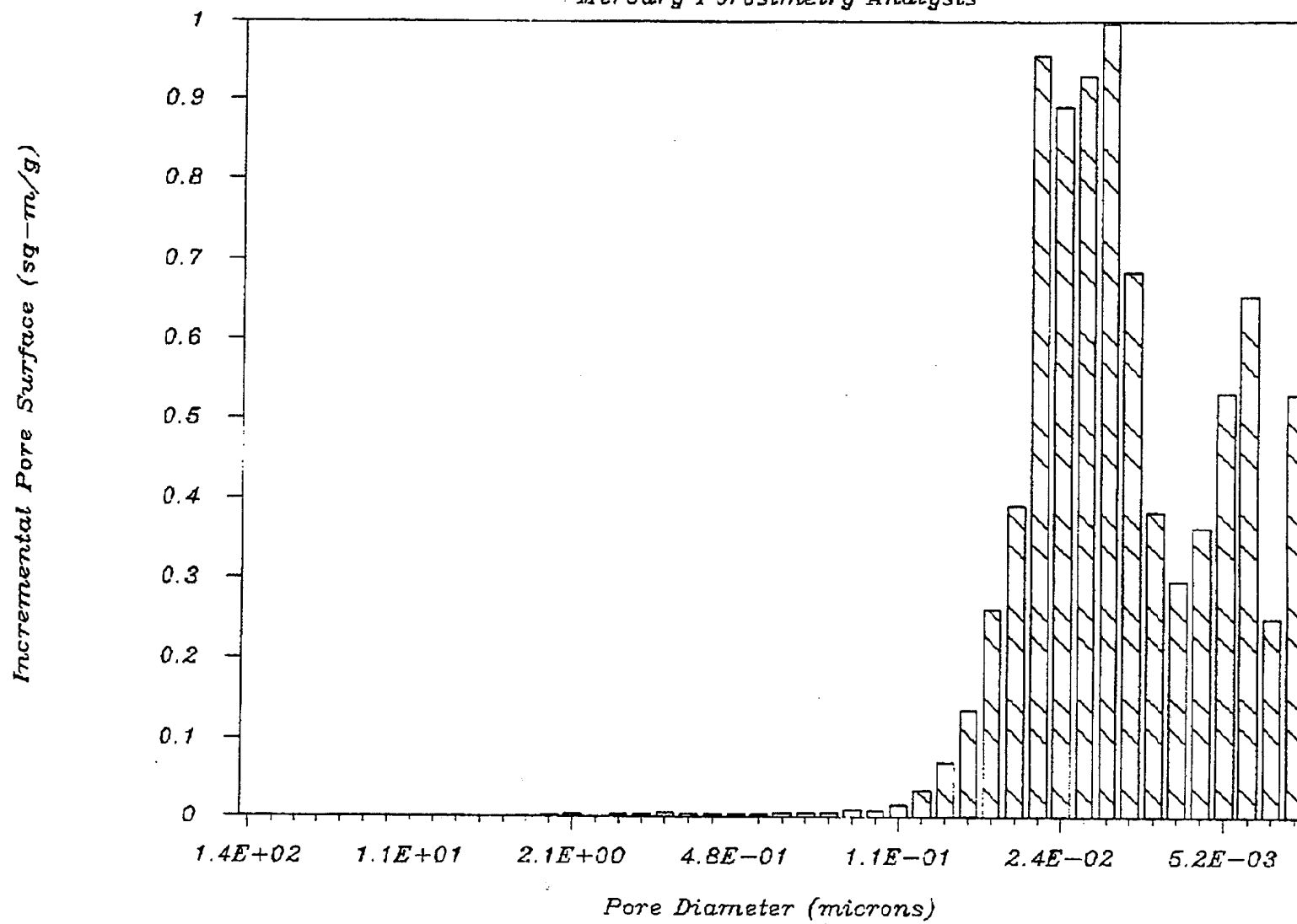
Wilder, D. G., W. Lin, S. Blair, T. Buscheck, R. Carlson, K. Lee, A. Meike, A. Ramirez, J. Wagoner, and J. Wang, Large Block test status report, UCRL-ID-128776, Lawrence Livermore Natl. Lab., Livermore, CA, 1997.

Appendix A

**Available Plots of
Incremental Pore Surface and
Incremental Pore Volume**

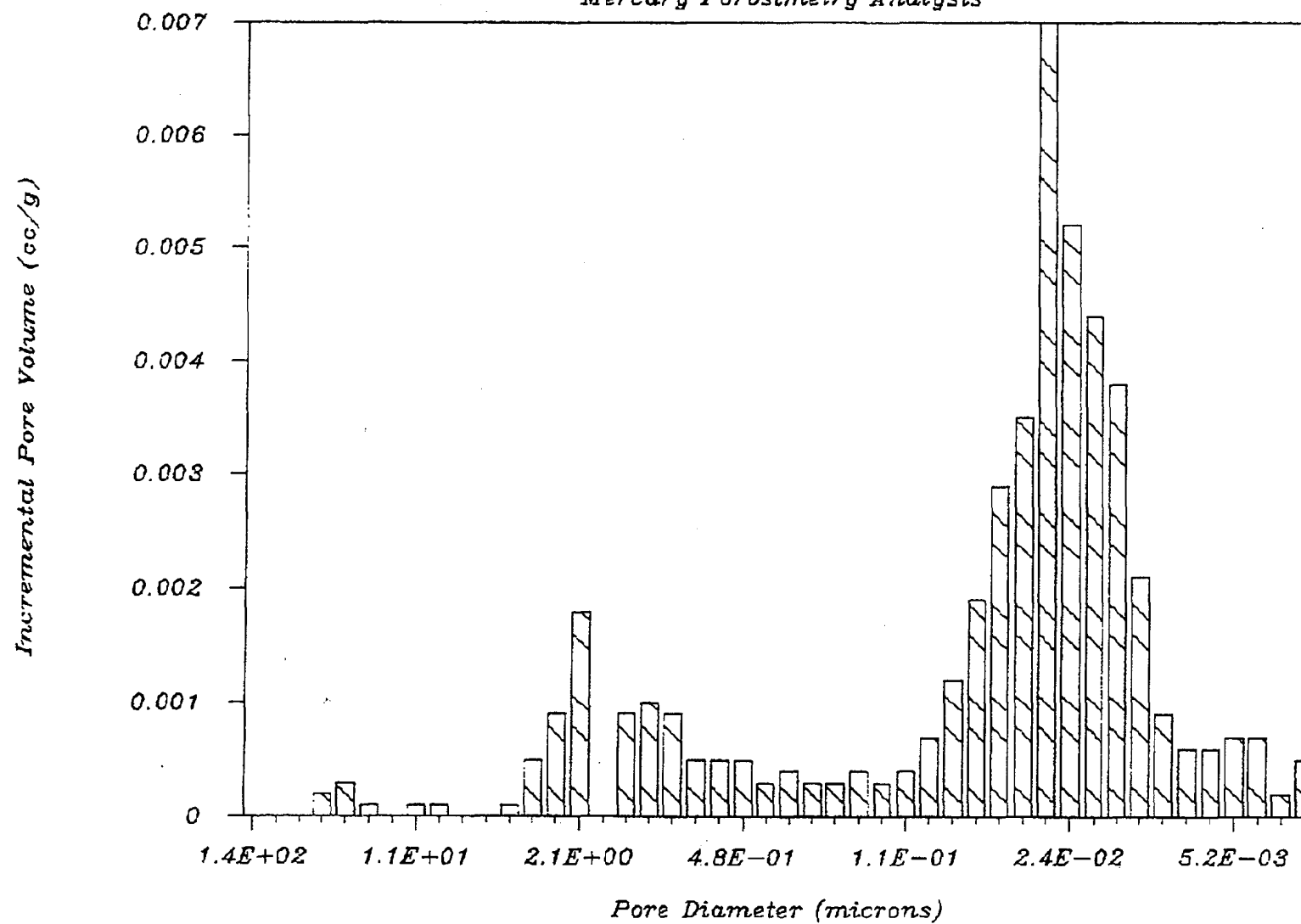
94047 32081.1-1 N1 11.0

Mercury Porosimetry Analysis



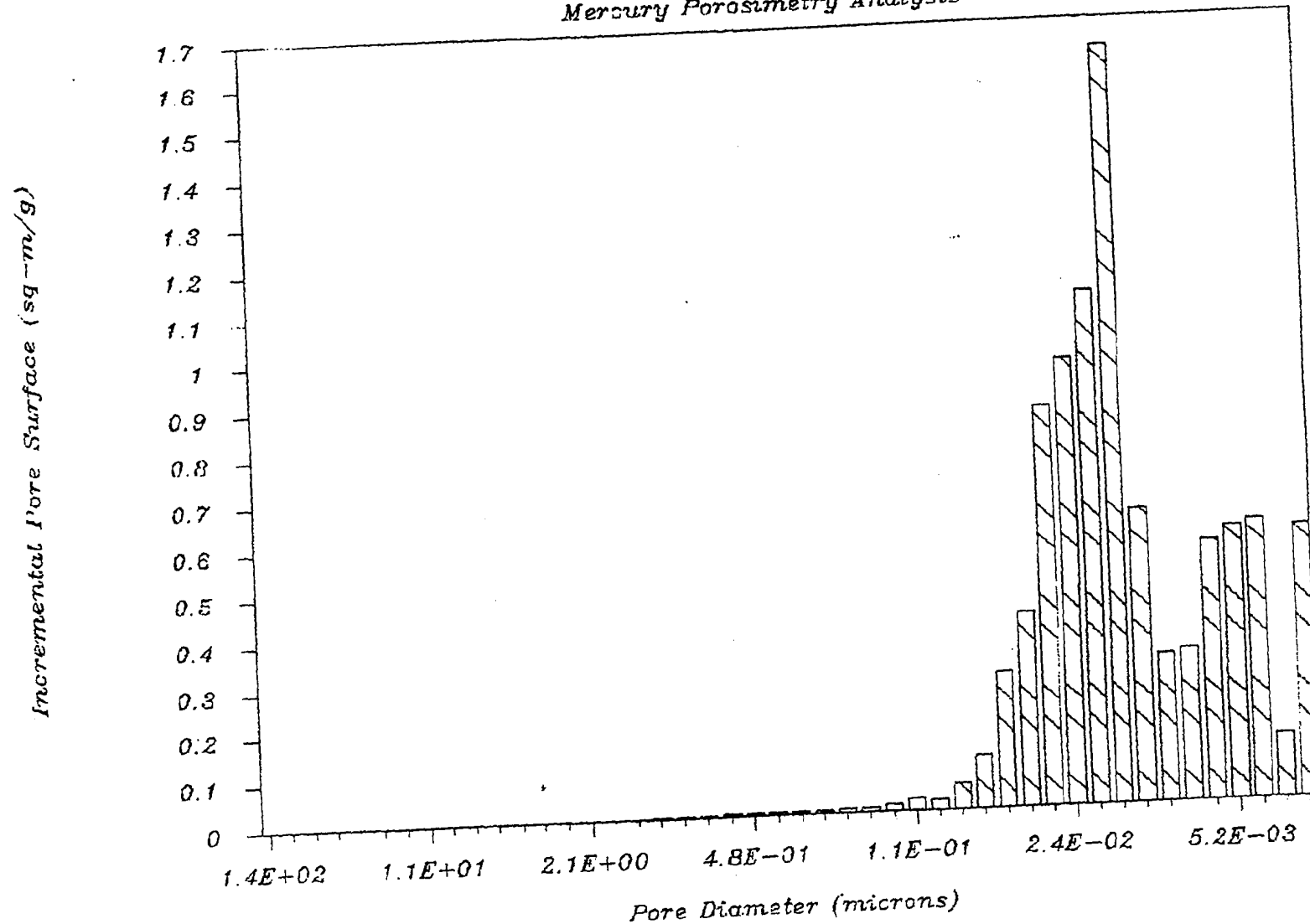
94047 32081.1-1 N1 11.0

Mercury Porosimetry Analysis



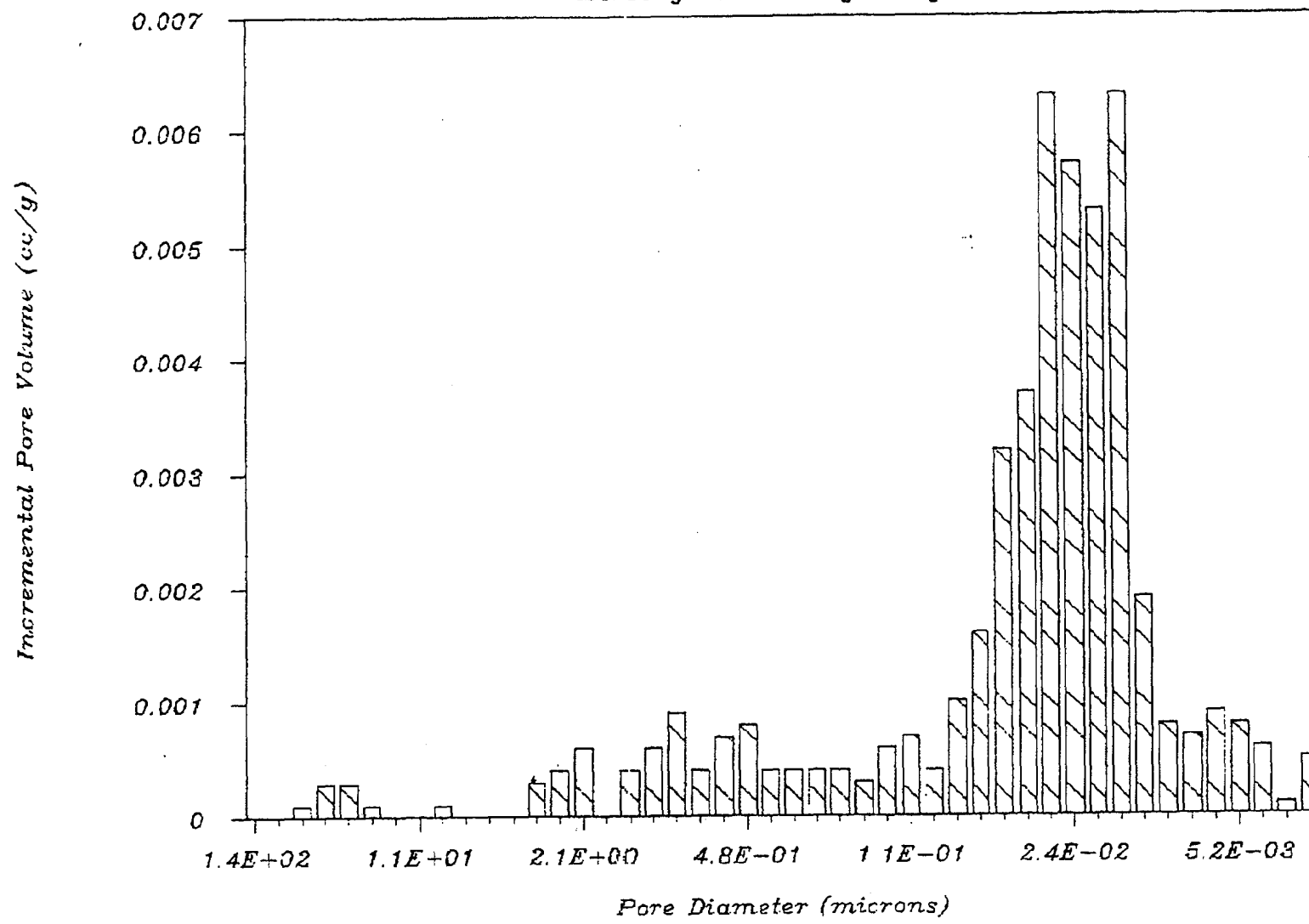
94050 32082.1-1 N1 13.4

Mercury Porosimetry Analysis



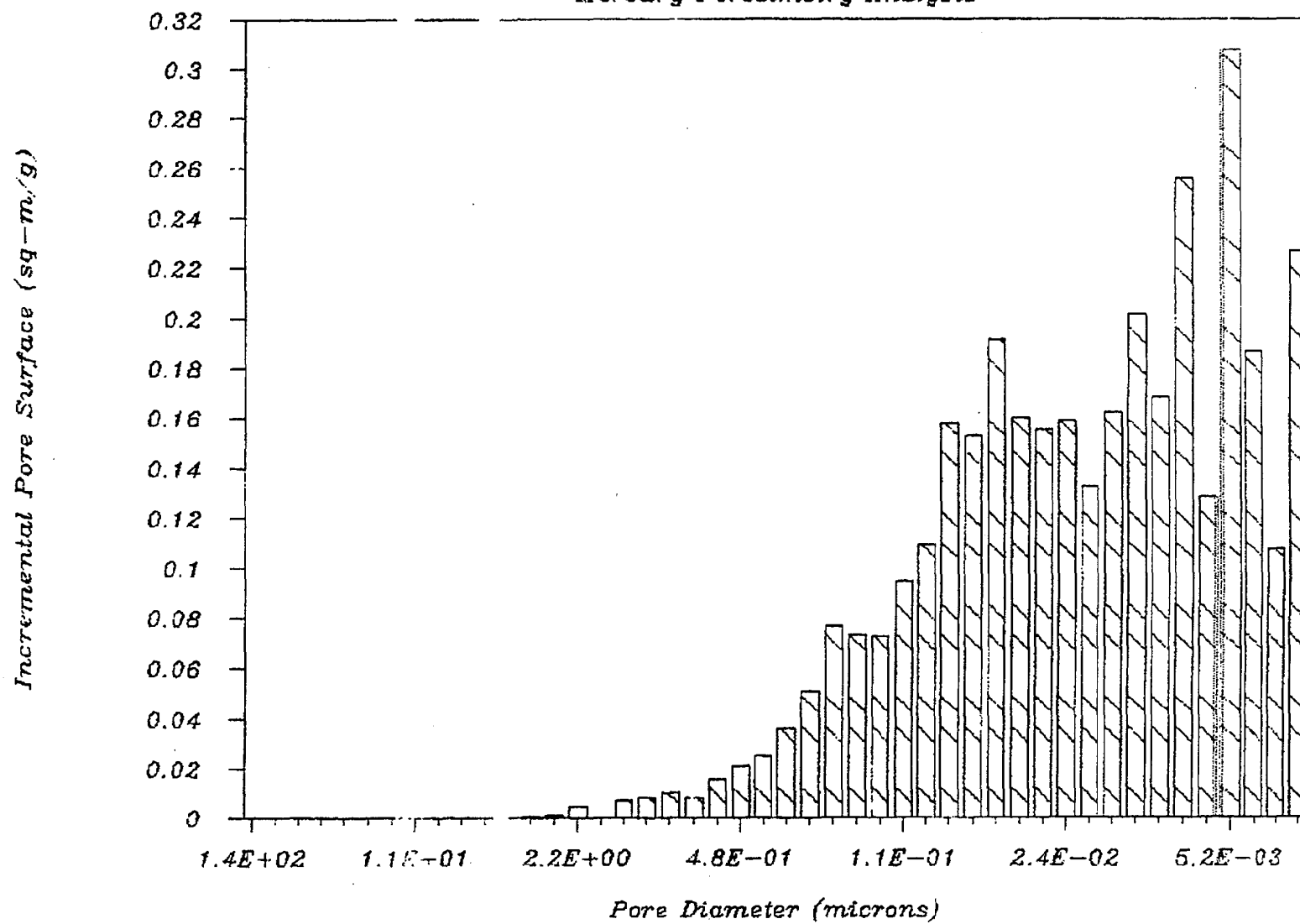
94050 32082.1-1 N1 13.4

Mercury Porosimetry Analysis



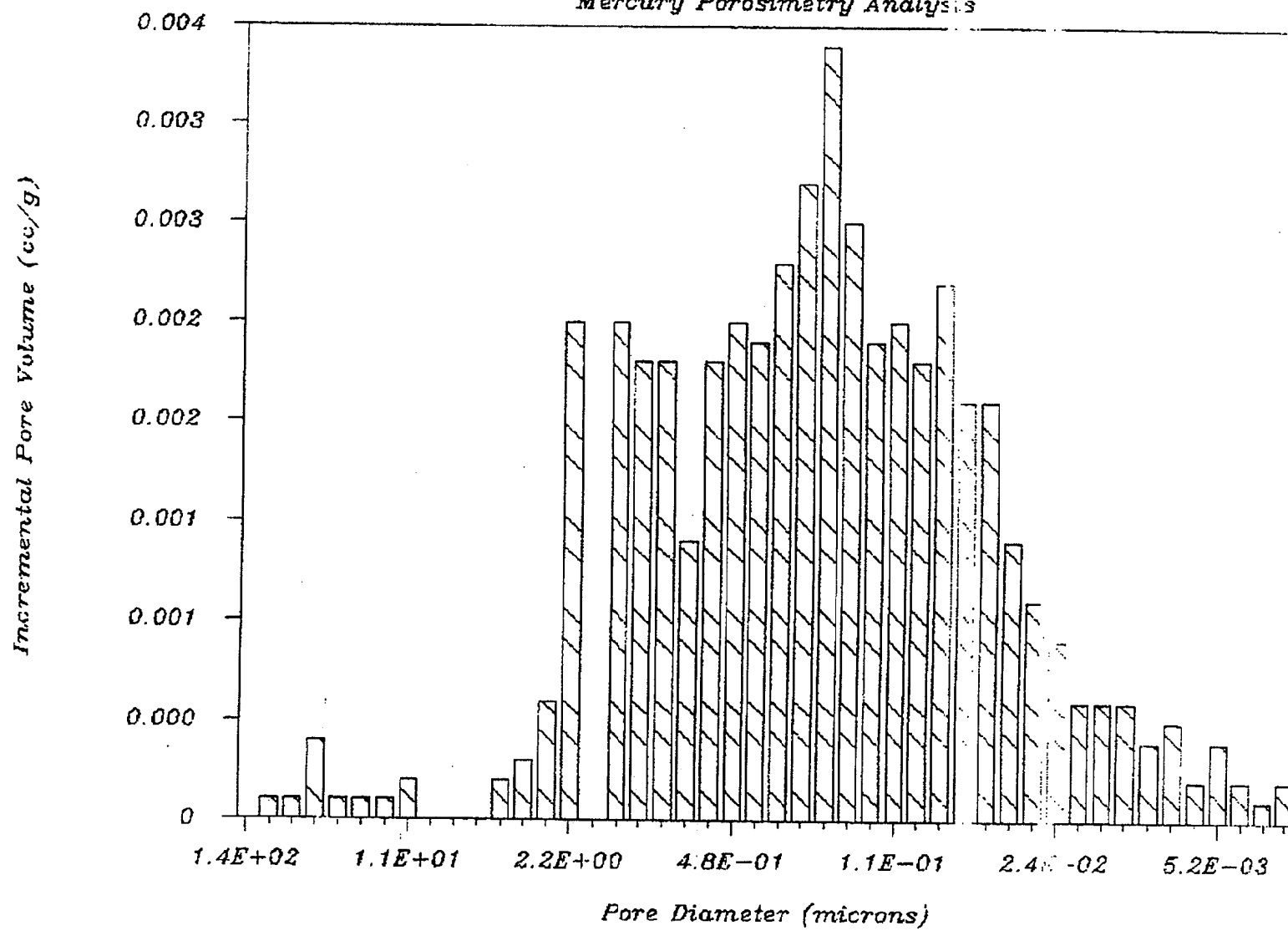
94030 32083.1 N1 16.9

Mercury Porosimetry Analysis



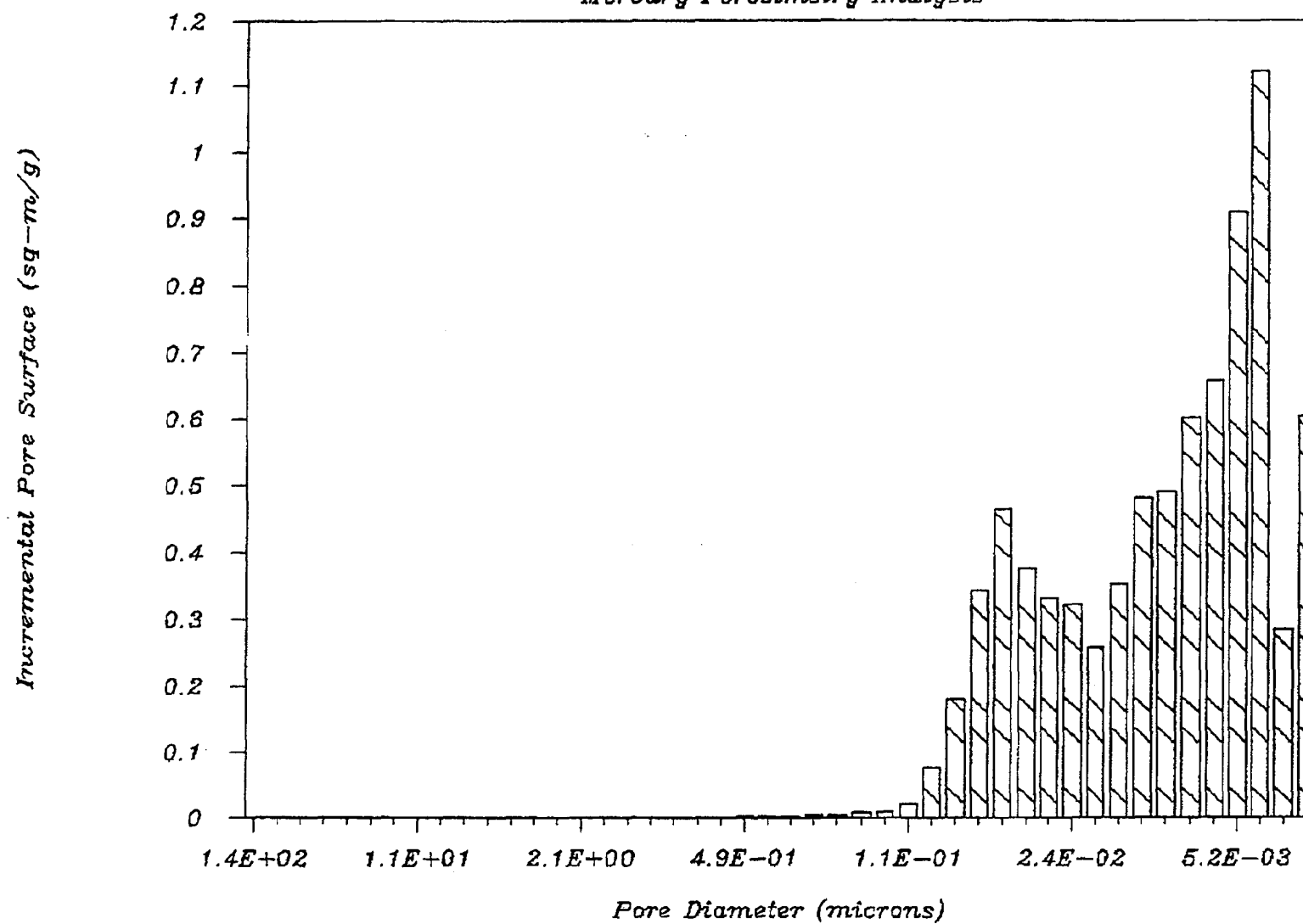
94030 32083.1 N1 16.9

Mercury Porosimetry Analysis



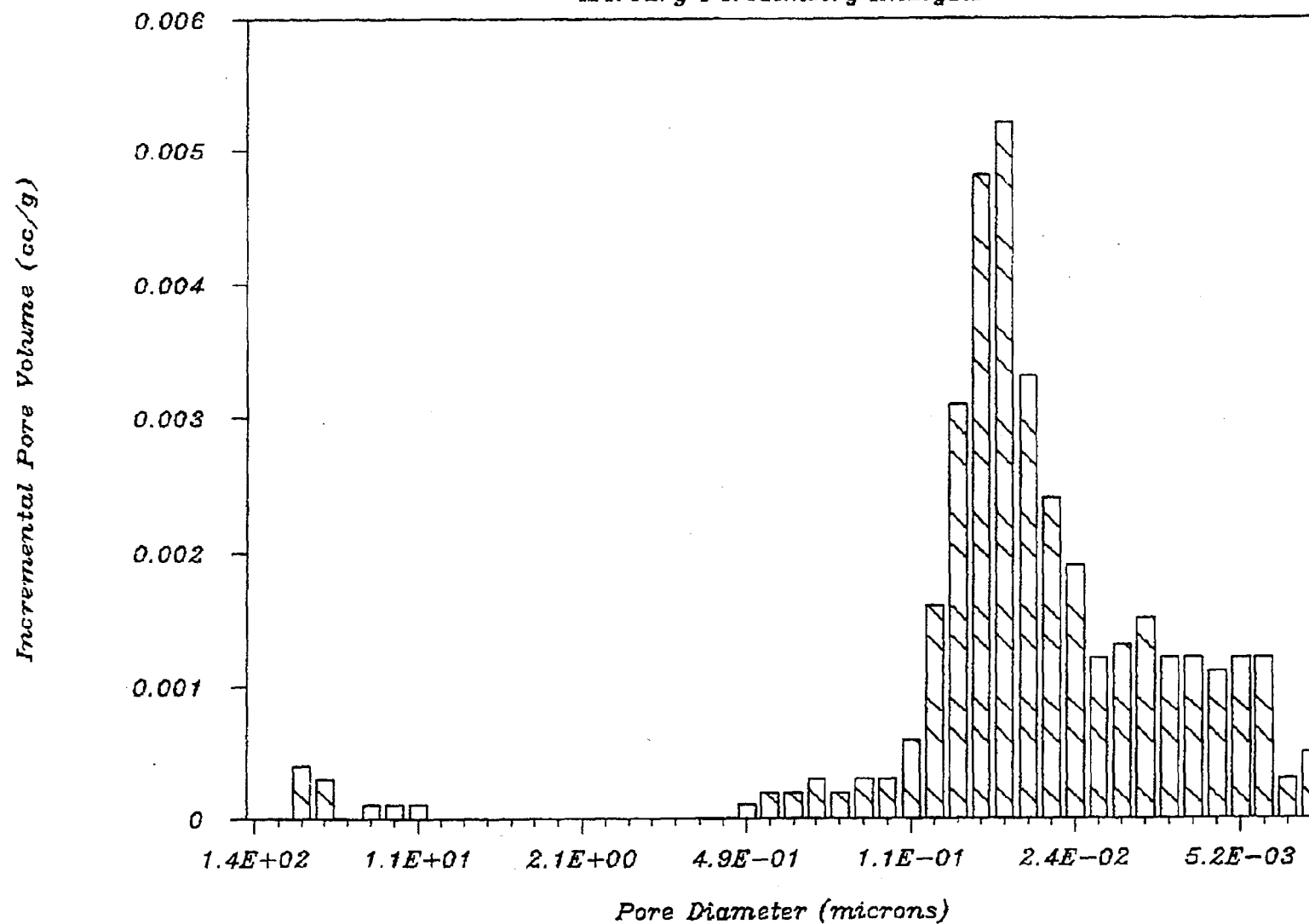
94052 32086.1 N2 4.3

Mercury Porosimetry Analysis



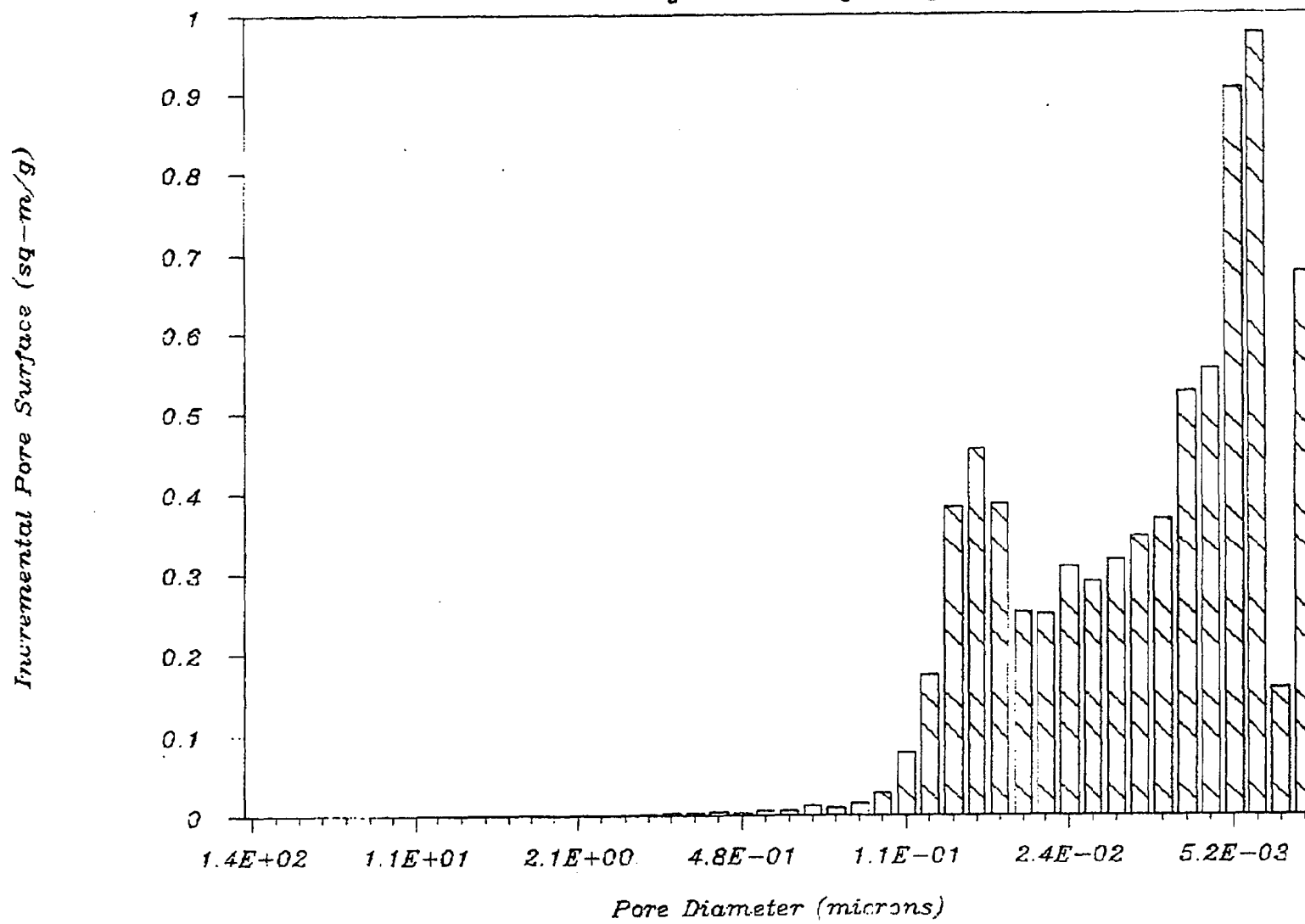
94052 32086.1 N2 4.3

Mercury Porosimetry Analysis



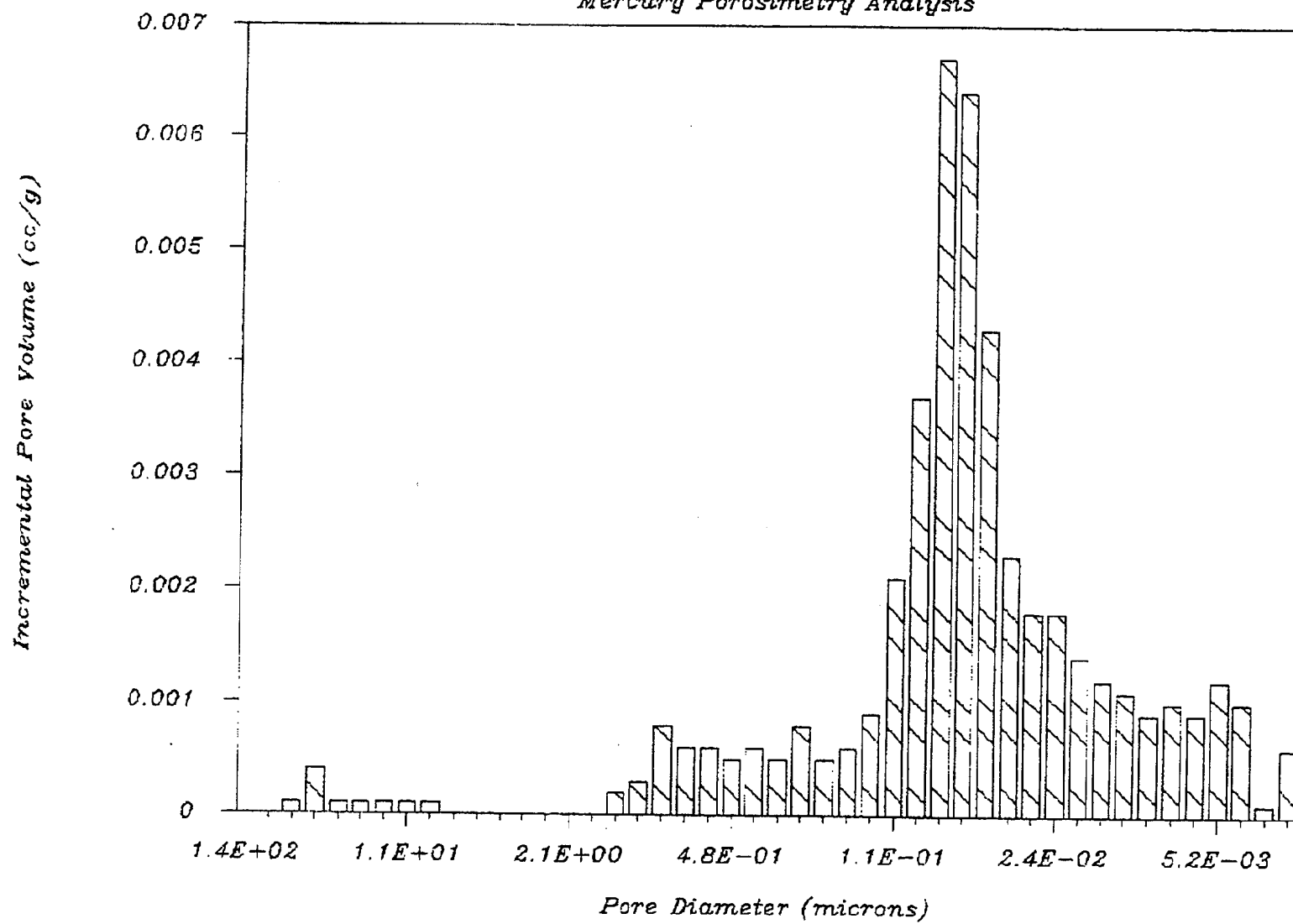
94056 32089.1 N2 11.1

Mercury Porosimetry Analysis



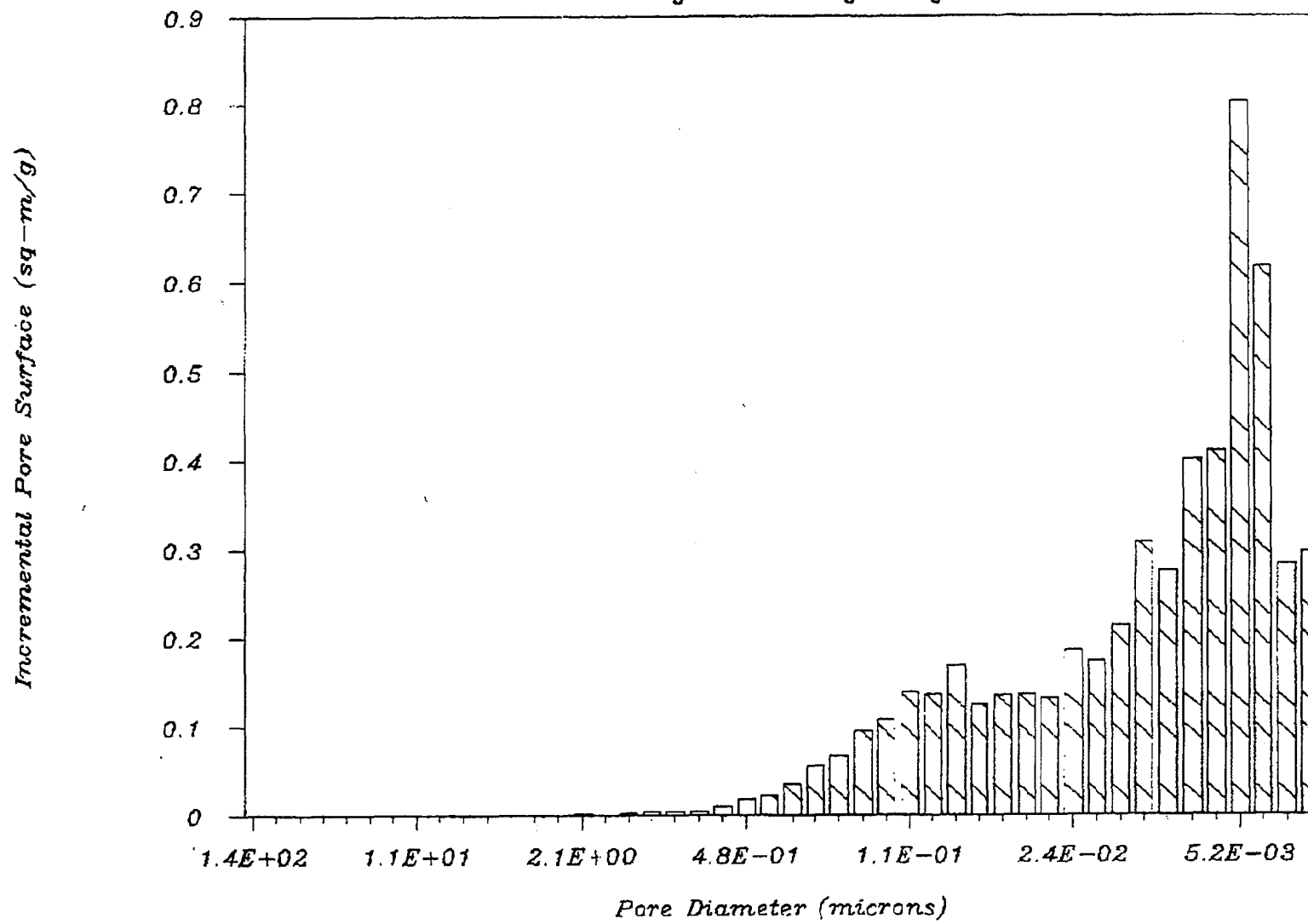
94056 32089.1 N2 11.1

Mercury Porosimetry Analysis



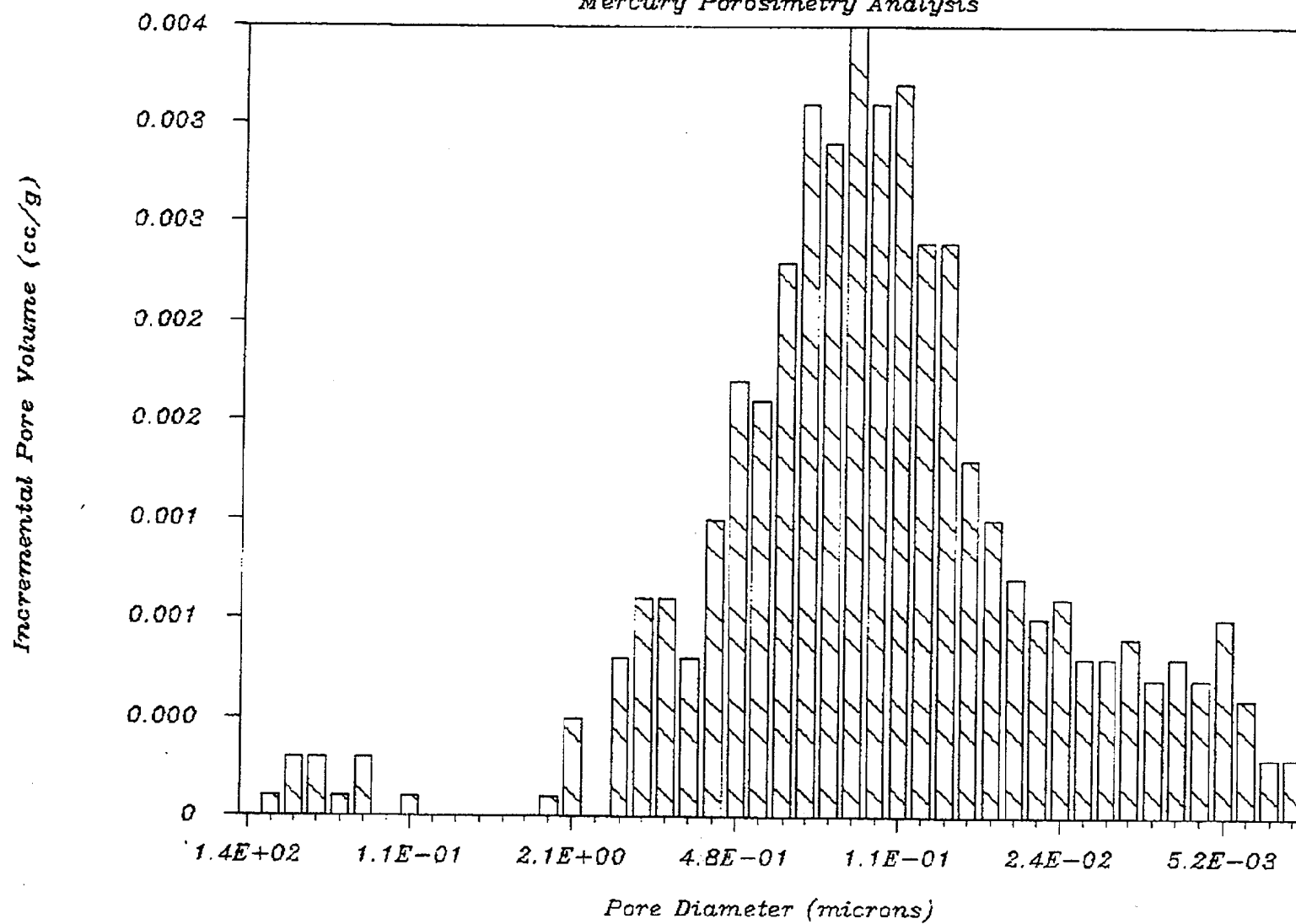
94061 32089.1 N2 11.25

Mercury Porosimetry Analysis



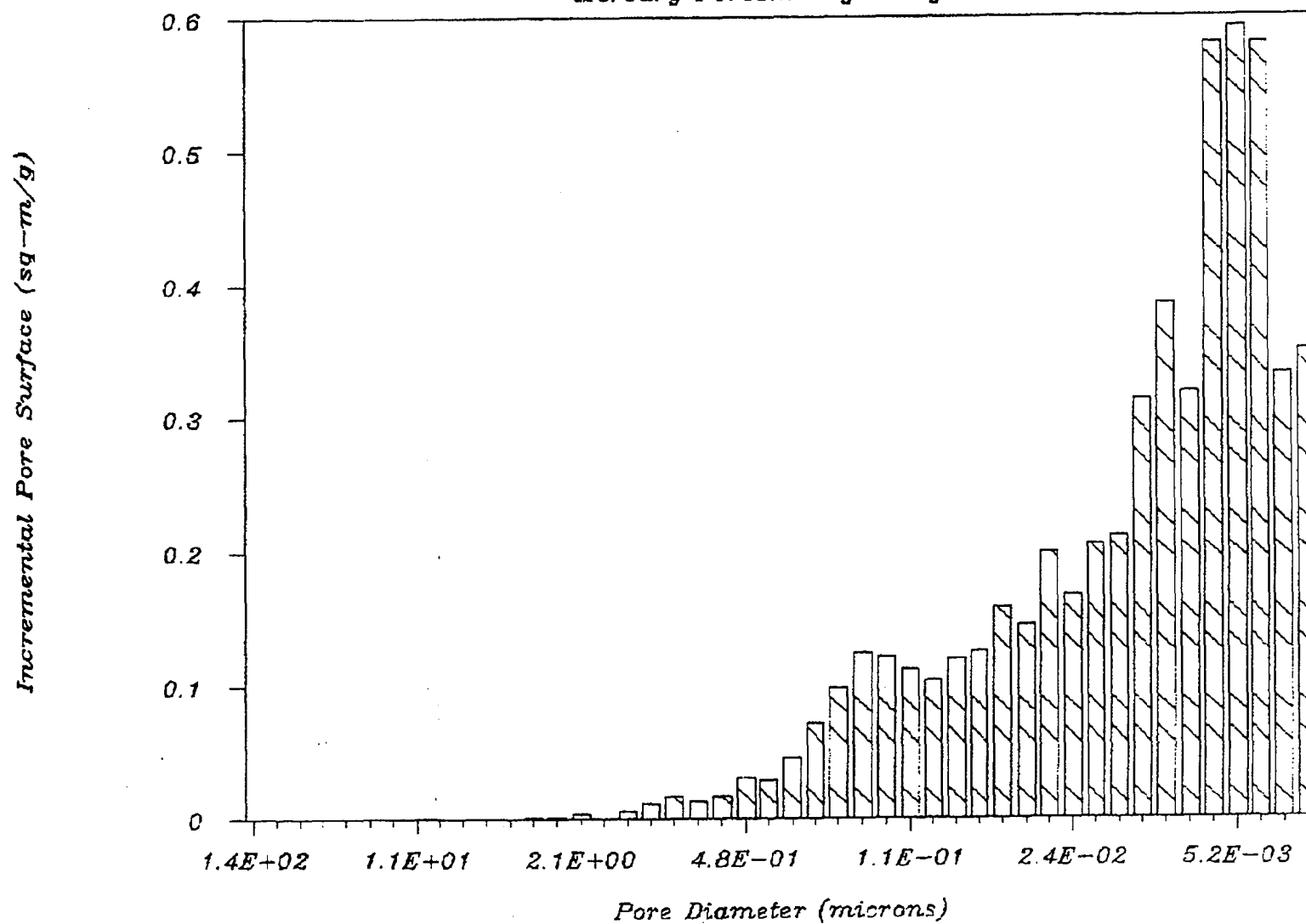
94061 32089.1 N2 11.25

Mercury Porosimetry Analysis



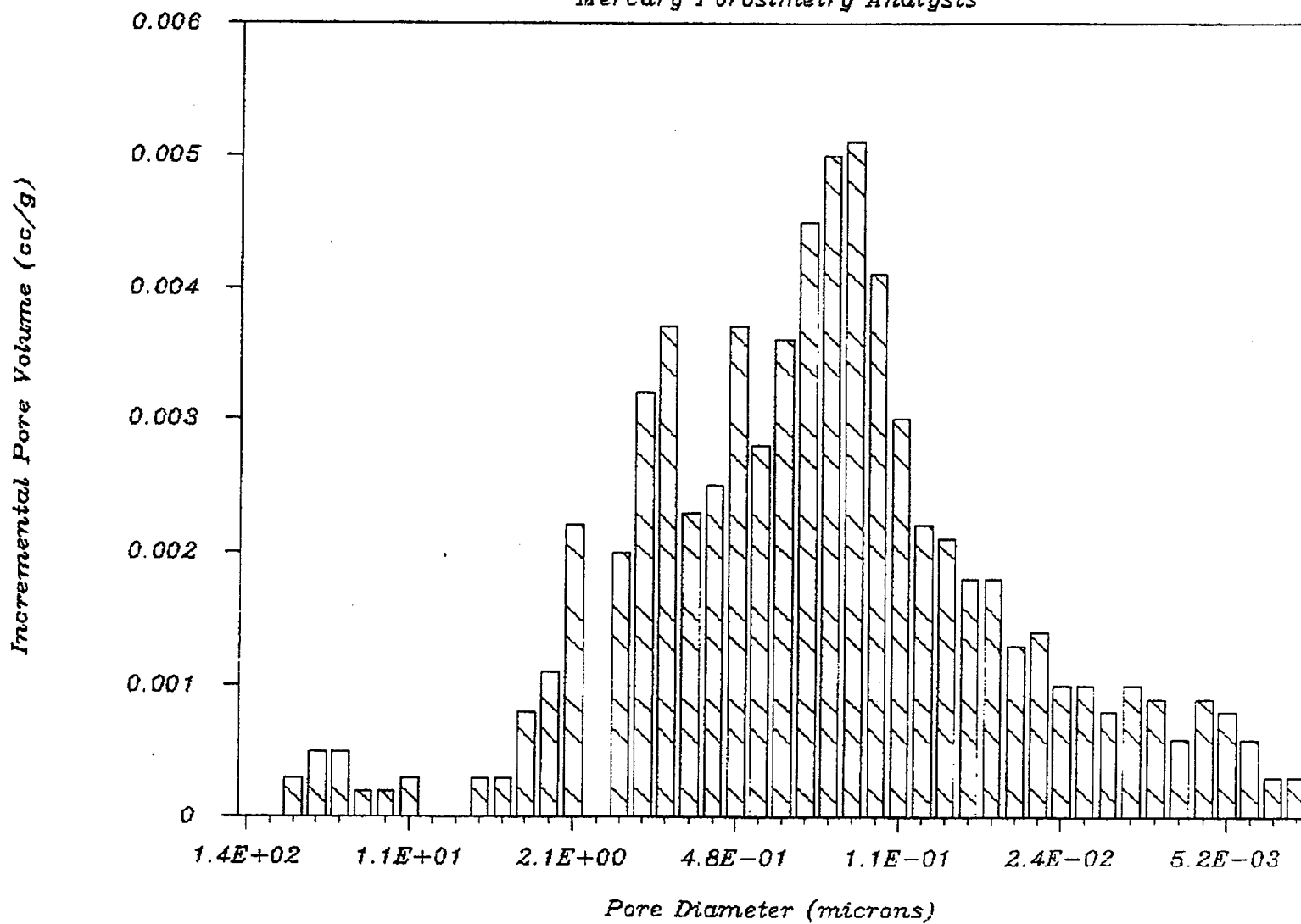
94048 32091.1 N2 13.9

Mercury Porosimetry Analysis



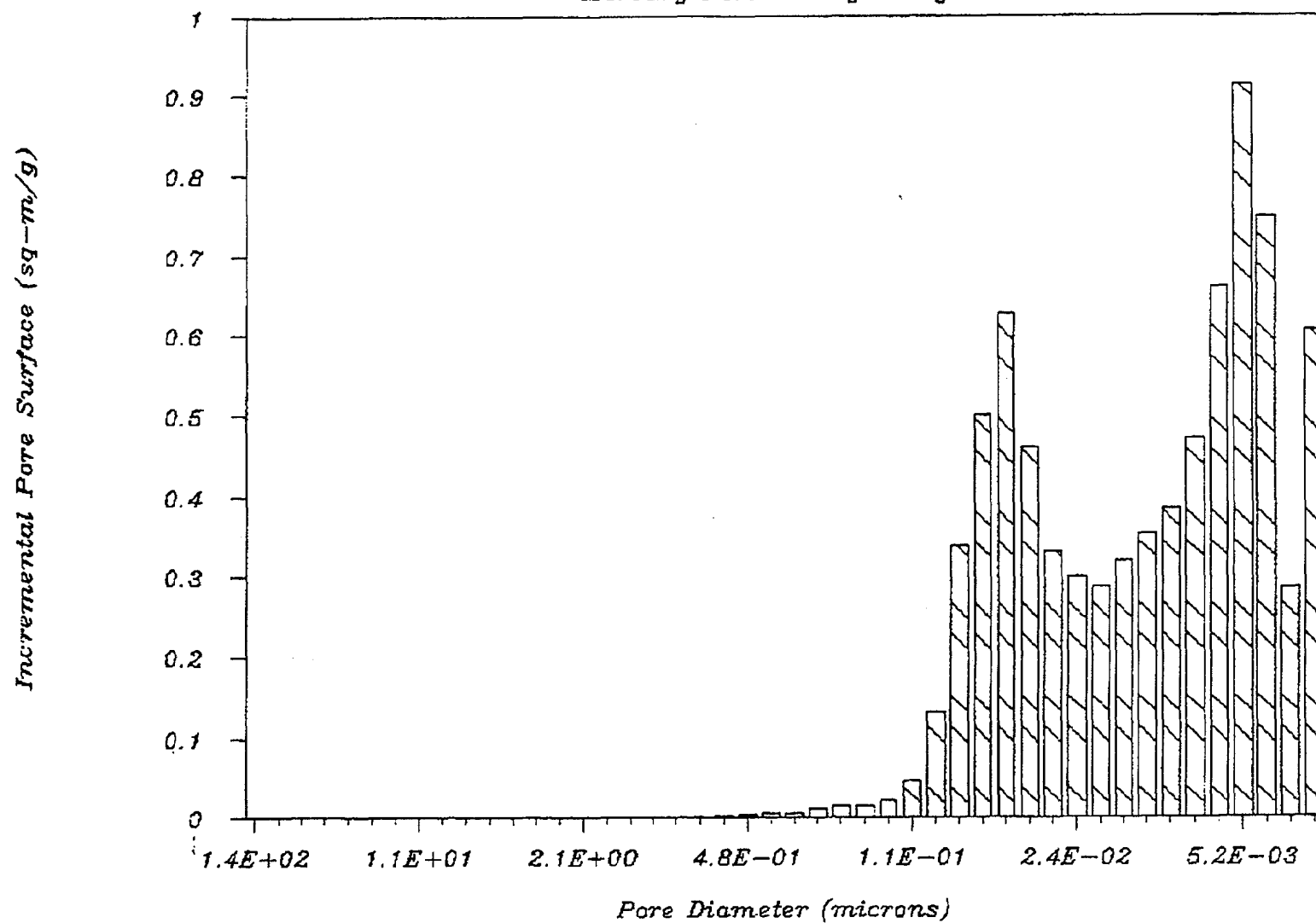
94048 32091.1 N2 13.9

Mercury Porosimetry Analysis



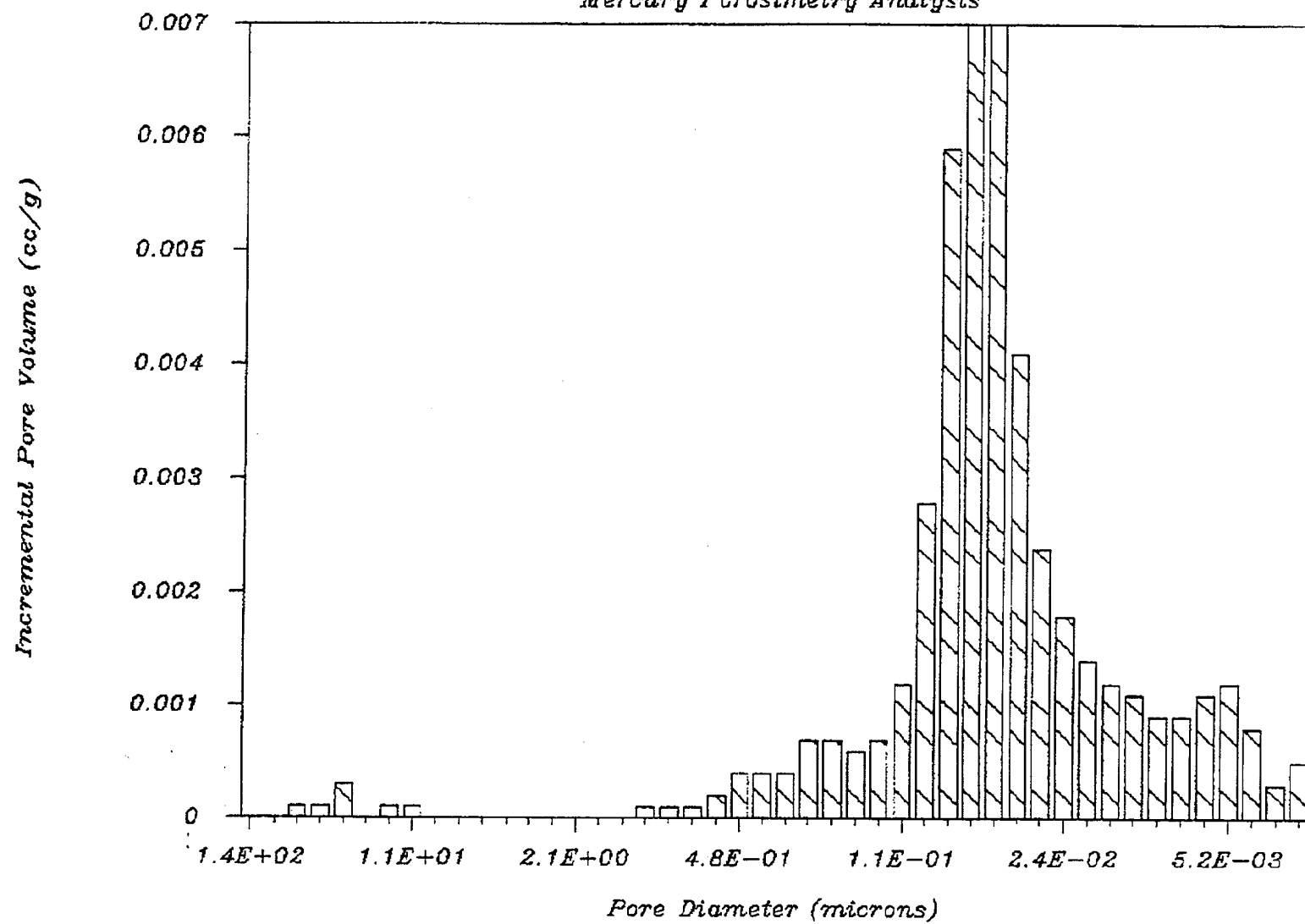
94060 32093.1 N2 19.2

Mercury Porosimetry Analysis



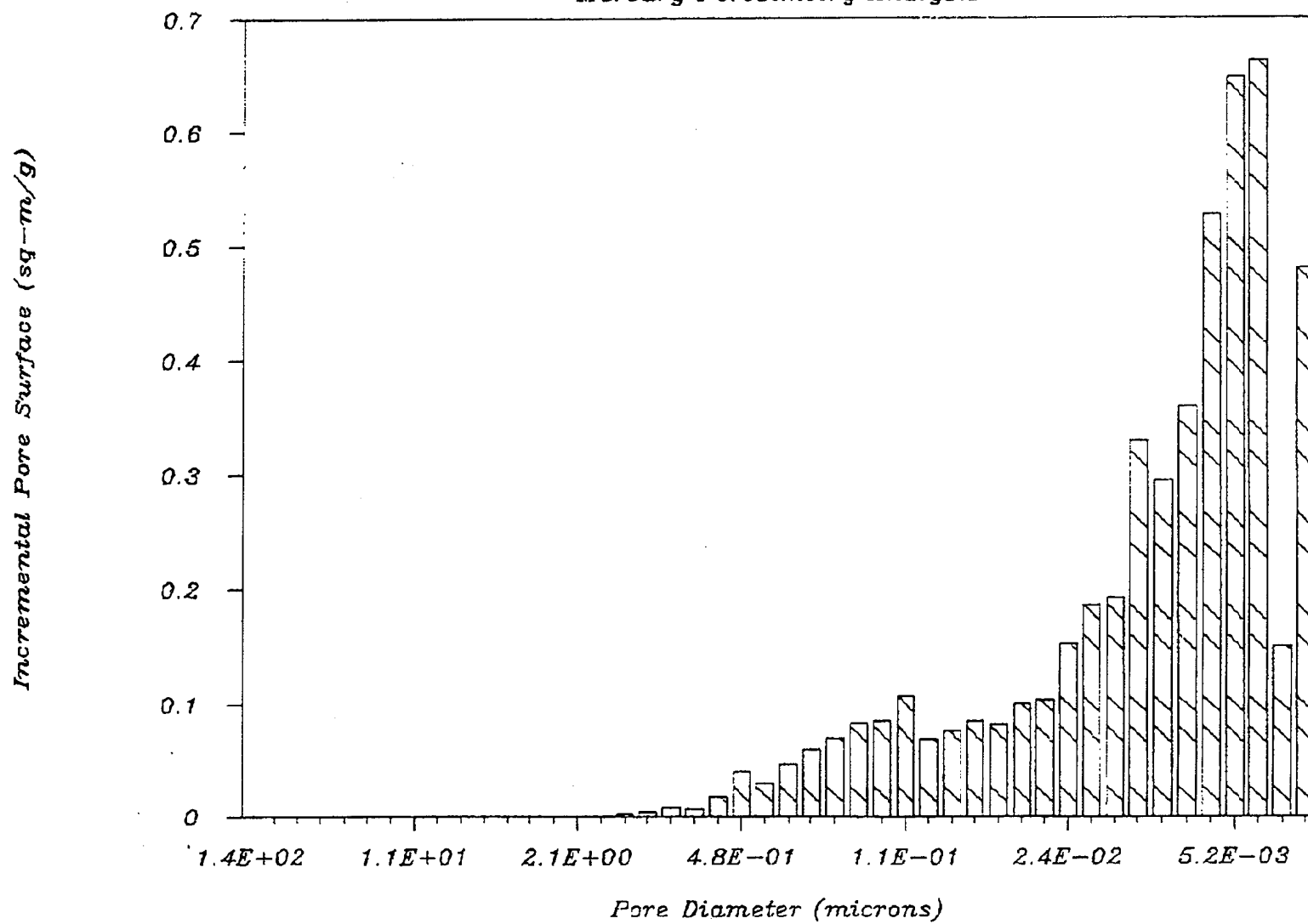
94060 32093.1 N2 19.2

Mercury Porosimetry Analysis



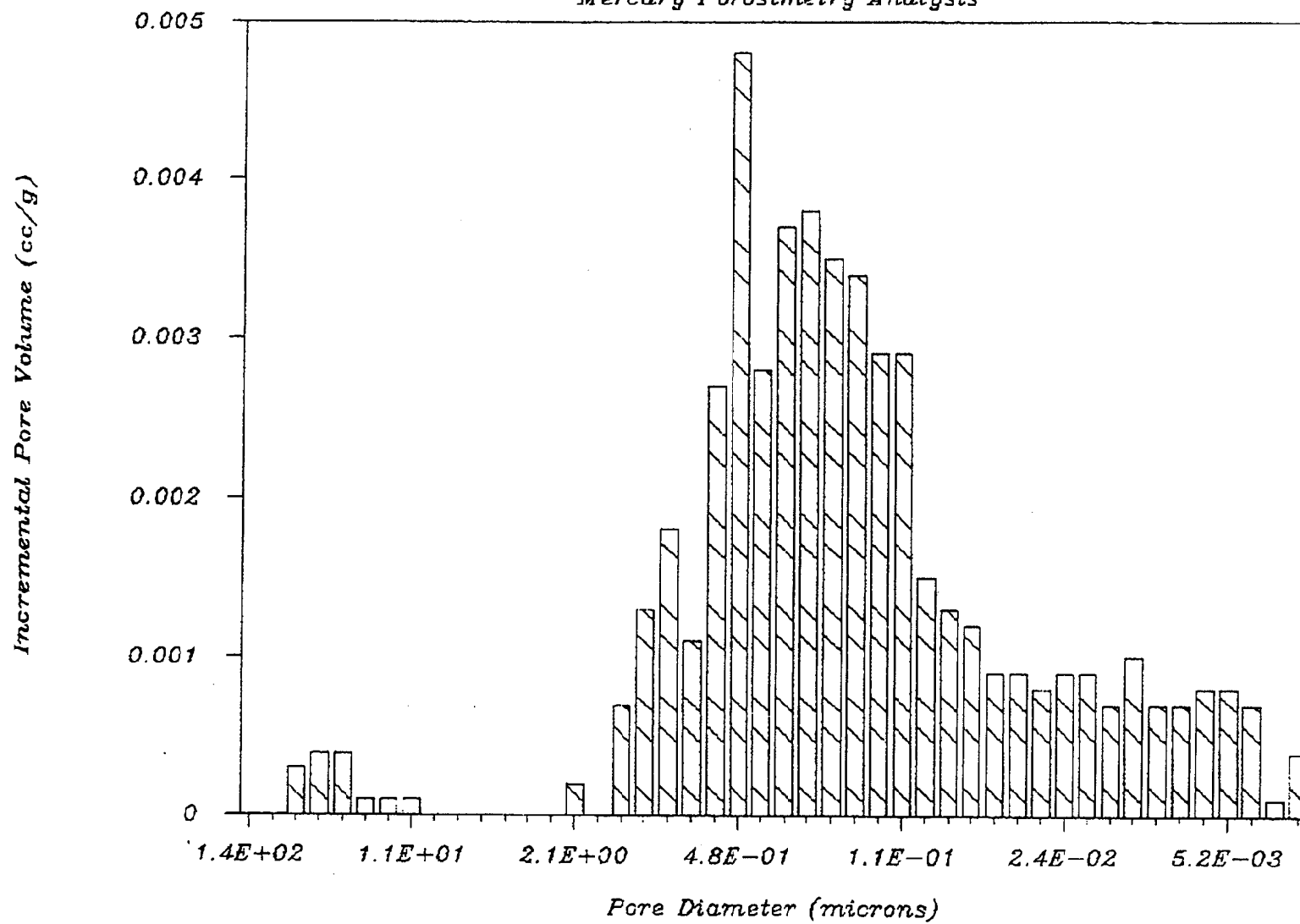
94063 32095.1 N3 4.5

Mercury Porosimetry Analysis



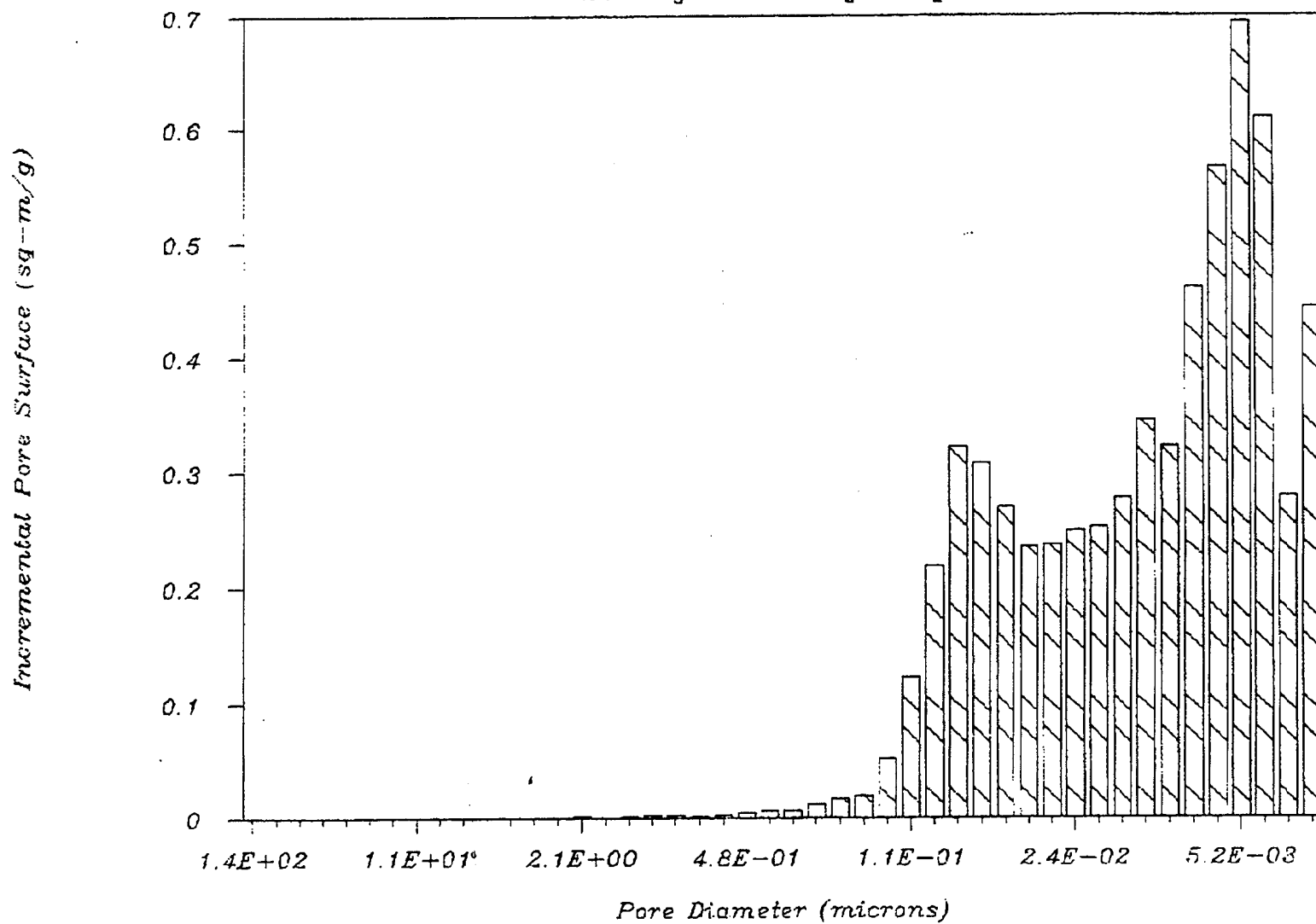
94063 32095.1 N3 4.5

Mercury Porosimetry Analysis



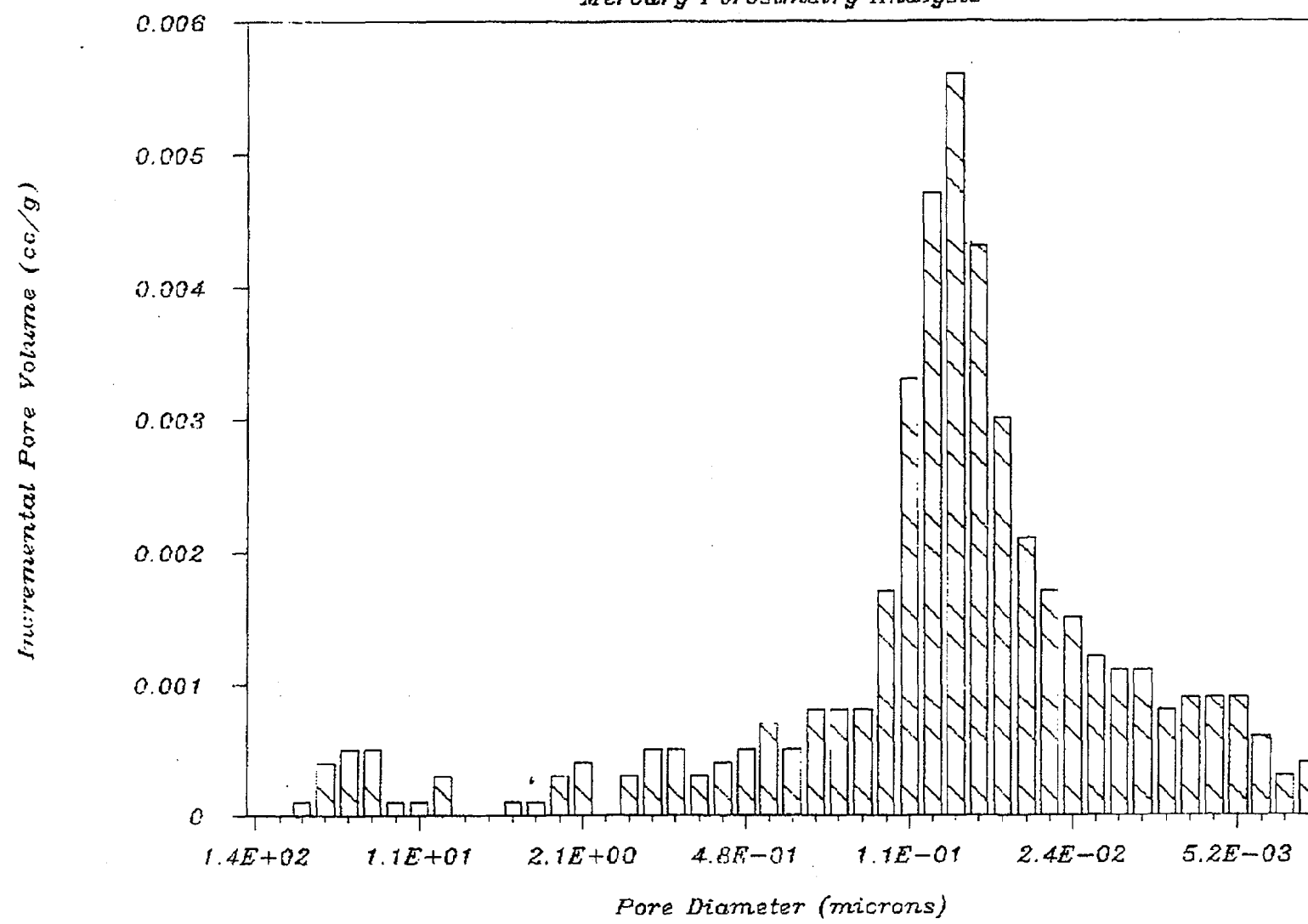
94049 32095.1 N3 4.75

Mercury Porosimetry Analysis



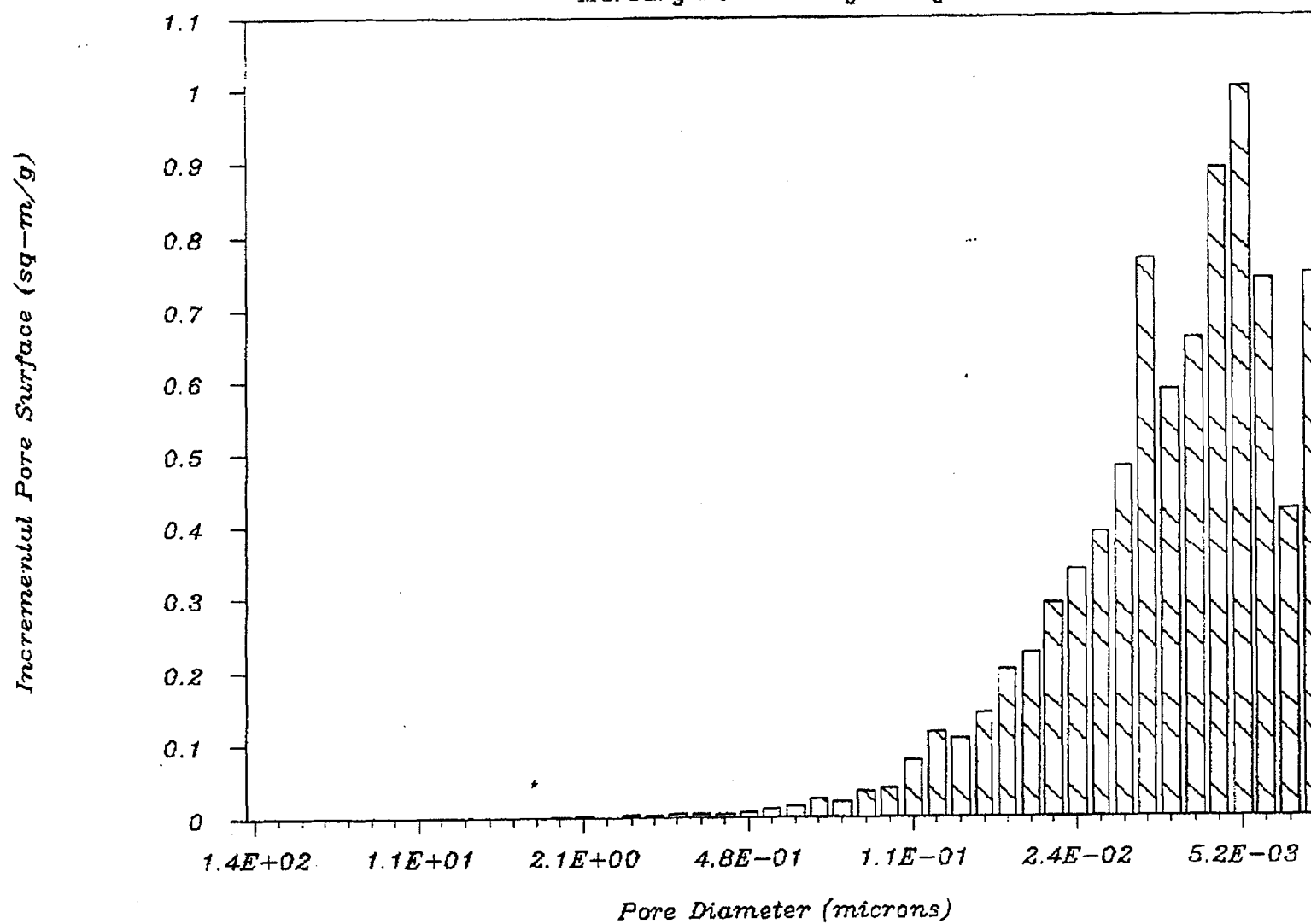
94049 32095.1 N3 4.75

Mercury Porosimetry Analysis



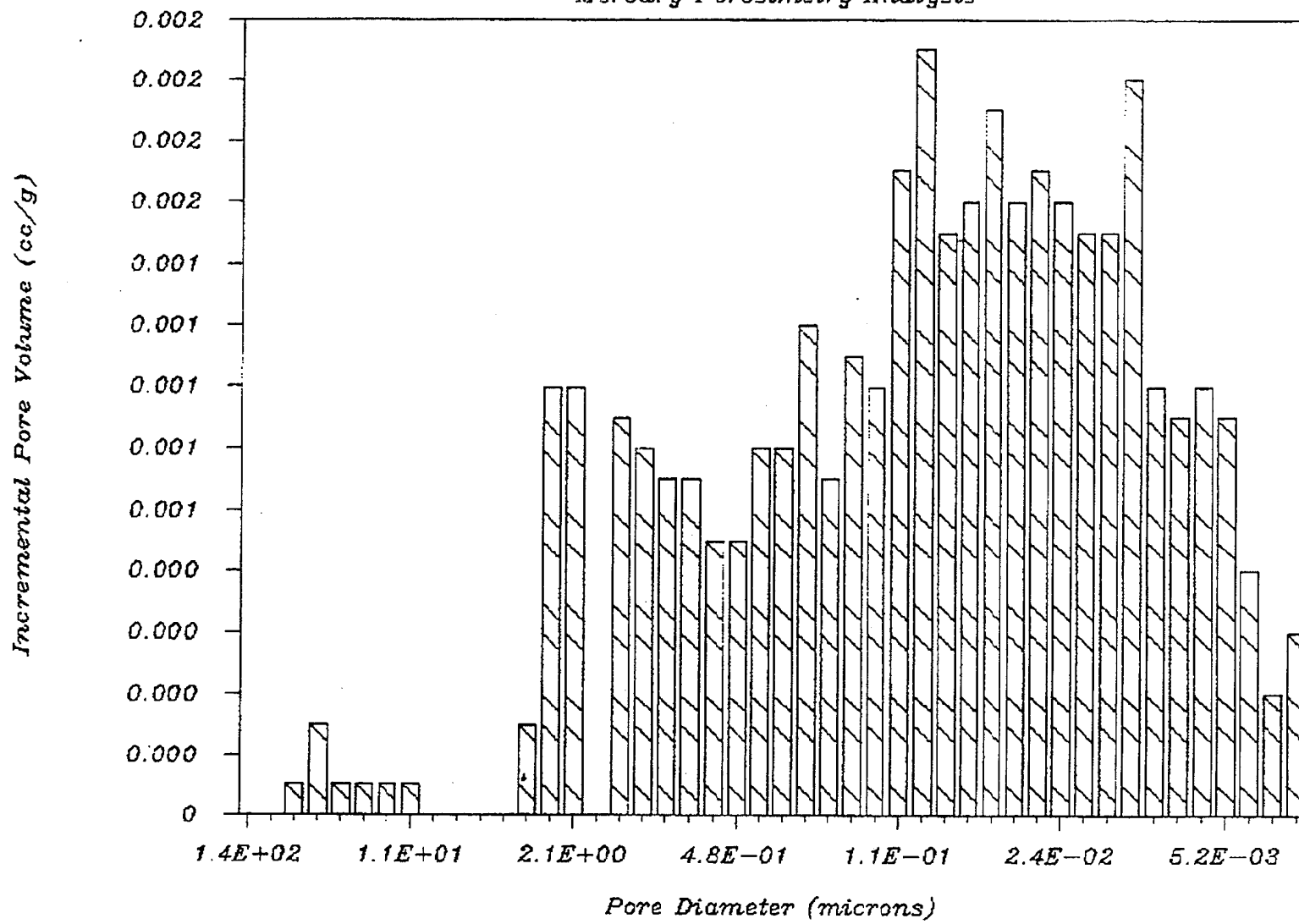
94051 34063.1 N3 11.0

Mercury Porosimetry Analysis



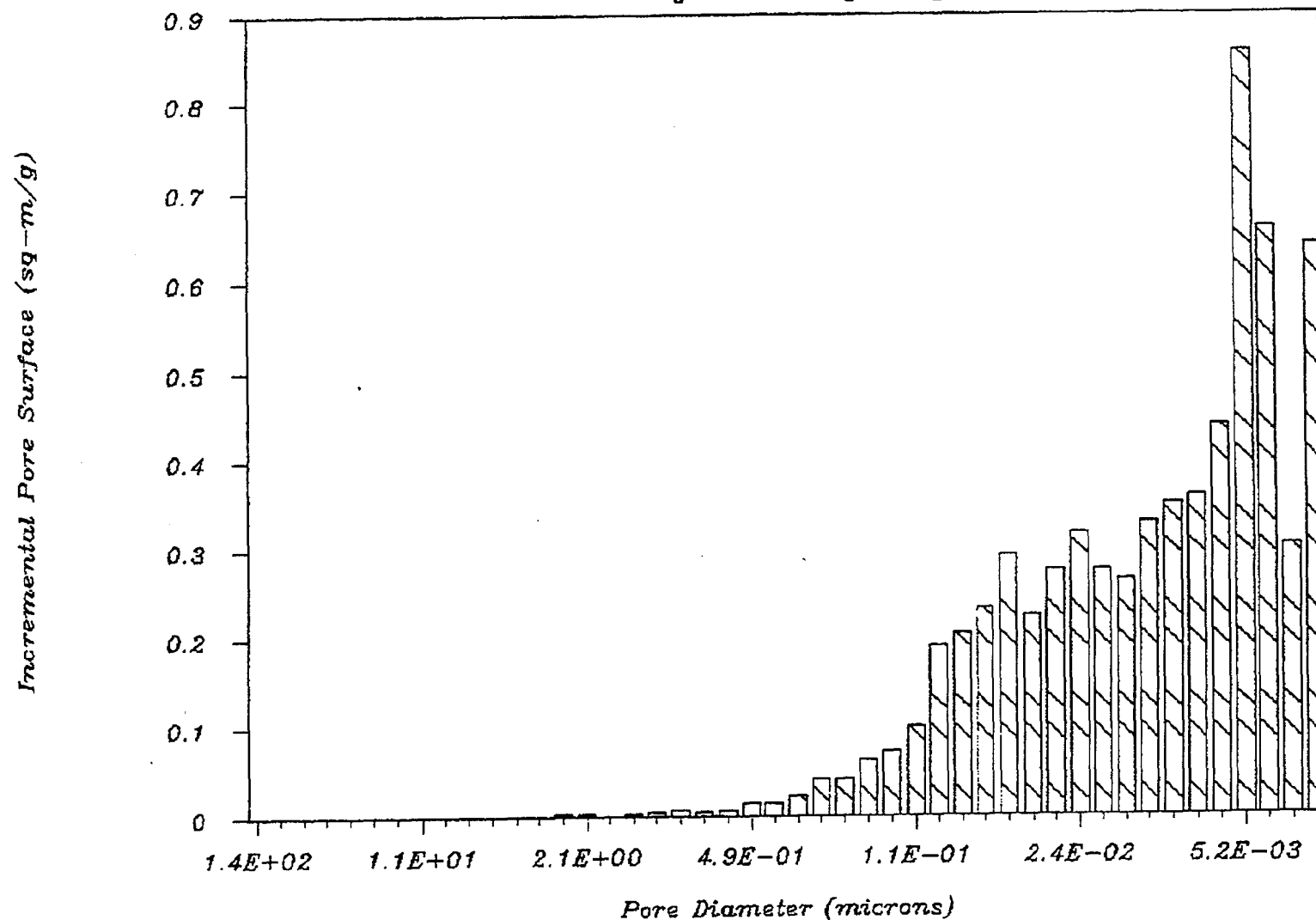
94051 34063.1 N3 11.0

Mercury Porosimetry Analysis



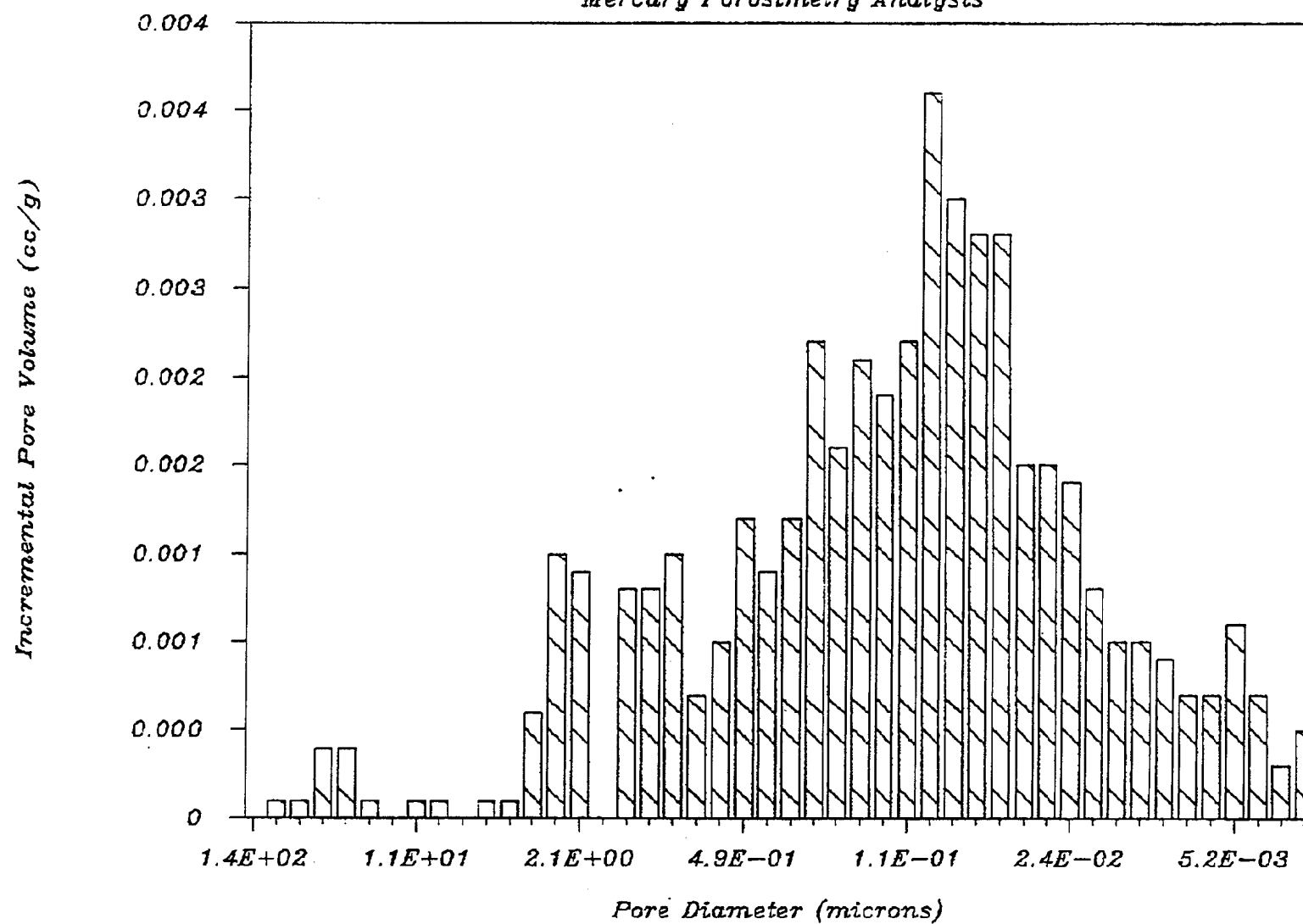
94053 32099.1 N3 15.2

Mercury Porosimetry Analysis



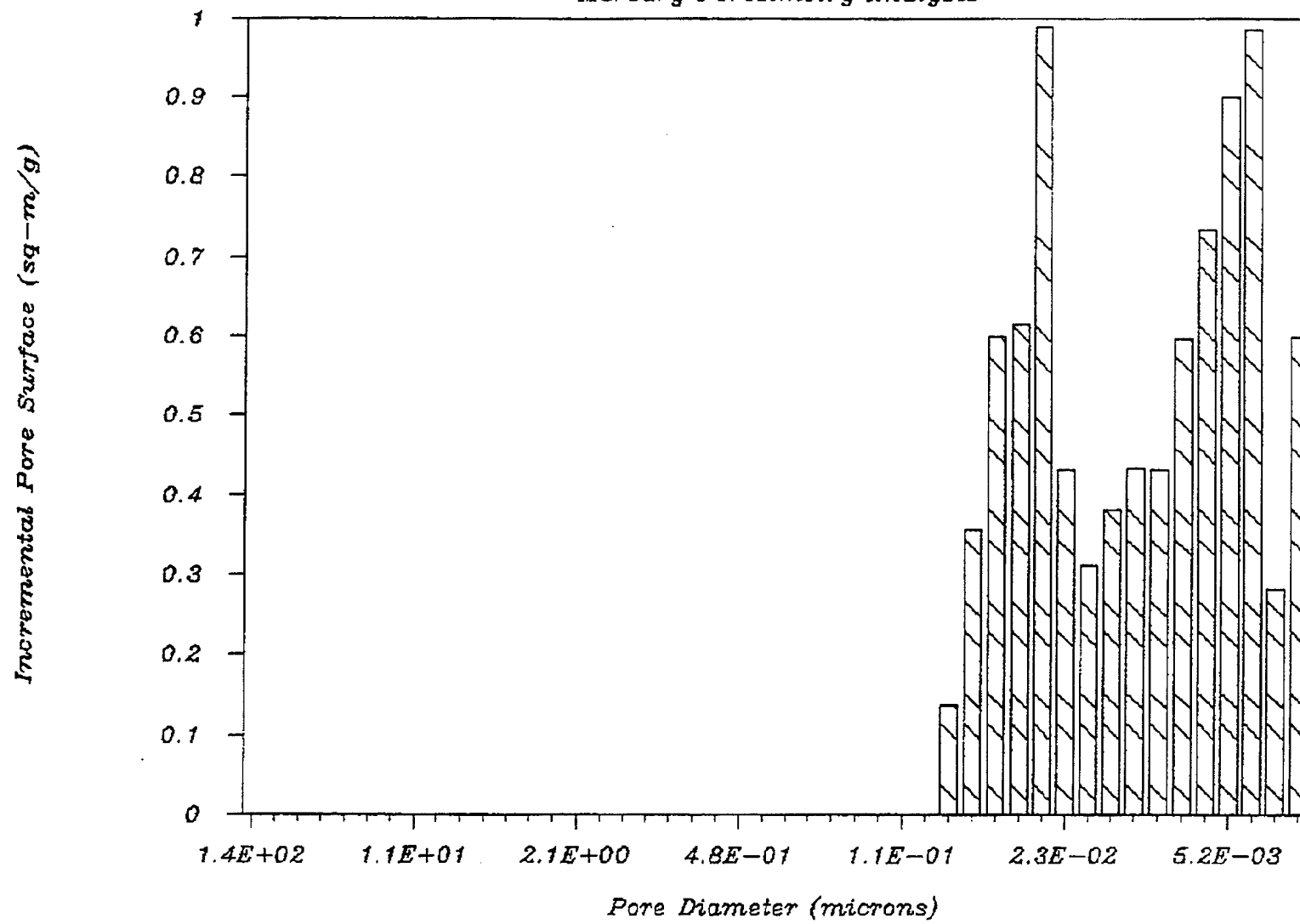
94053 32099.1 N3 15.2

Mercury Porosimetry Analysis



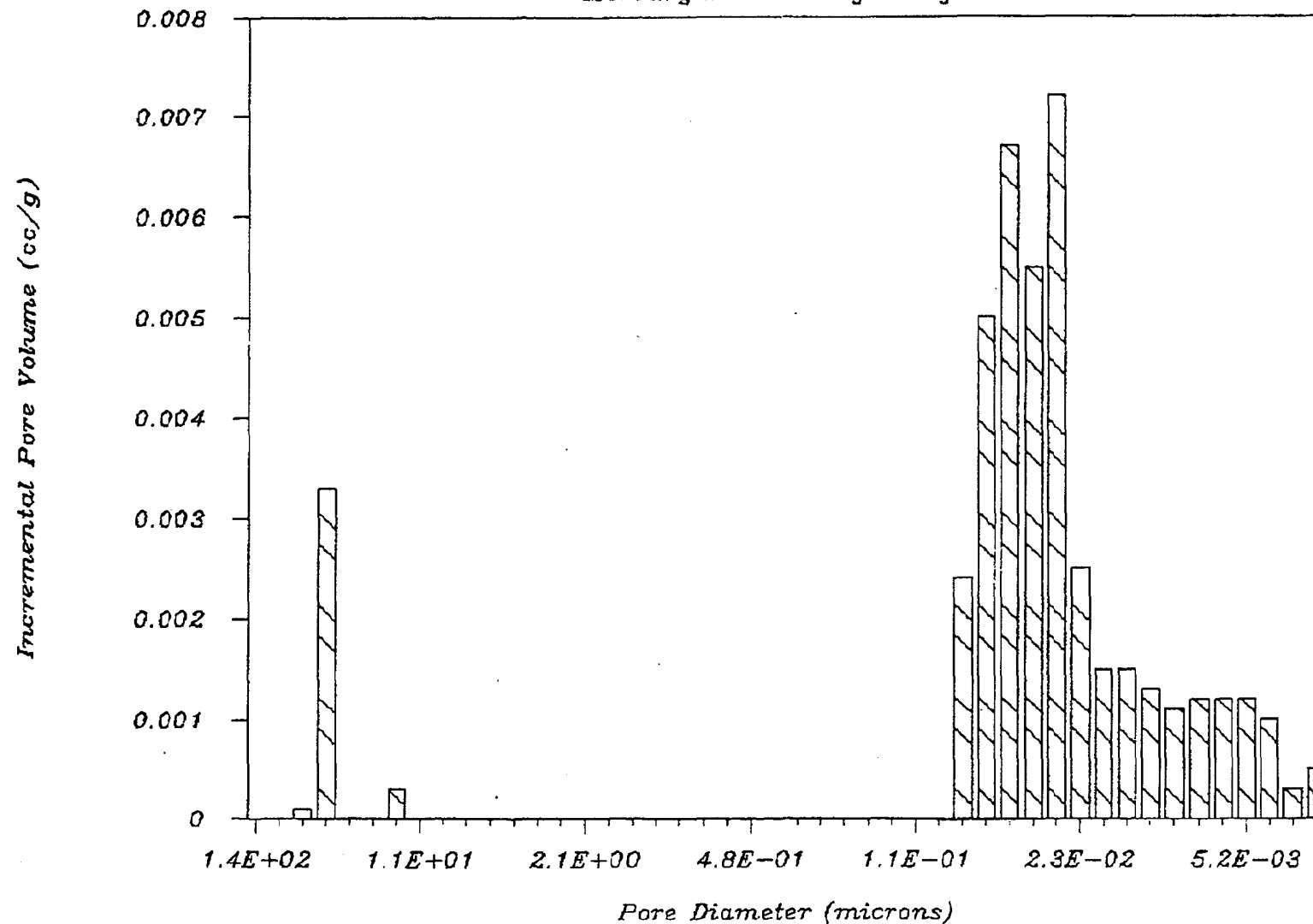
94057 32101.1 N3 20.4

Mercury Porosimetry Analysis



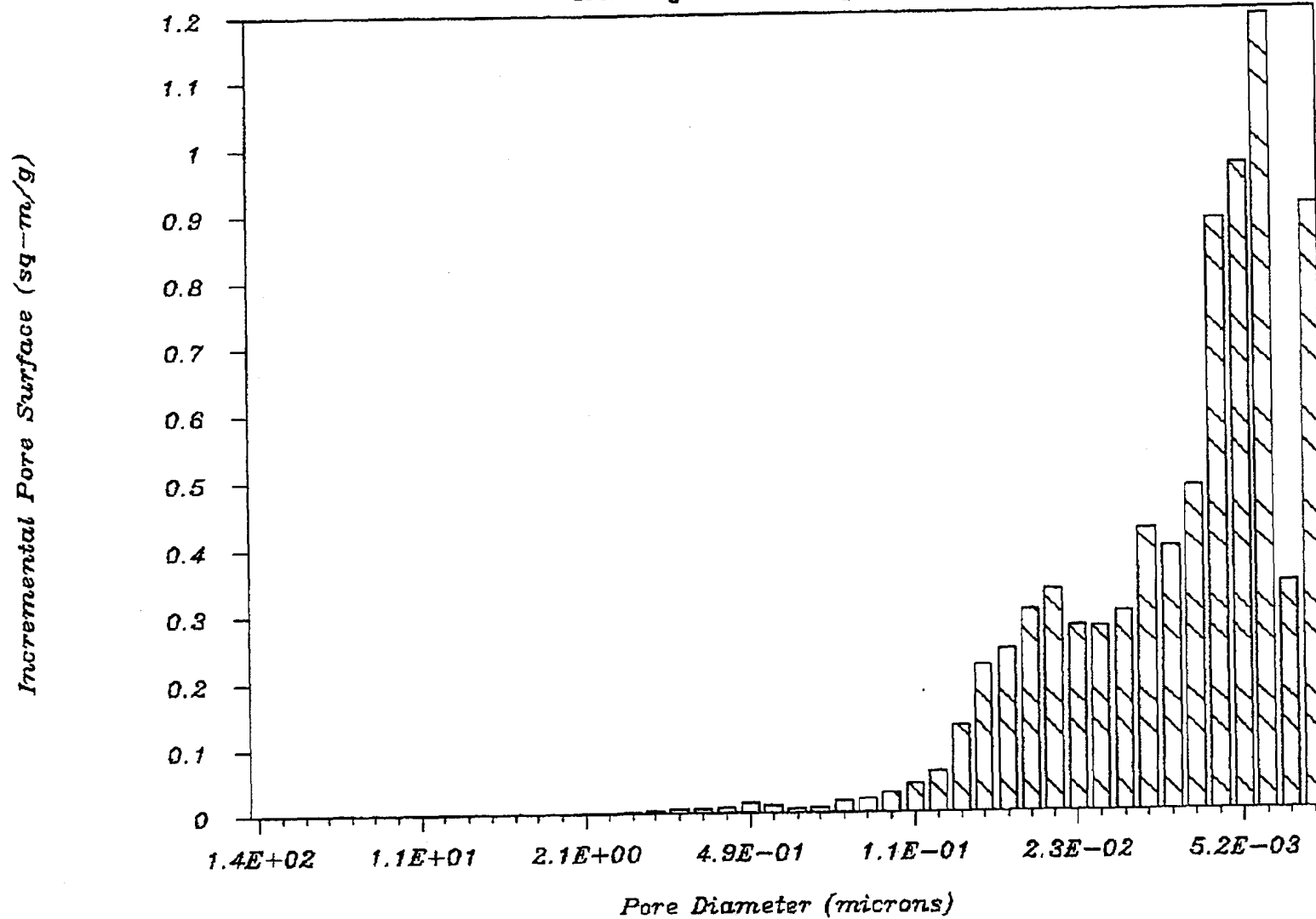
94057 32101.1 N3 20.4

Mercury Porosimetry Analysis



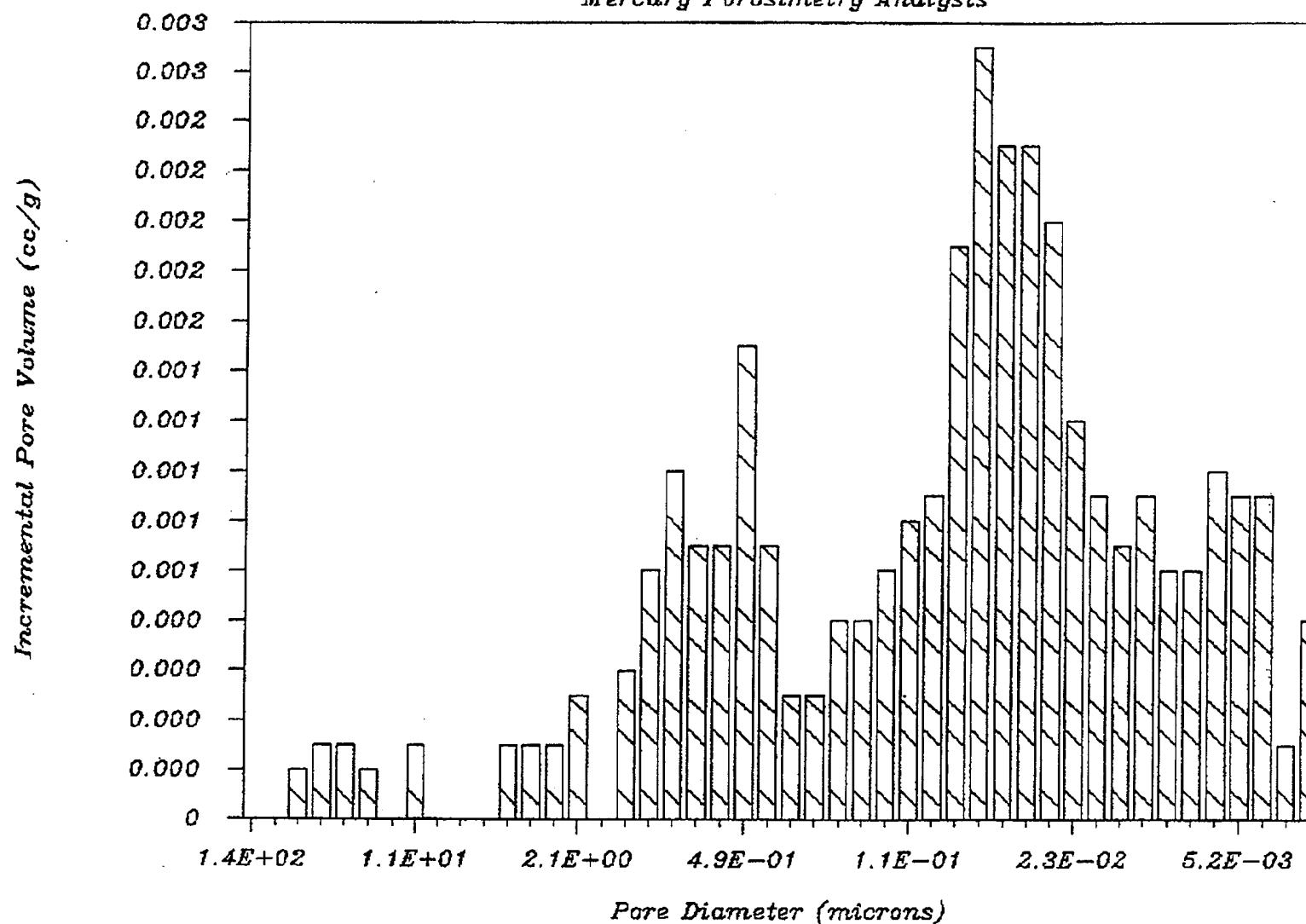
94032 32102.1 N4 5.3

Mercury Porosimetry Analysis



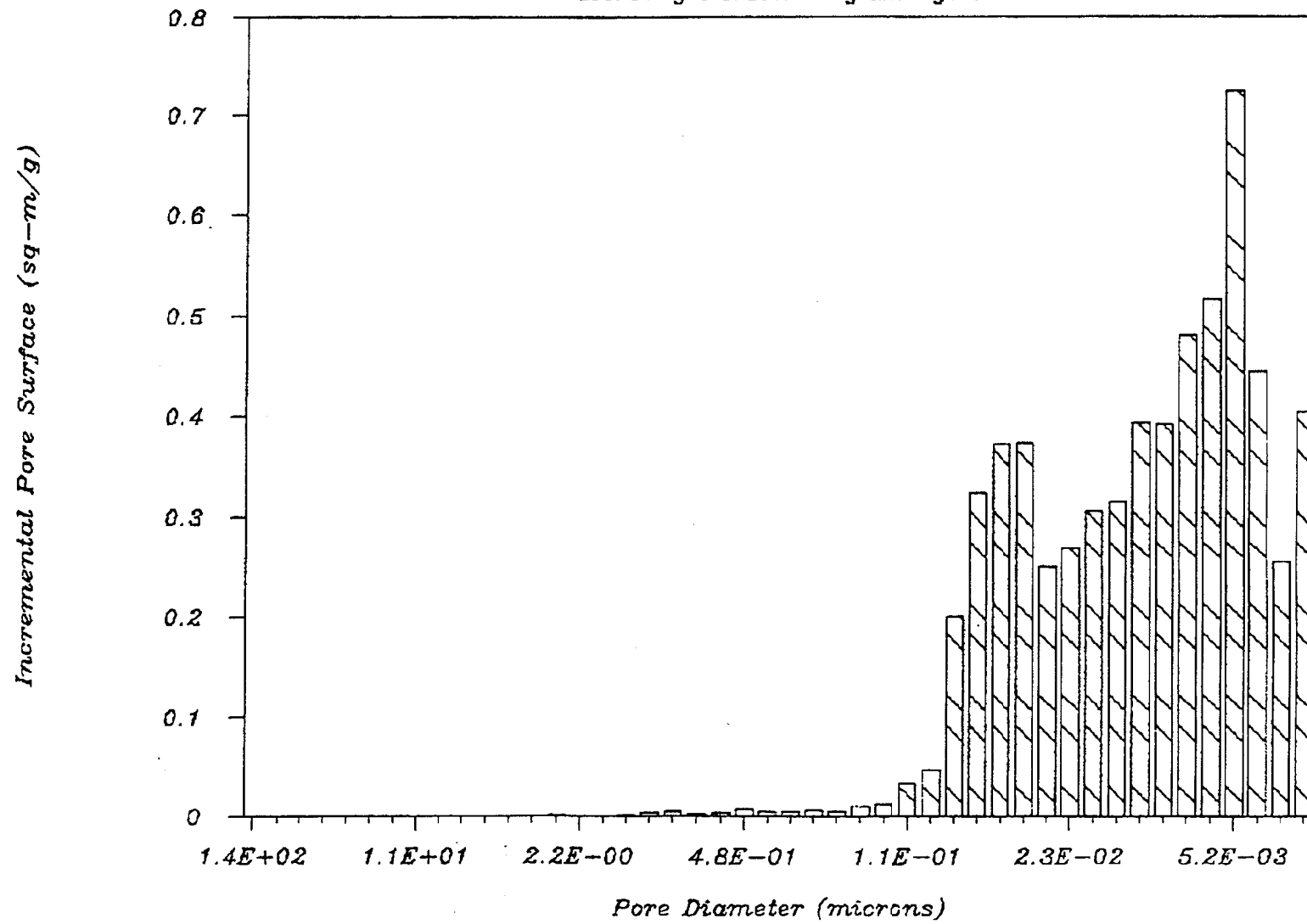
94032 32102.1 N4 5.3

Mercury Porosimetry Analysis



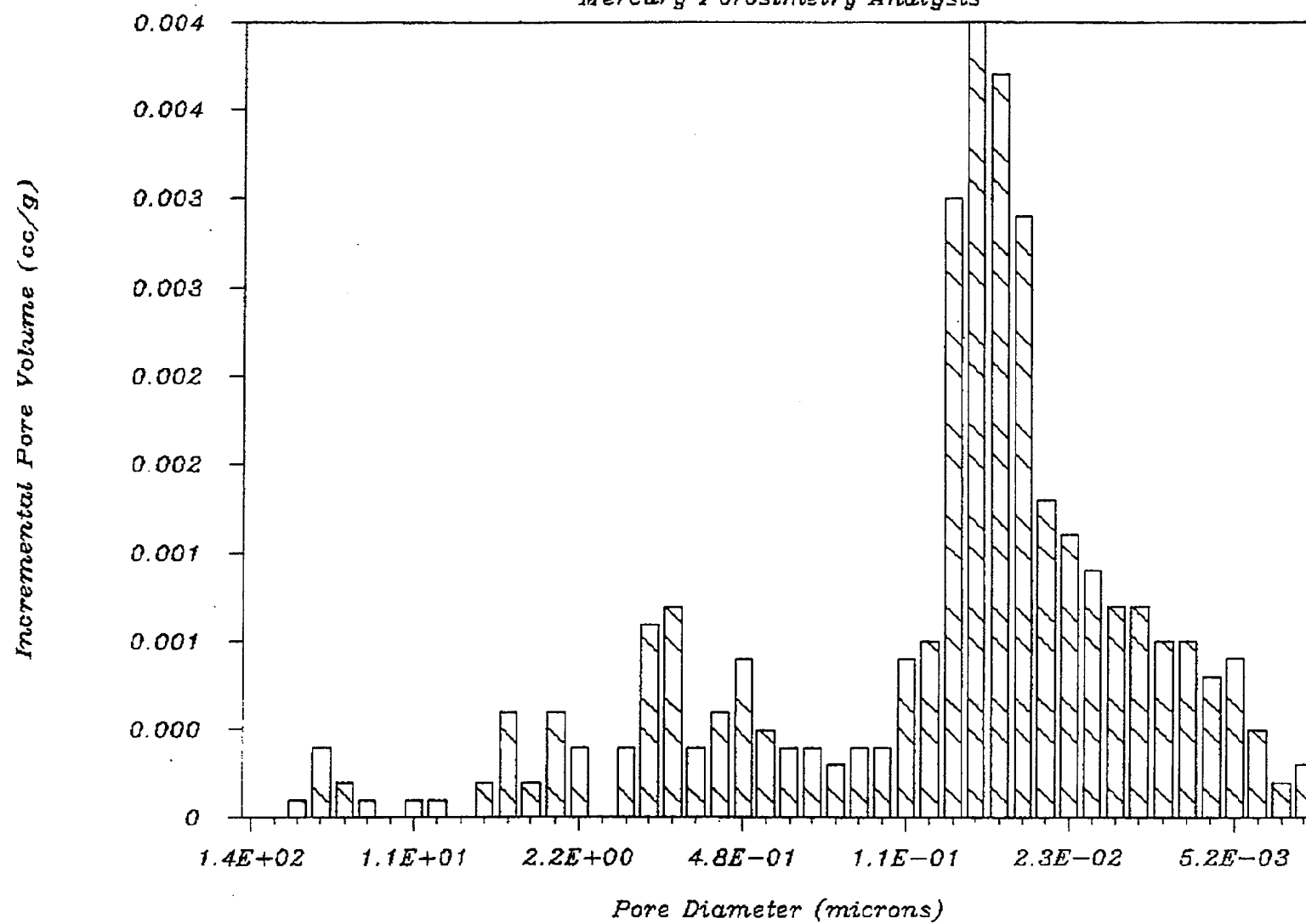
94041 32104.1 N4 11.6

Mercury Porosimetry Analysis



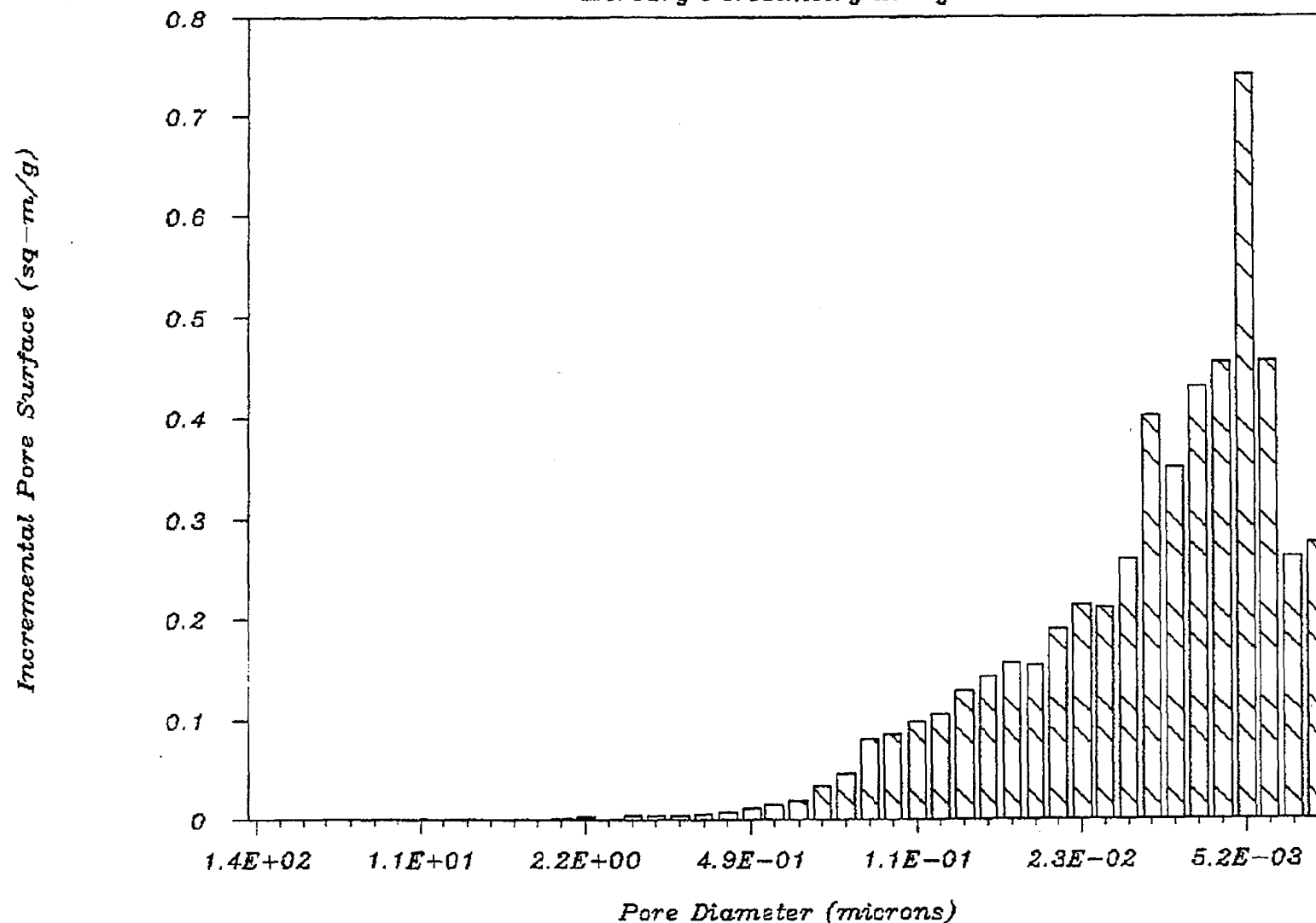
94041 32104.1 N4 11.6

Mercury Porosimetry Analysis



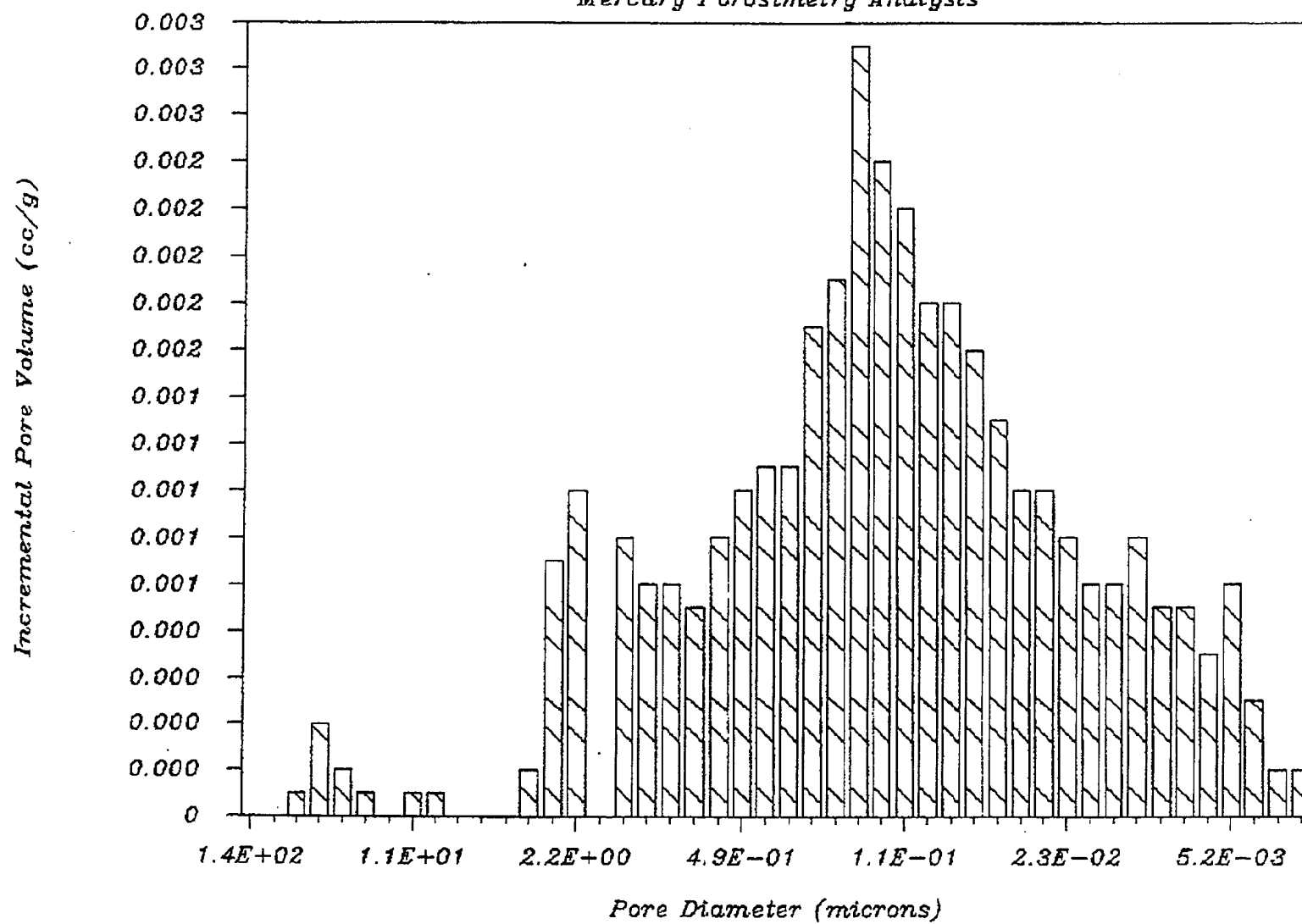
94037 32105.1 N4 14.5

Mercury Porosimetry Analysis



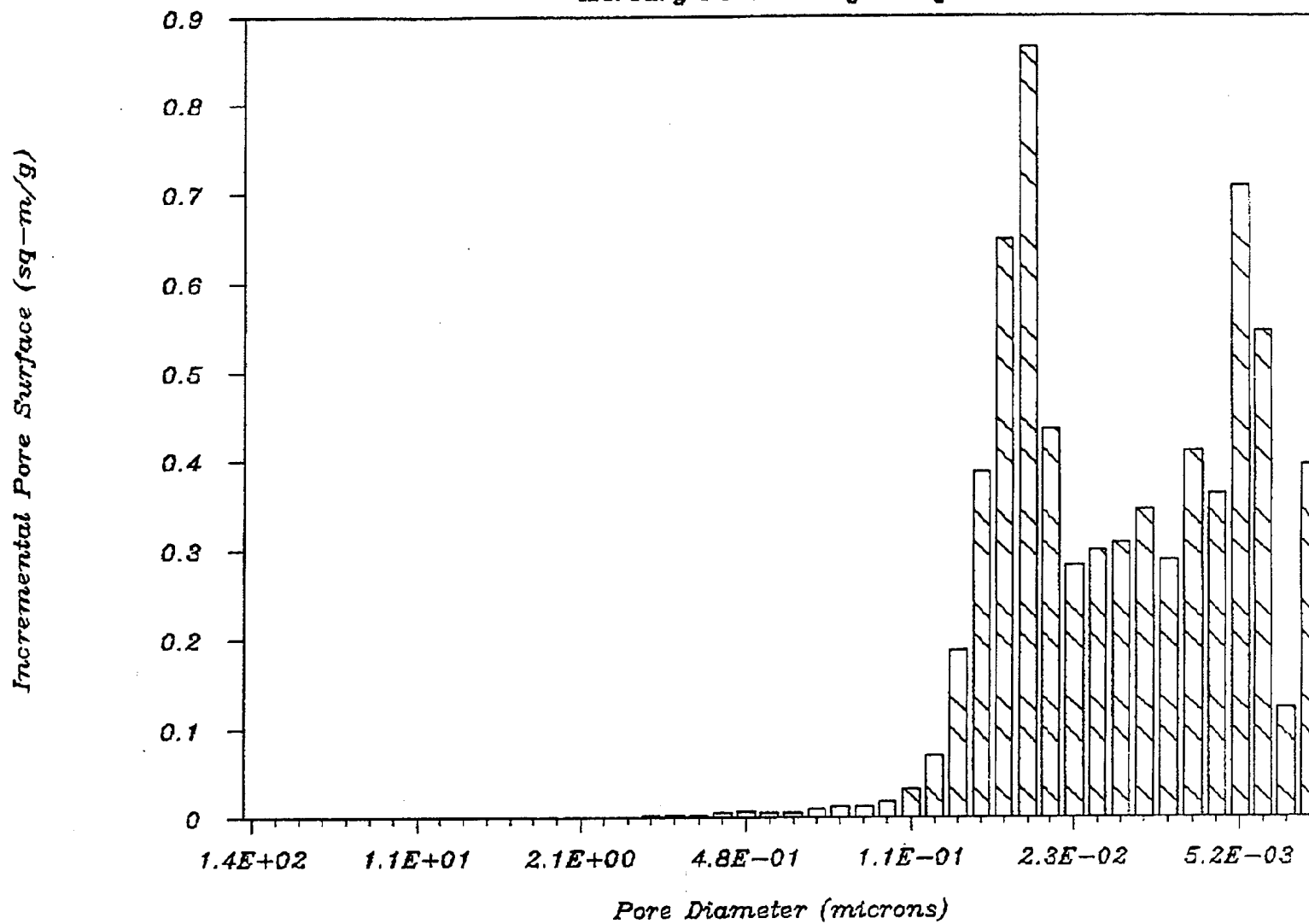
94037 32105.1 N4 14.5

Mercury Porosimetry Analysis



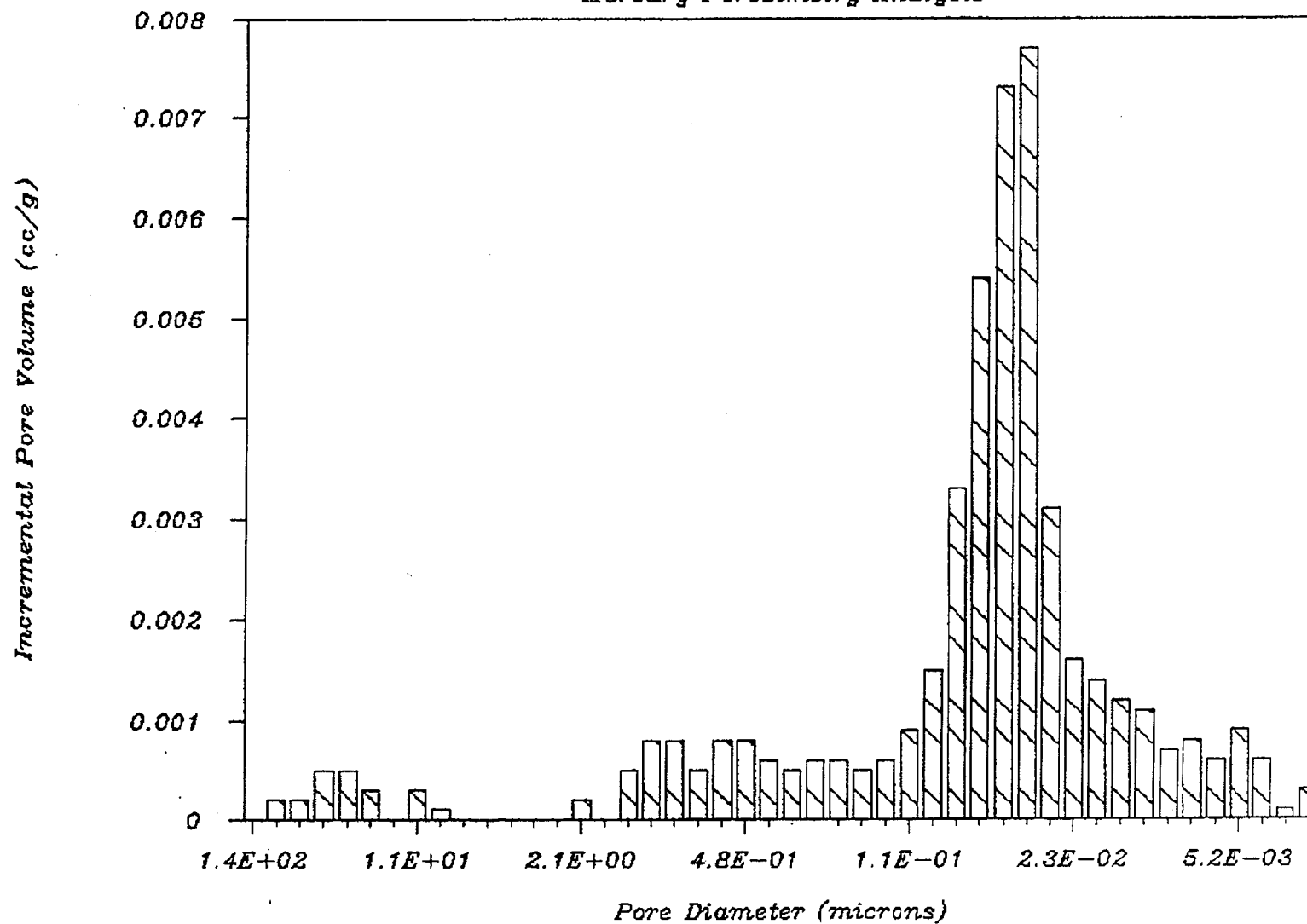
94043 32106.1 N4 19.0

Mercury Porosimetry Analysis



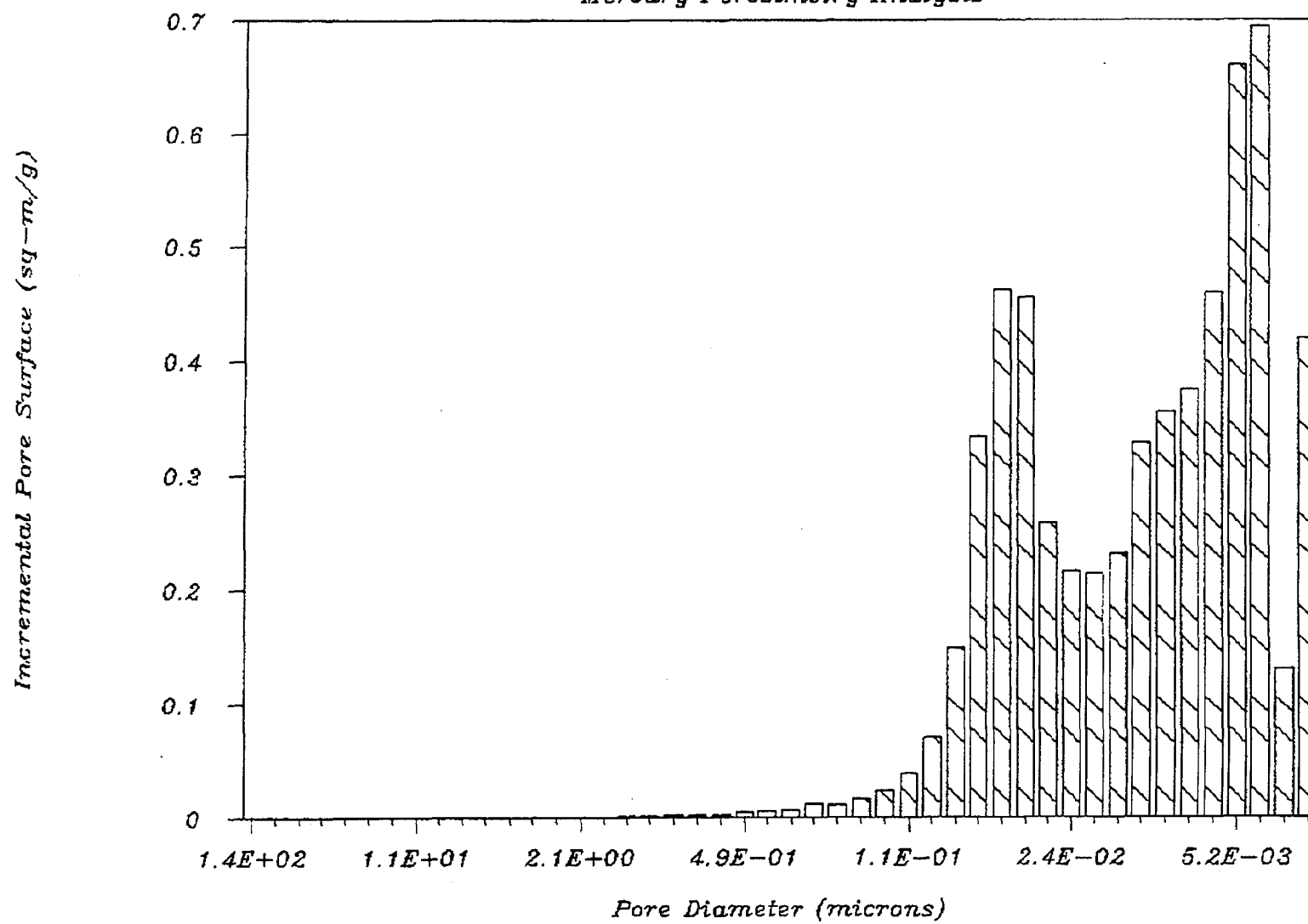
94043 32106.1 N4 19.0

Mercury Porosimetry Analysis



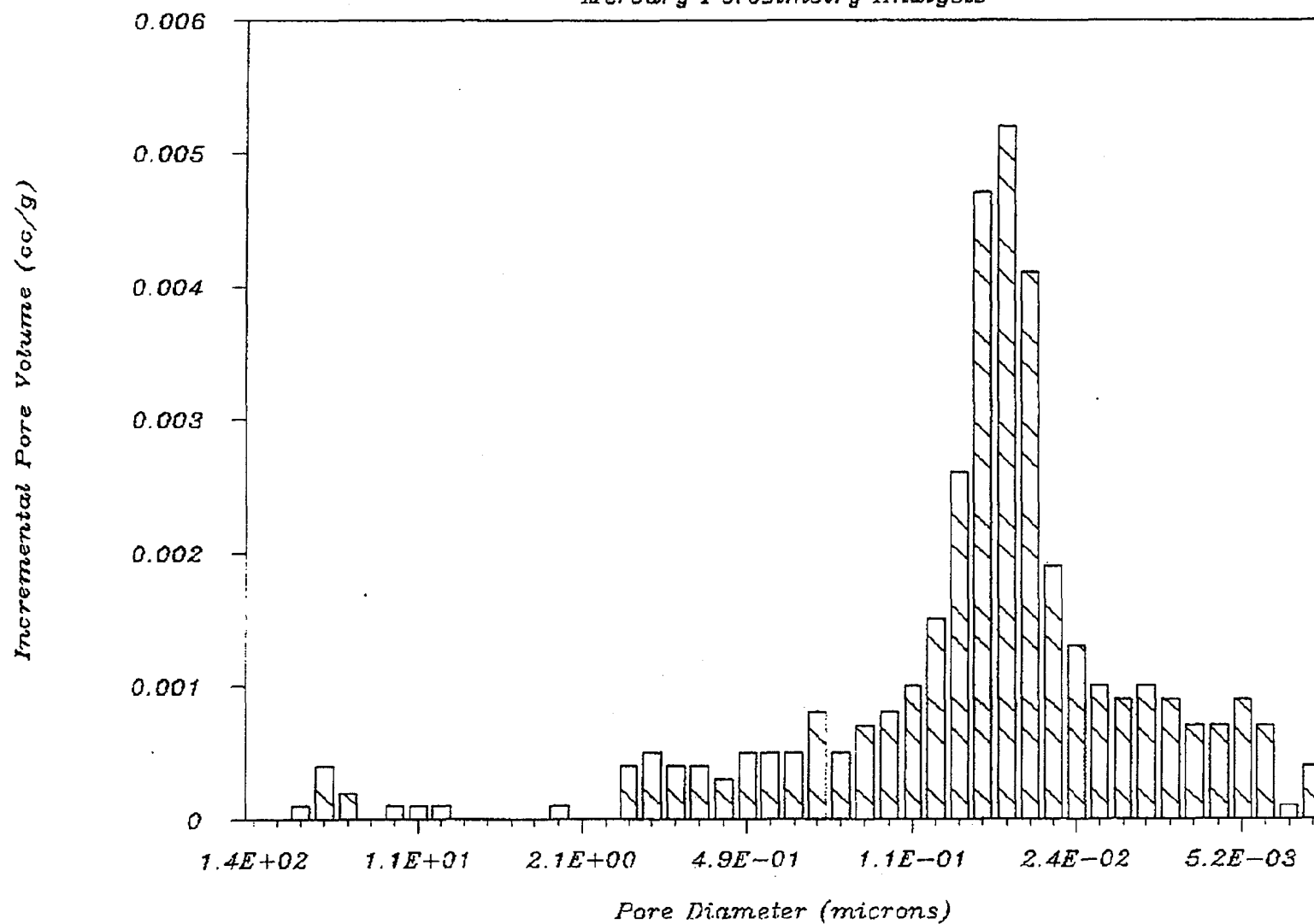
94046 32107.1 N5 4.9

Mercury Porosimetry Analysis



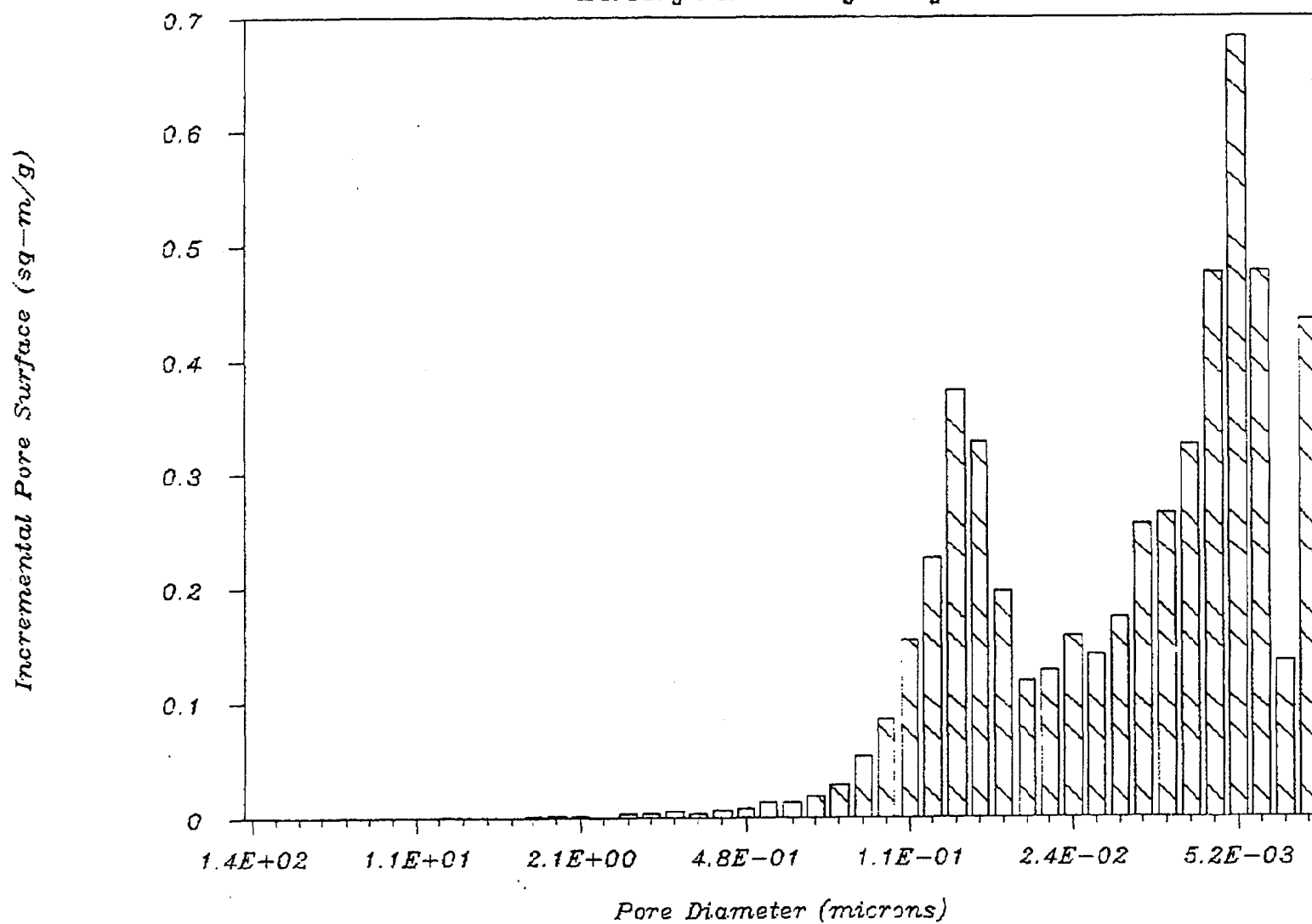
94046 32107.1 N5 4.9

Mercury Porosimetry Analysis



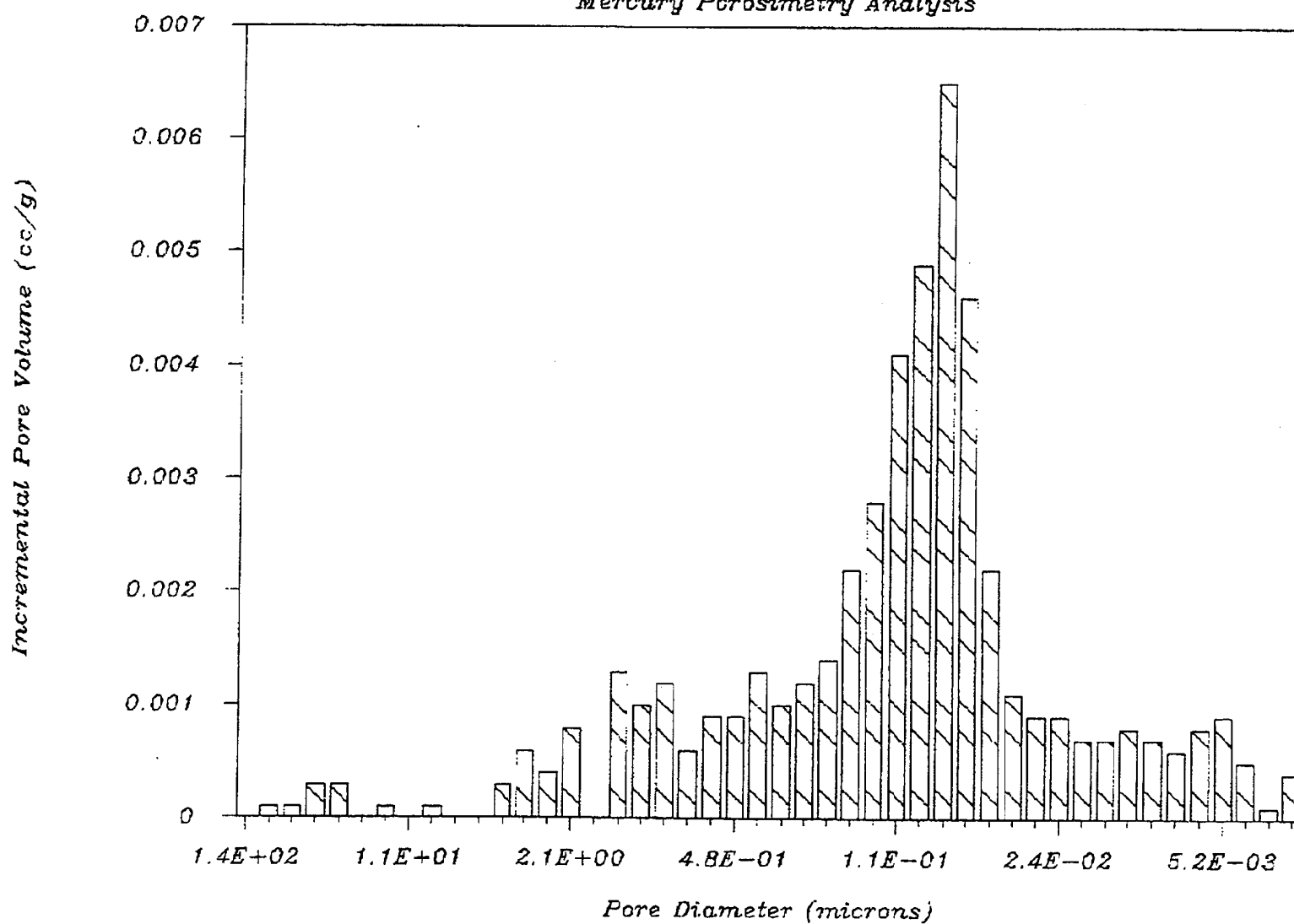
94055 32109.1 N5 11.15

Mercury Porosimetry Analysis



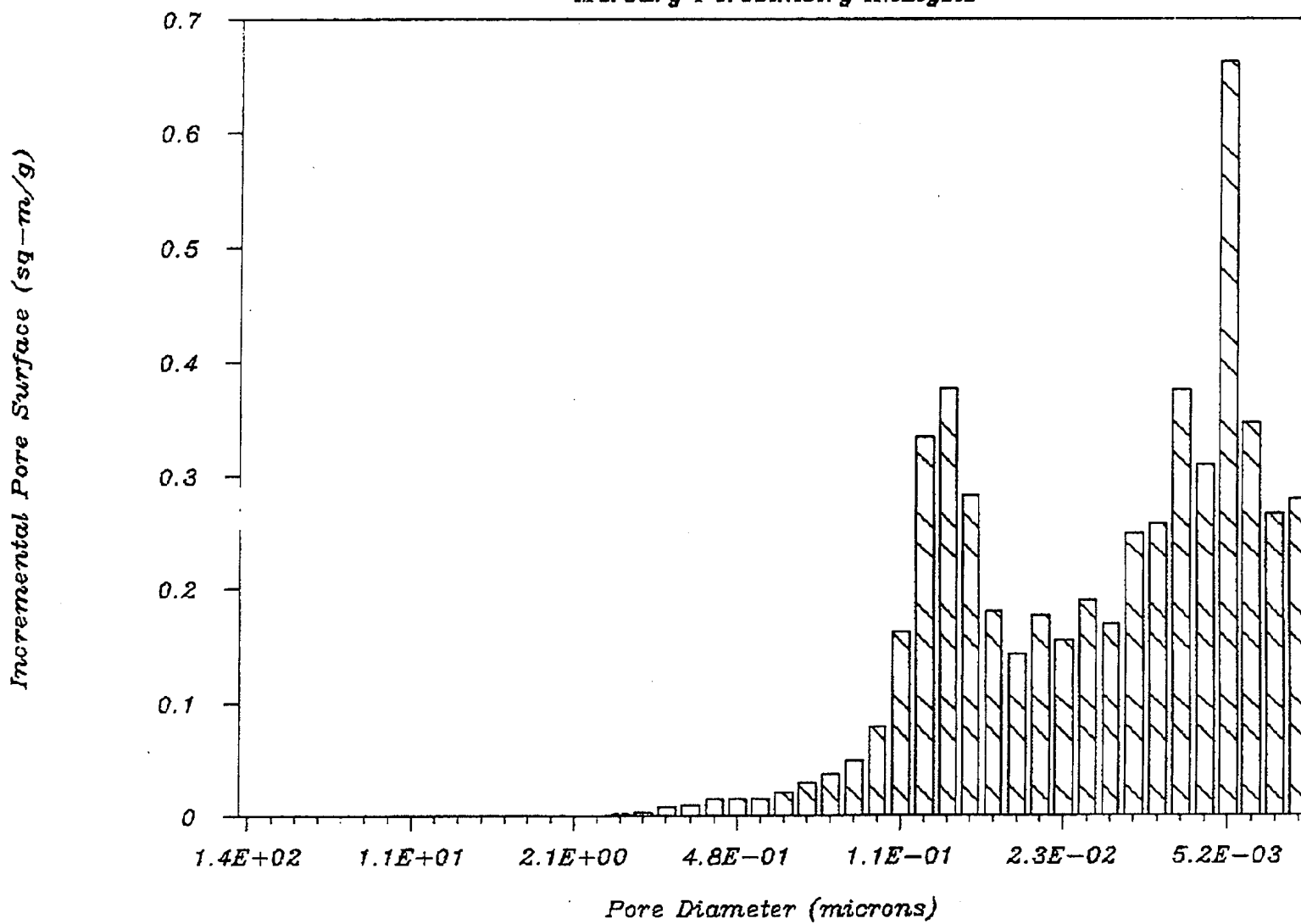
94055 32109.1 N5 11.15

Mercury Porosimetry Analysis



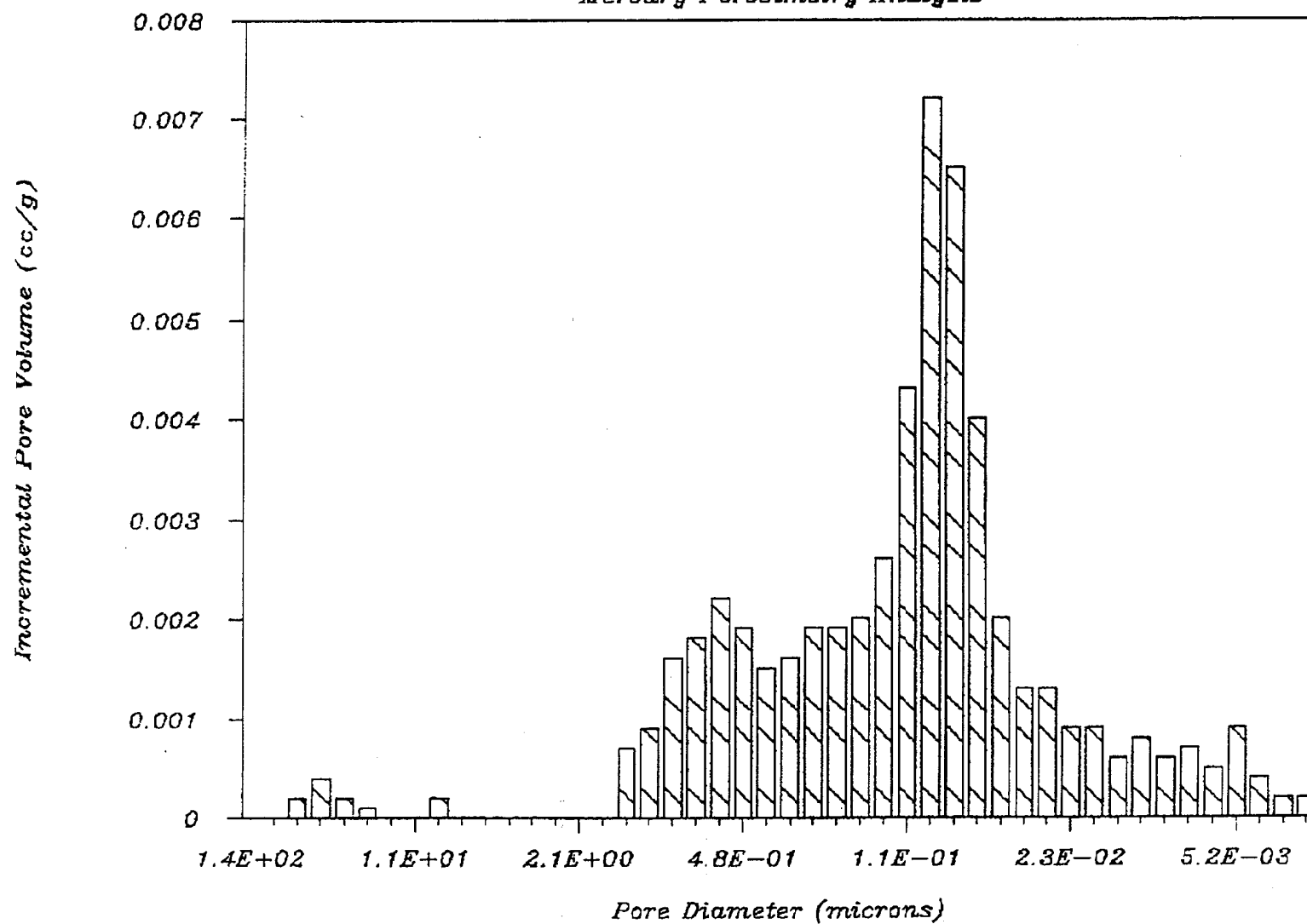
94044 32110.1 N5 14.8

Mercury Porosimetry Analysis



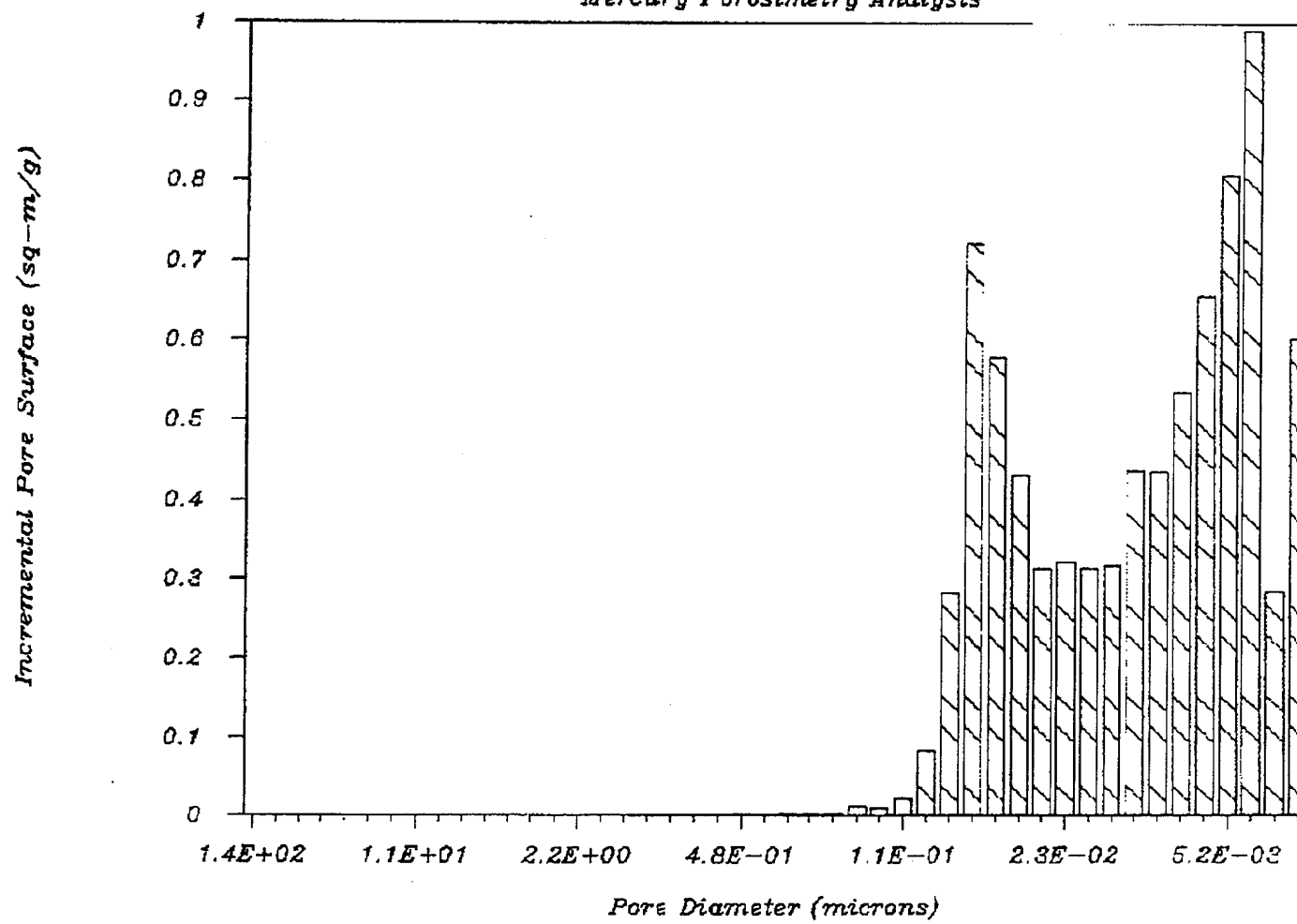
94044 32110.1 N5 14.8

Mercury Porosimetry Analysis



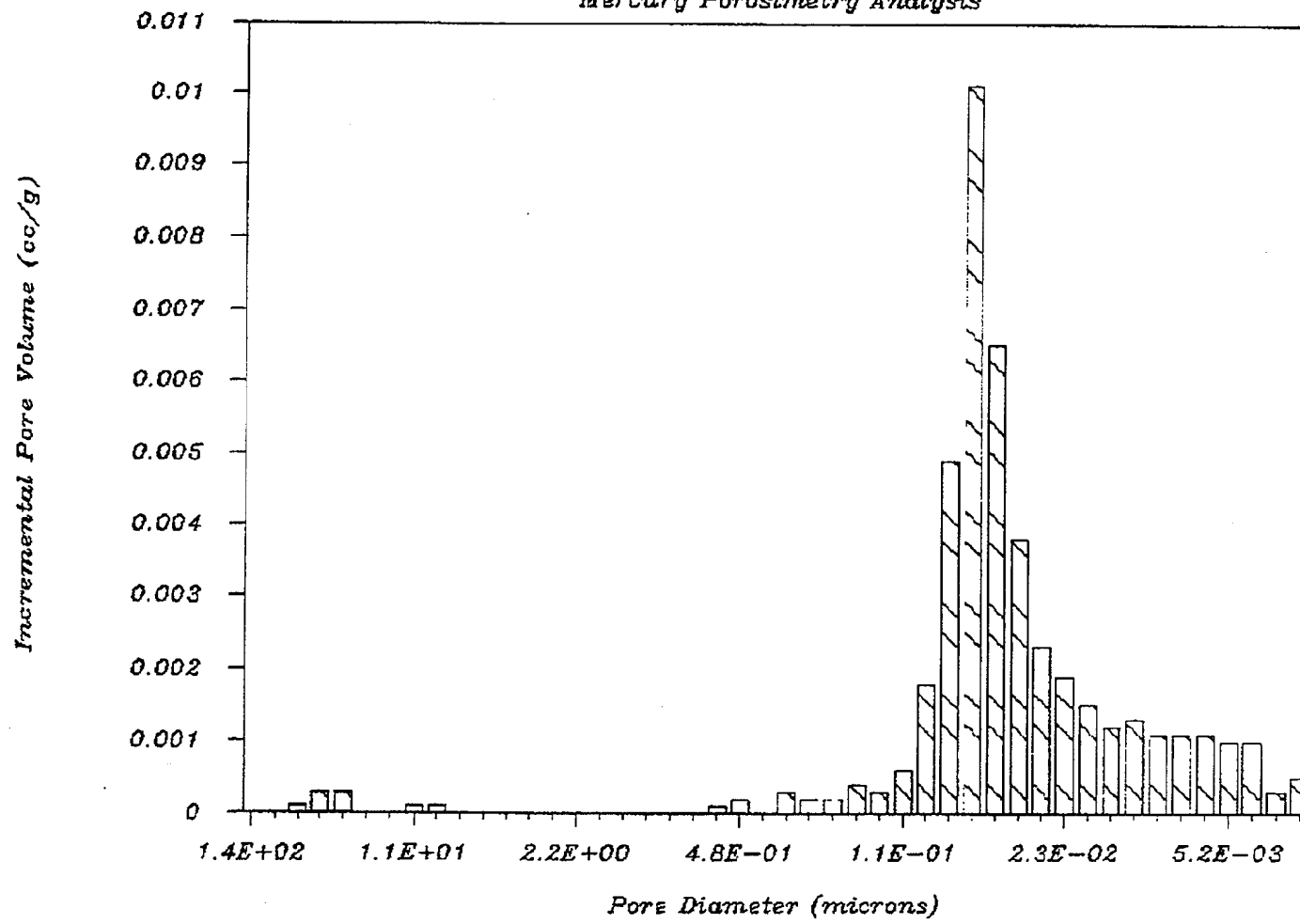
94036 32111.1 N5 20.1

Mercury Porosimetry Analysis



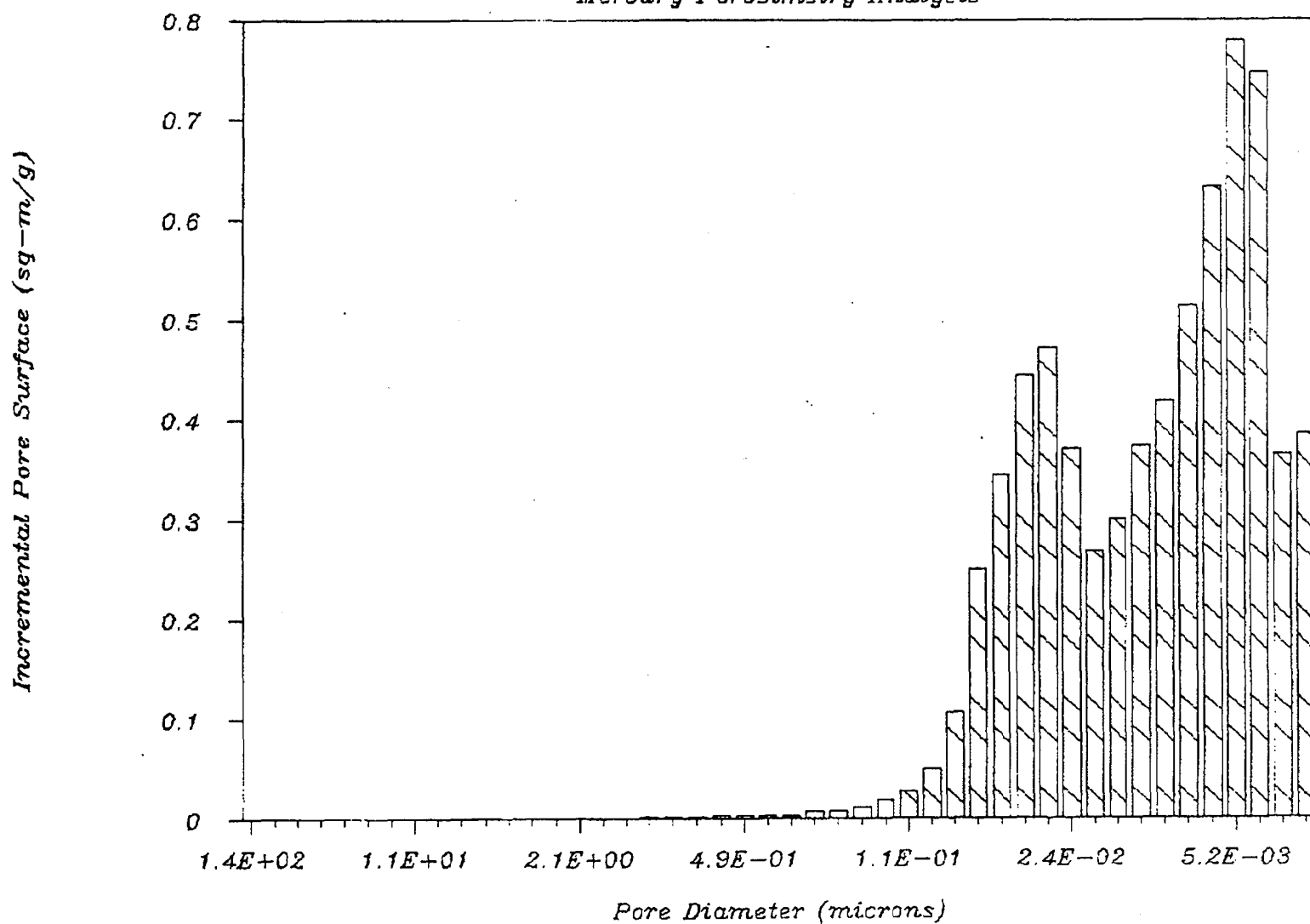
94036 32111.1 N5 20.1

Mercury Porosimetry Analysis



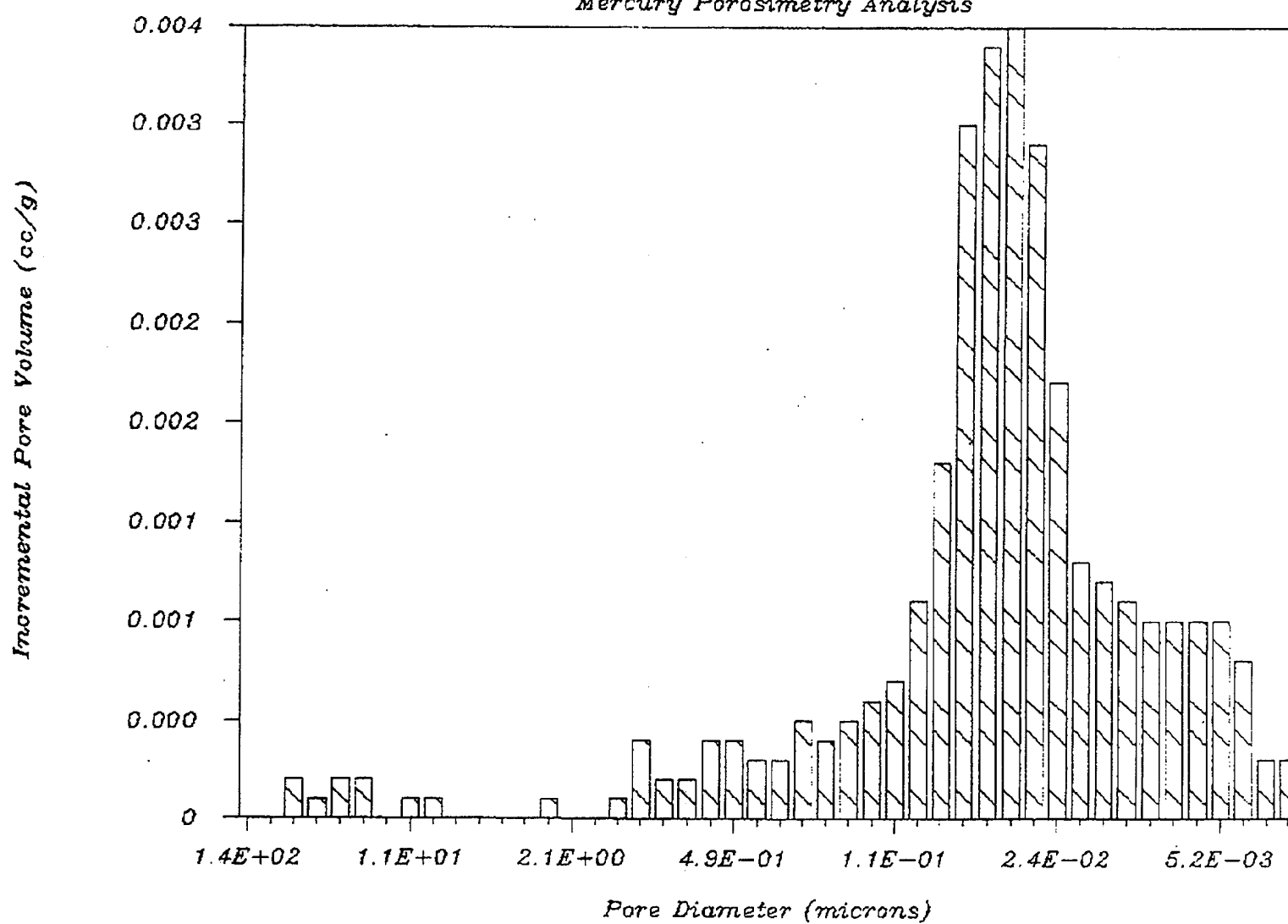
94040 32112.1 N6 4.8

Mercury Porosimetry Analysis



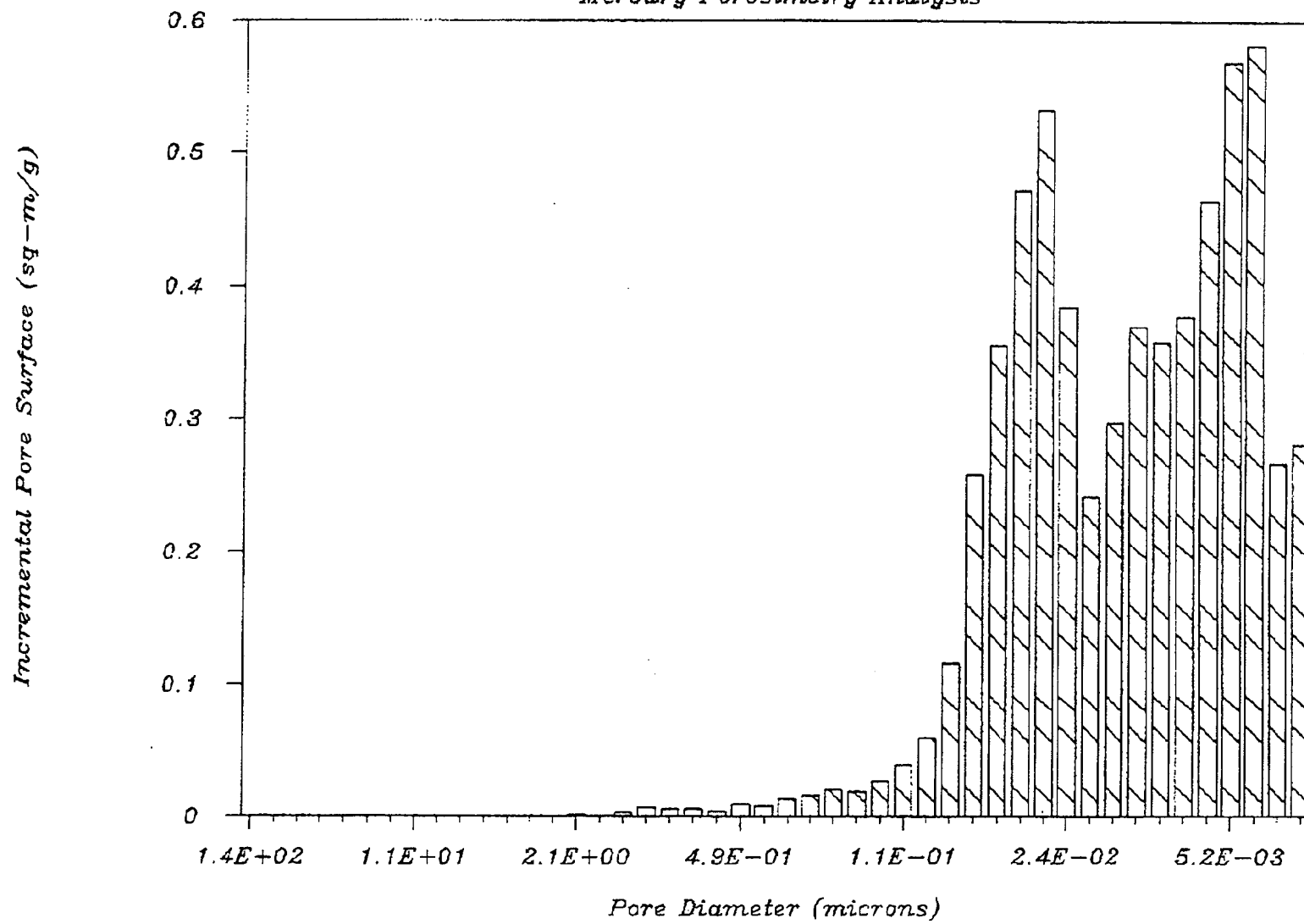
94040 32112.1 N6 4.8

Mercury Porosimetry Analysis



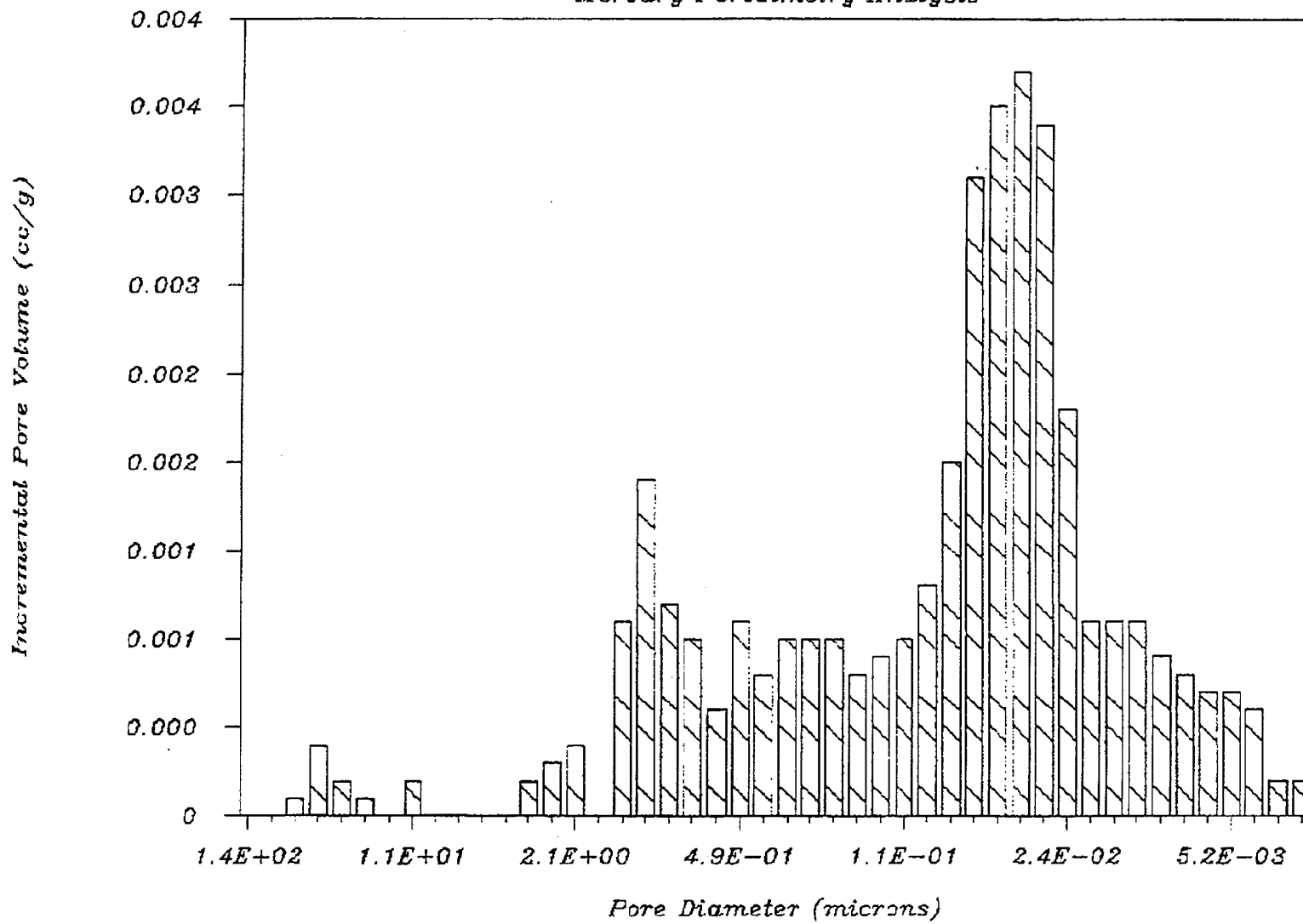
94045 32115.1 N6 11.0

Mercury Porosimetry Analysis



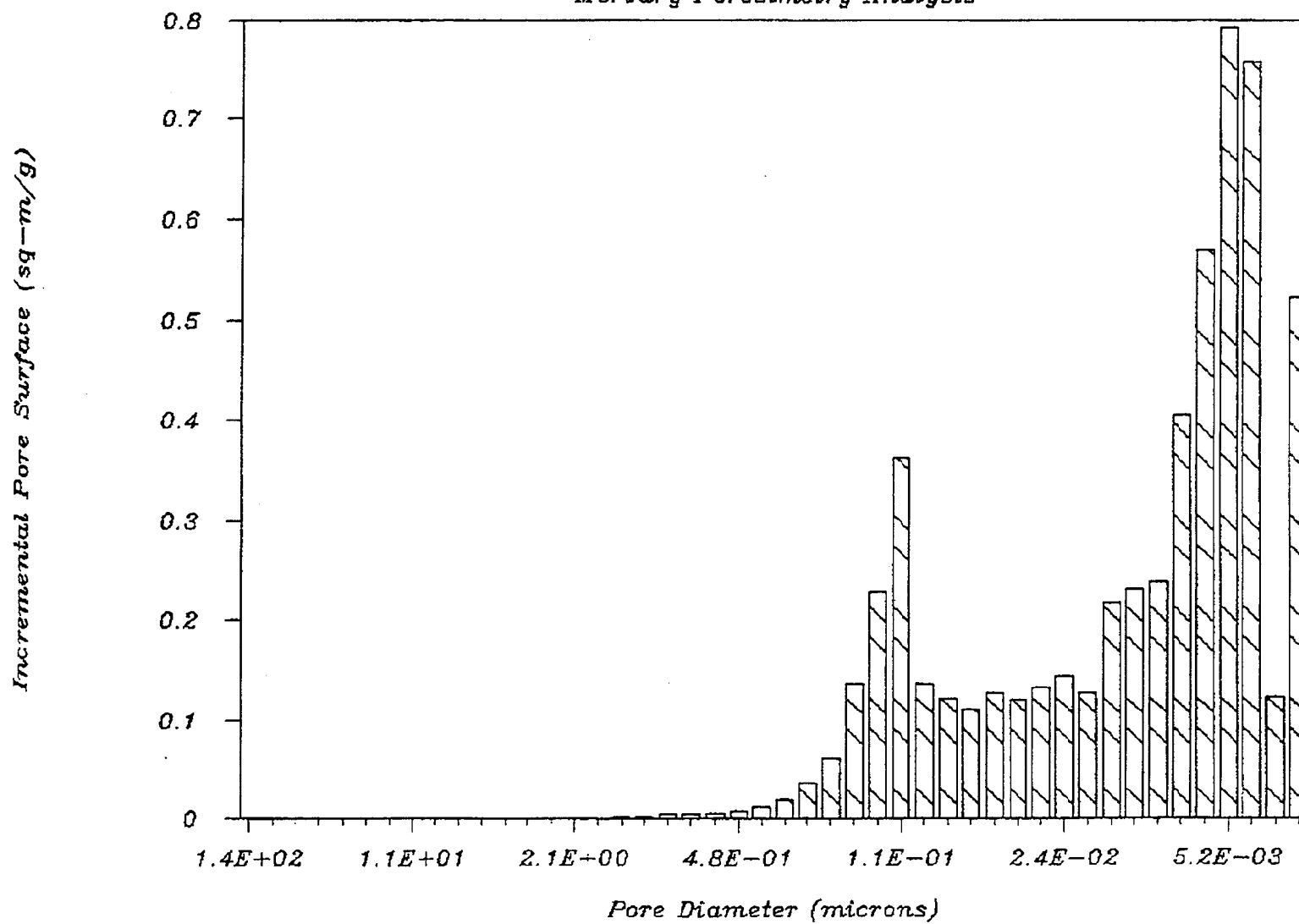
94045 32115.1 N6 11.0

Mercury Porosimetry Analysis



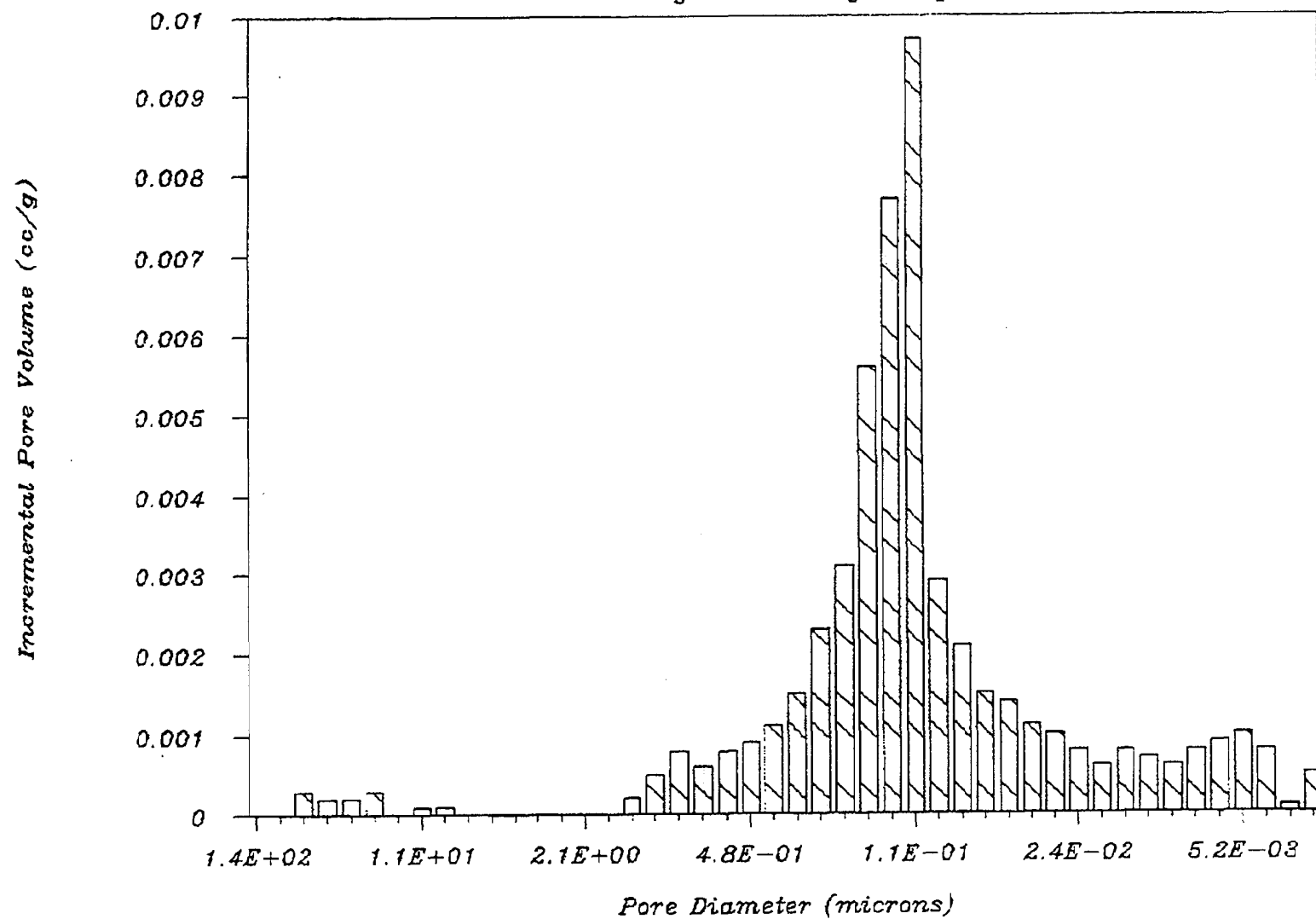
94059 32116.1 N6 14.5

Mercury Porosimetry Analysis



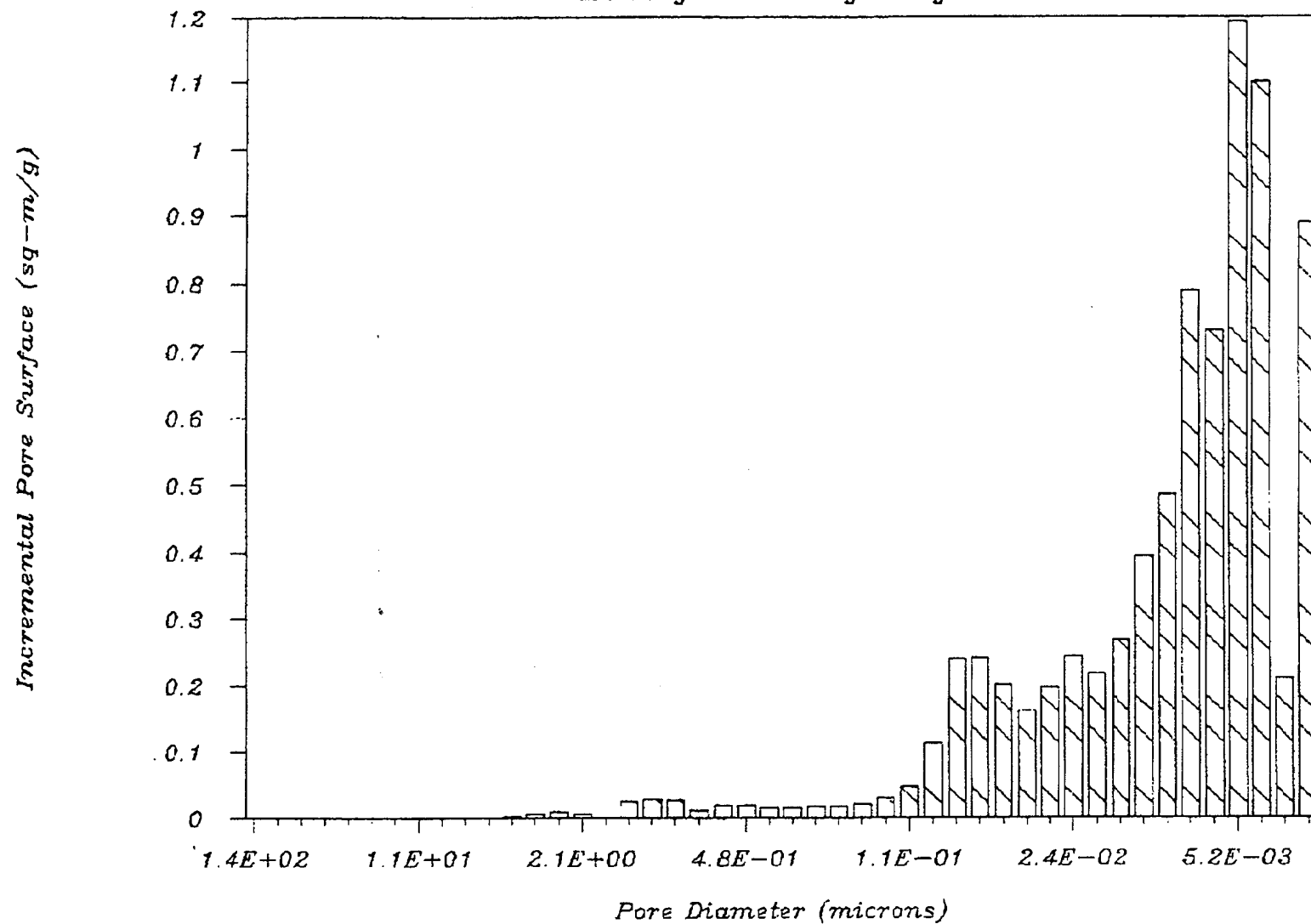
94059 32116.1 N6 14.5

Mercury Porosimetry Analysis



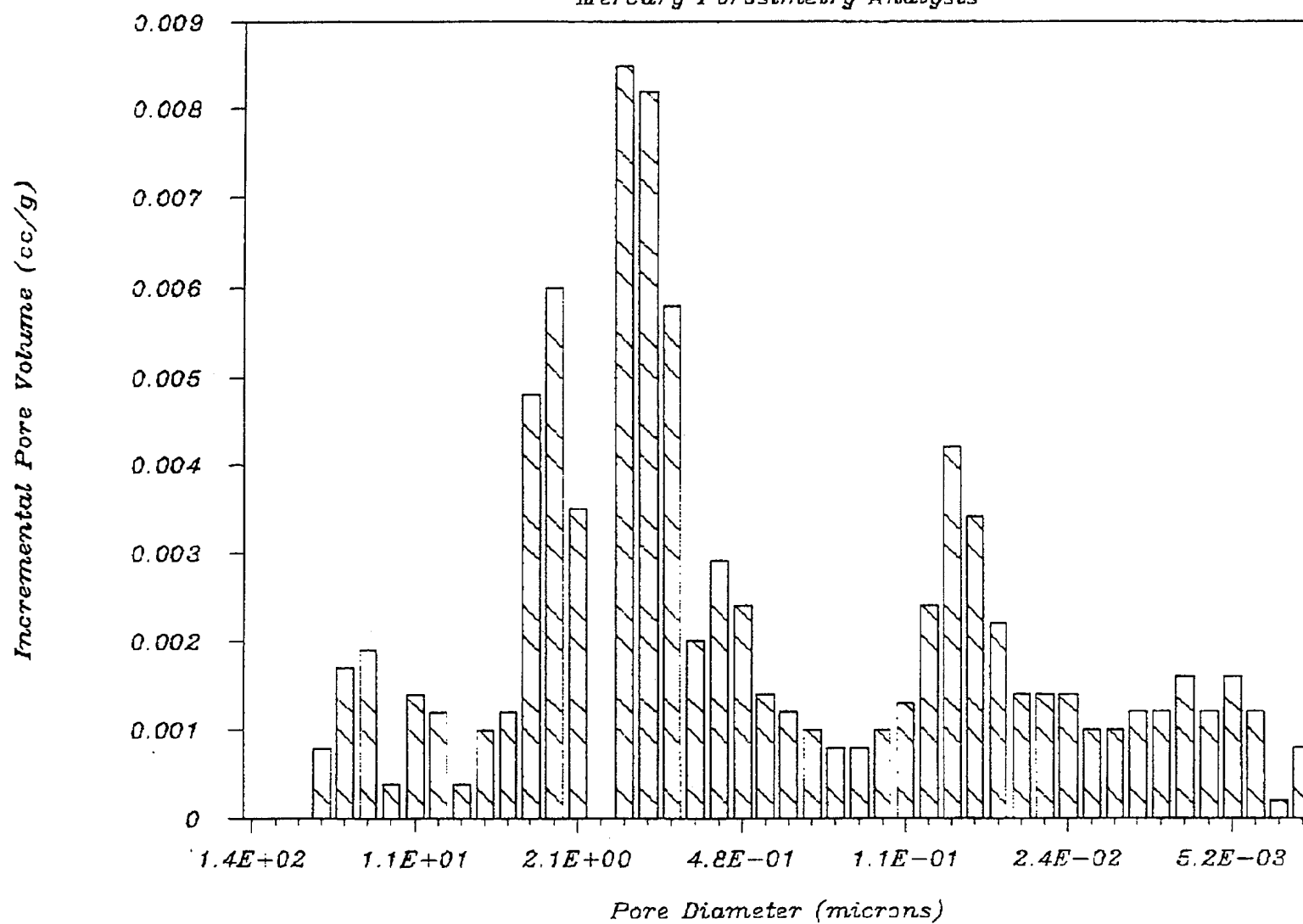
94062 34061.1 N6 20 2

Mercury Porosimetry Analysis



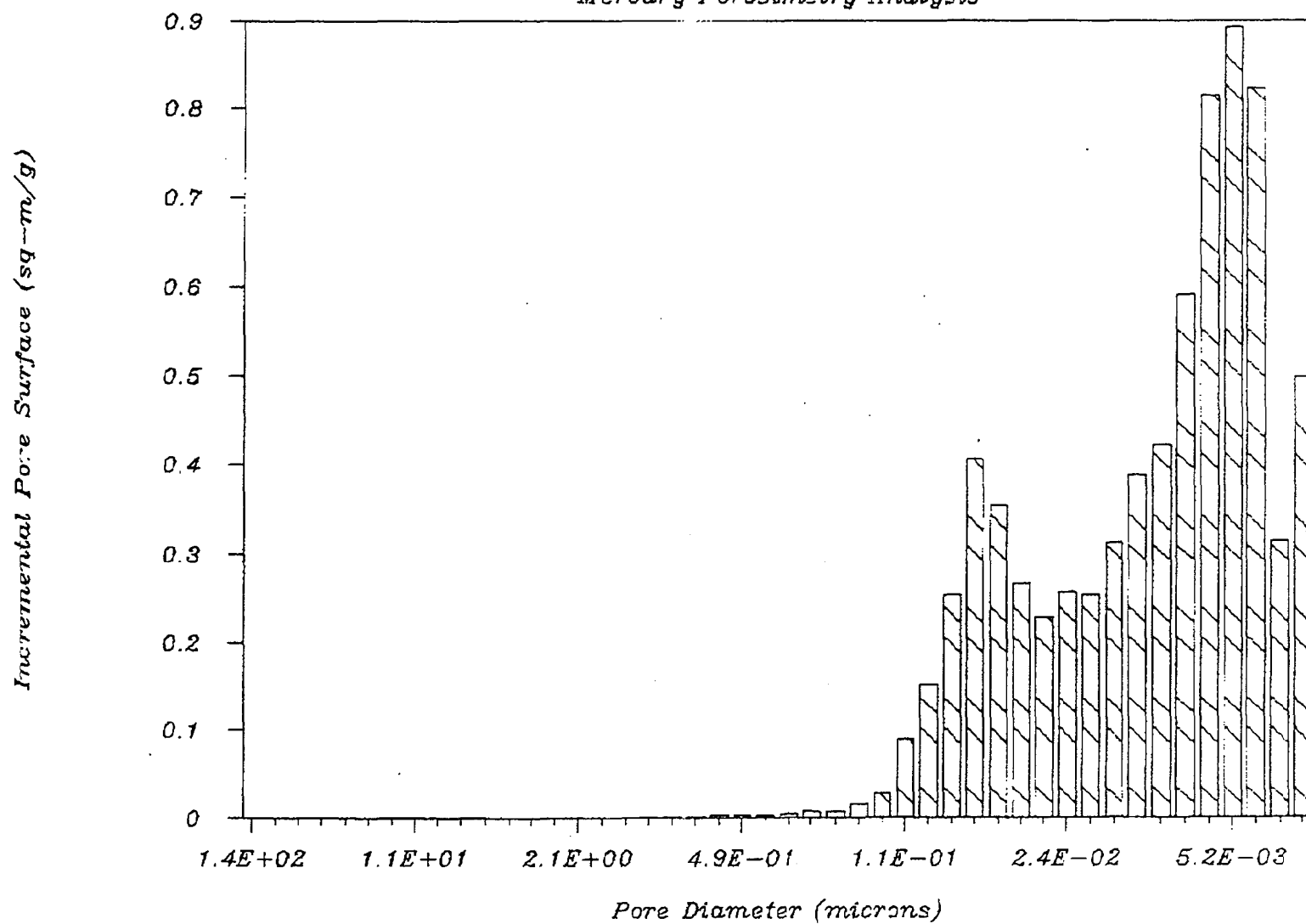
94062 34061.1 N6 20 2

Mercury Porosimetry Analysis



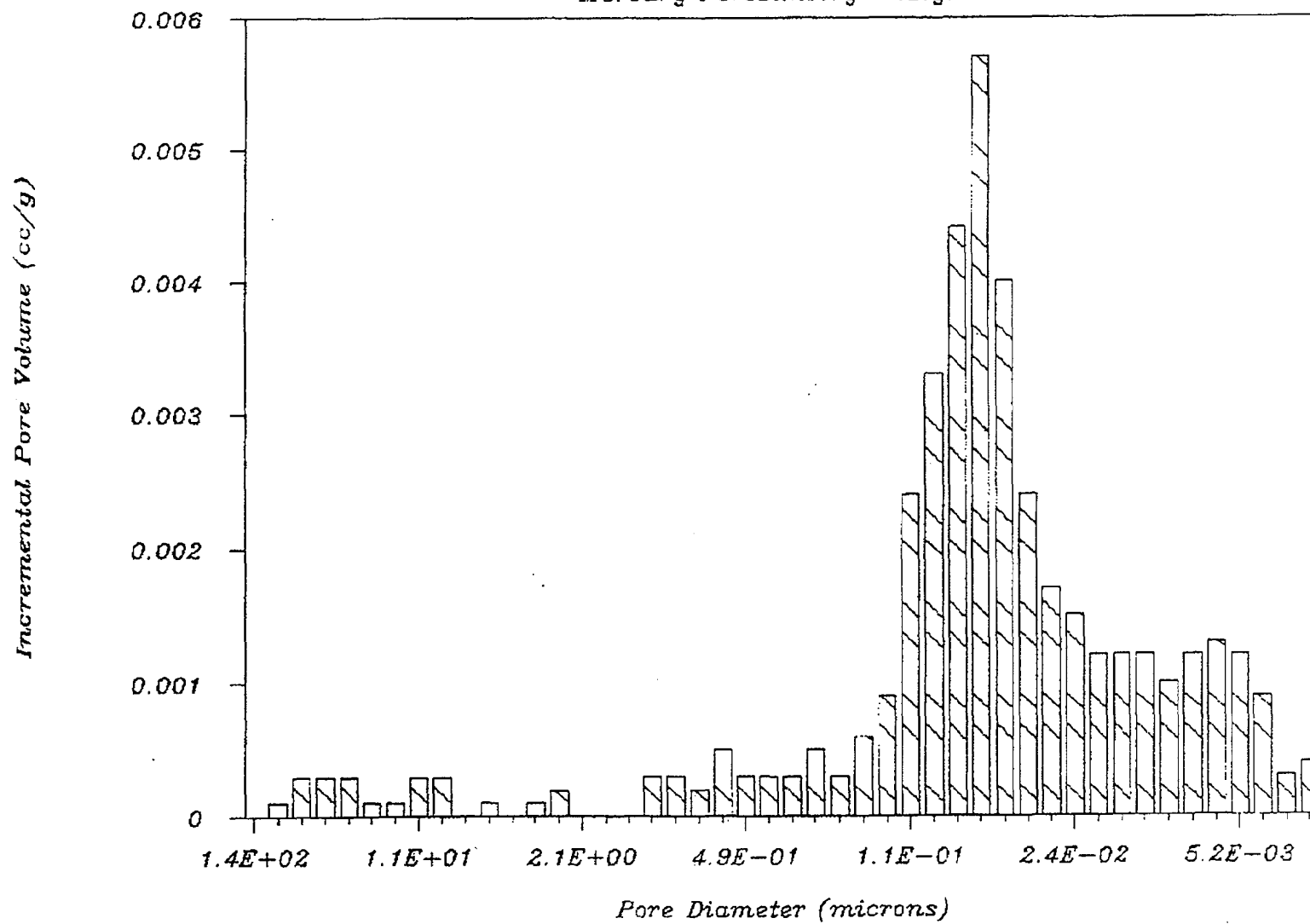
94039 32120.1 N7 5.0

Mercury Porosimetry Analysis



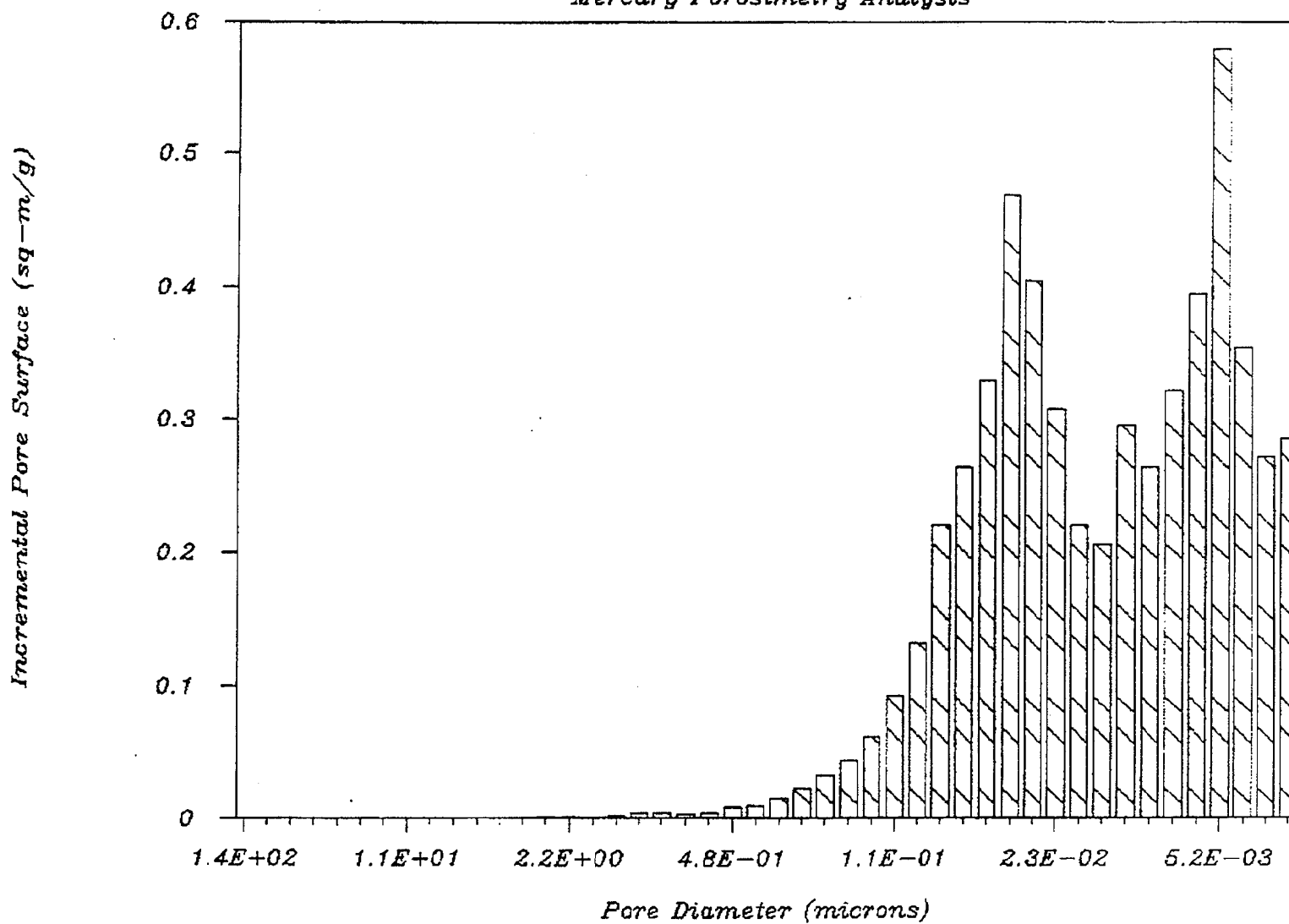
94039 32120.1 N7 5.0

Mercury Porosimetry Analysis



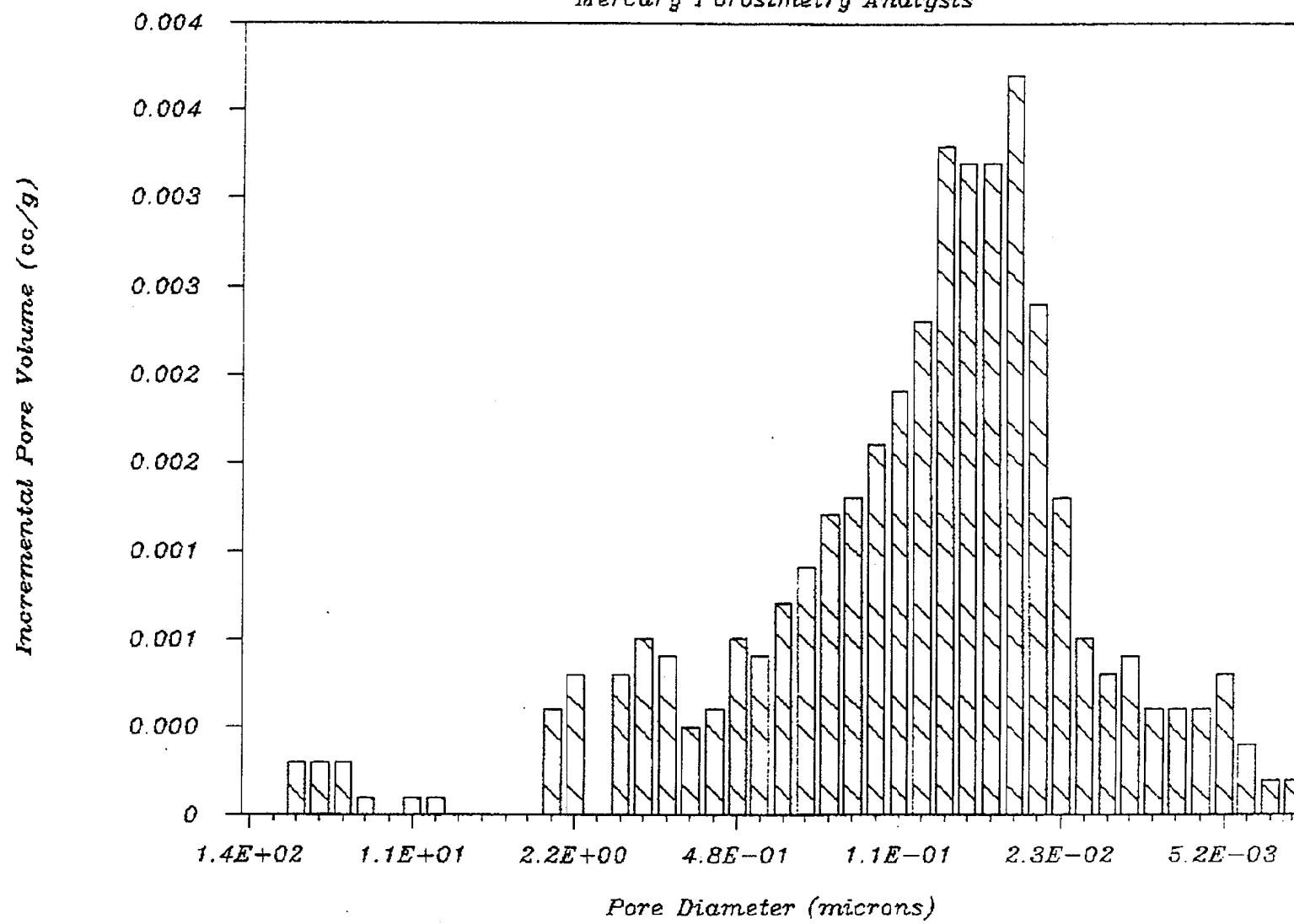
94042 32123.1 N7 10.9

Mercury Porosimetry Analysis



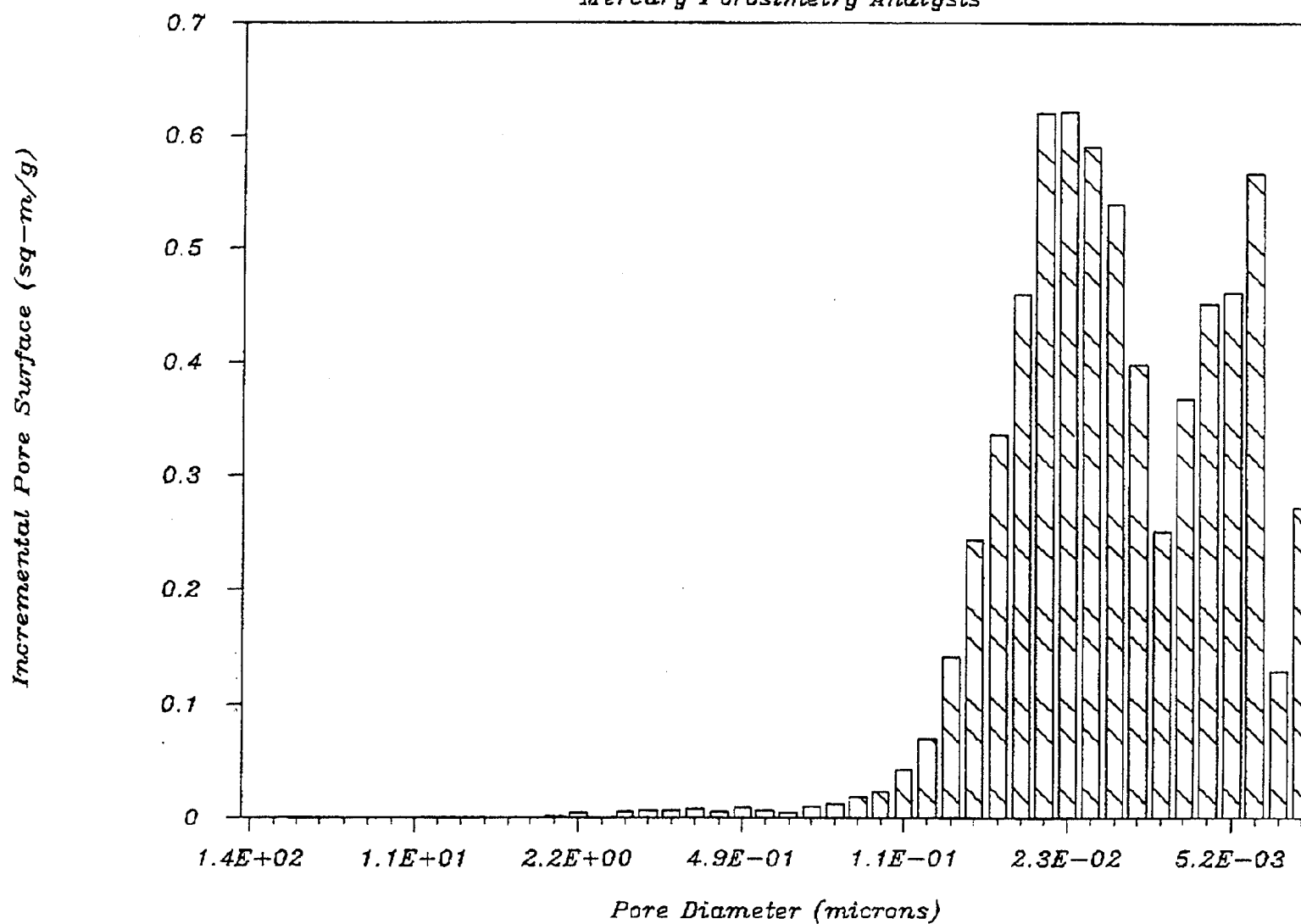
94042 32123.1 N7 10.9

Mercury Porosimetry Analysis



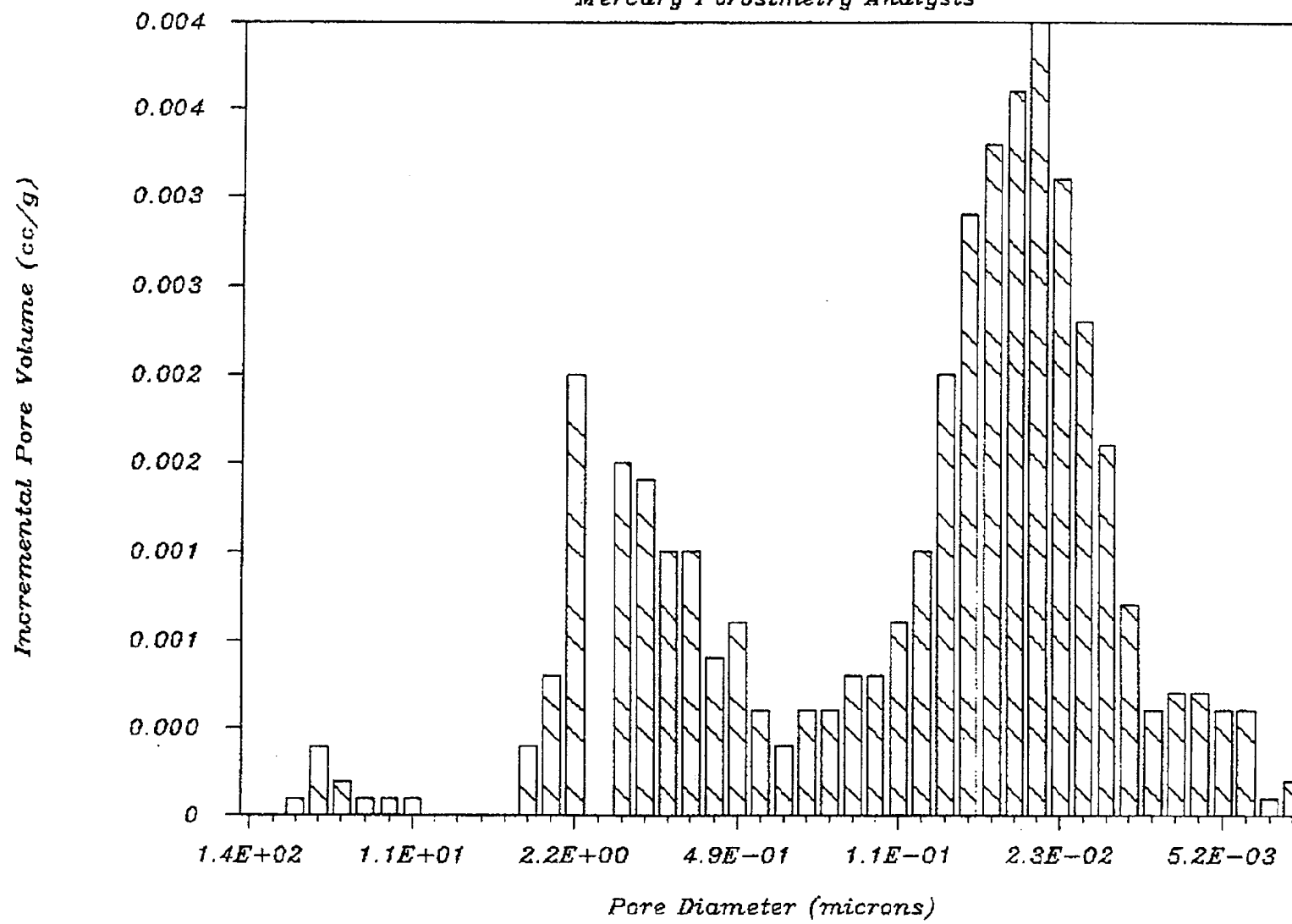
94038 32124.1 N7 14.3

Mercury Porosimetry Analysis



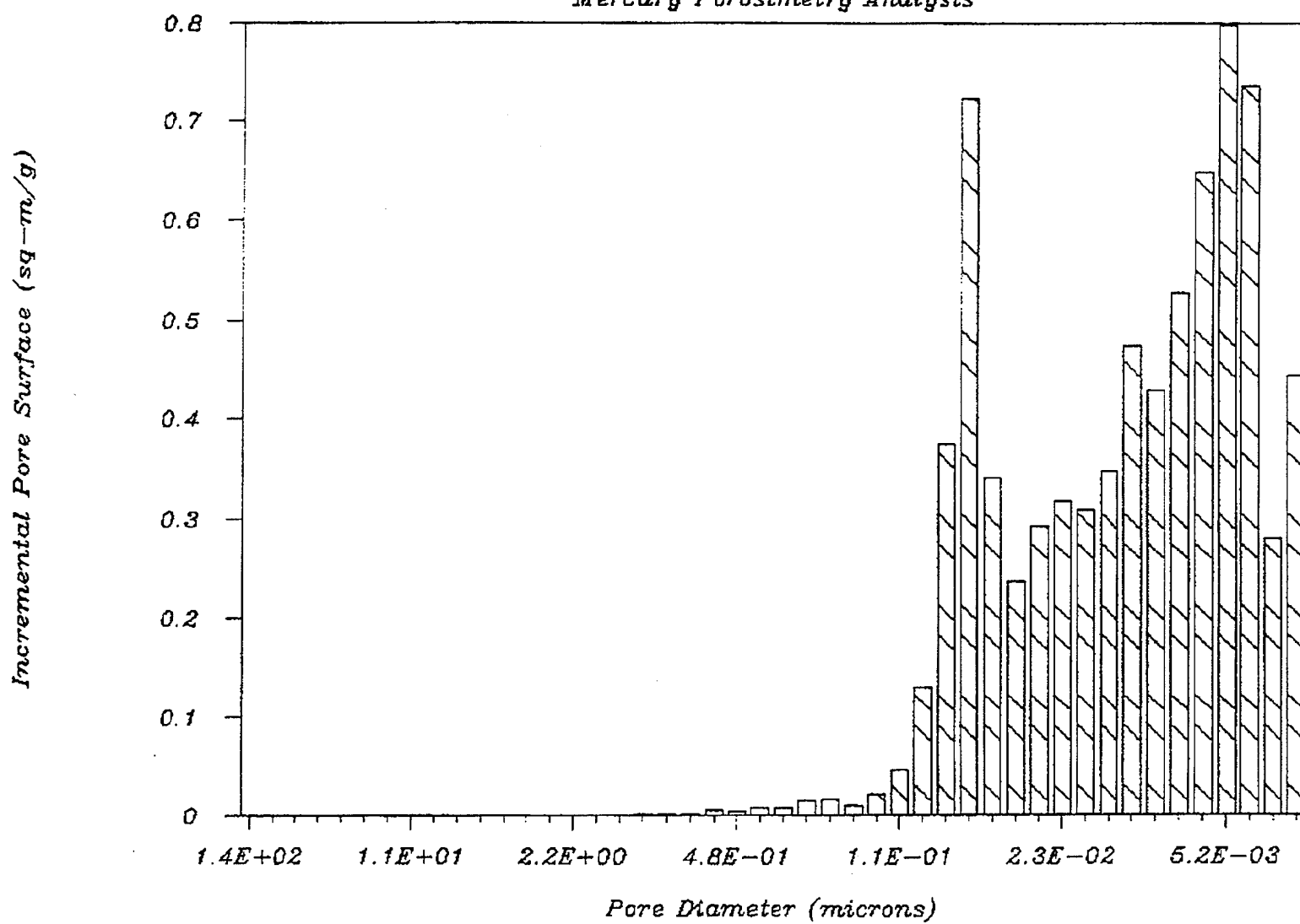
94038 32124.1 N7 14.3

Mercury Porosimetry Analysis



94035 32131.1 E2 19.5

Mercury Porosimetry Analysis



94035 32131.1 E2 19.5

Mercury Porosimetry Analysis

